

10/2/00
2

Breakdown Properties of Atmospheric Air for Short Gap Distances in Extremely Non Uniform Field with Switching and Lightning Impulse Voltages

by
JAGDISH CHOUDHARY



DEPARTMENT OF ELECTRICAL ENGINEERING
INDIAN INSTITUTE OF TECHNOLOGY KANPUR

April, 2000

Breakdown Properties of Atmospheric Air for Short Gap Distances in Extremely Non Uniform Field with Switching and Lightning Impulse Voltages

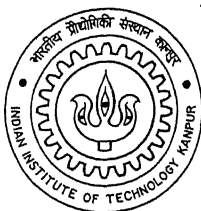
A Thesis Submitted

*in Partial Fulfillment of the Requirements
for the Degree of*

MASTER OF TECHNOLOGY

By

JAGDISH CHOUDHARY



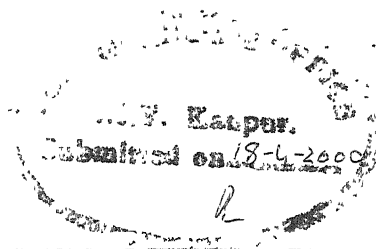
to the

DEPARTMENT OF ELECTRICAL ENGINEERING
INDIAN INSTITUTE OF TECHNOLOGY, KANPUR
APRIL, 2000

14 JUN 2000^{EE}
CENTRAL LIBRARY
I. I. T., KANPUR
A 131073



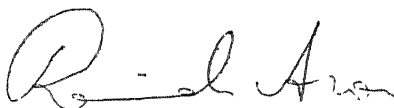
A131073



Certificate

It is to certify that the work contained in the thesis entitled "*Breakdown Properties of Atmospheric Air for short gap distances in Extremely Non Uniform Field with Switching and Lightning impulse voltages*" by Jagdish Choudhary (9810425) has been carried out under my supervision and that this work has not been submitted elsewhere for a degree.

(April, 2000)


(Dr. R. Arora)

Professor
Department of Electrical Engineering
Indian Institute of Technology
Kanpur – 208016
India.

Acknowledgement

I wish to acknowledge my deep sense of gratitude to Dr. Ravindra Arora for his invaluable guidance, patient supervision and encouragement throughout of the thesis work

My thanks to Mr. S V Ghorpade of our lab for his help in preparing the experiment setups and using the HV equipment. I also thanks Mr. Ram Avtaar for his prompt services. Specially thanks to Mr. Devi Charan of electronics lab who devote his time to detecting the fault of impulse generator in control cubicle when work has been impeded in mid way. I also thanks to Mr. Tiwari of workshop for preparing electrodes for setup.

I acknowledge to my colleague Mr. R Banwari for providing joyful company during the experiments. I also thanks to Jaan group viz. S P Singh, Dhiraj, Manish, Shobit, Jainu, Praveen, Pandey₂ and Jangir for their immemorable company during my stay of IITK. At the end I wish to thank to my parents, brother Munnu and sister Dr Sumitra for source of inspiration and moral support during the alma meter of IITK.

Jagdish Choudhary

Name of Student : **JAGDISH CHOUDHARY**

Roll No. : **9810425**

Degree for which submitted : **M. Tech.**

Department : **Electrical Engineering**

Thesis Title : **Breakdown Properties of Atmospheric Air for Short Gap Distances in
Extremely Non Uniform Field with Switching and Lightning Impulse
Voltages**

Thesis Supervisor : **Dr. R. Arora**

Month and Year of Submission : **April, 2000**

Abstract

Laboratory investigations are carried out to study the insulation breakdown strength of air in extremely non uniform field. U_{b50} Breakdown characteristics and Average field intensity characteristics are obtained for three electrode configurations with three types of impulse voltage waveshapes. $si1$, $si2$ and li by impulse generator. Effect of electrode configuration, shape of voltage and its polarity are analysed in extremely non uniform field. Propagation characteristics as Propagation time and Propagation velocity are also studied. During the course of experimental investigations accurate measurement of magnitude of impulse voltage and propagation time were accomplished with the help of digital oscilloscope.

Contents

| | |
|--|----------|
| 1. Introduction | 1 |
| 2 Generation of Impulse Voltages | |
| 2.1 Standard impulse voltage waveshapes | 4 |
| 2.2 Theory of impulse generator | 6 |
| 2.2.1 Single stage generator circuits | 6 |
| 2.2.2 Multistage impulse generator circuits | 9 |
| 2.2.3 Design and operation of impulse generator | 10 |
| 3 Field Classification and Theory of Breakdown in Extremely non uniform field | |
| 3.1 Field classification | 12 |
| 3.2 Degree of uniformity of electric field | 13 |
| 3.3 Theory of breakdown of air under impulse voltage | 13 |
| 3.3.1 Breakdown in extremely non uniform field | 15 |
| 3.3.2 Effect of polarity in extremely non uniform field | 18 |
| 3.4 Propagation of Breakdown Channel | 19 |
| 4 Experimental Setup | |
| 4.1 Experimental setup | 22 |
| 4.1.1 Impulse generator | 22 |
| 4.1.2 Load unit | 23 |
| 4.1.3 DC generator | 23 |
| 4.2 Oscilloscope | 26 |
| 4.3 Electrode preparation | 26 |
| 4.4 Atmospheric conditions | 27 |
| 5 Investigations | |
| 5.1 Introduction | 28 |
| 5.2 Experimental procedure | 28 |
| 5.2.1 Determination of 50 % breakdown voltage | 29 |
| 5.3 Results with switching impulse | 30 |

| | | |
|----------|--|----|
| 5.3.1 | Results with 190/1900 μs switching impulse | 30 |
| 5.3.2 | Results with 250/2500 μs switching impulse | 33 |
| (a) | U_{b50} characteristics | 33 |
| (b) | Average field intensity characteristic | 38 |
| 5.3.3 | Comparison of two switching impulse | 41 |
| 5.4 | Results with lightning impulse | 43 |
| 5.4.1 | U_{b50} characteristics with $\pm 1.2/50$ μs lightning impulse | 43 |
| 5.4.2 | Average field intensity characteristics | 49 |
| 5.5 | Comparison of switching and lightning impulse | 52 |
| 6 | Investigations of Propagation Time and Propagation Velocity of Leader | |
| 6.1 | Investigations with 250/2500 μs switching impulse | 54 |
| 6.2 | Investigations with 1.2/50 μs lightning impulse | 73 |
| 7 | Conclusion and scope for future work | 76 |
| | References | 79 |

List of figures

| | | |
|-----|--|----|
| 2.1 | A typical lightning impulse | 5 |
| 2.2 | T typical switching impulse | 5 |
| 2.3 | (a) Single stage impulse generator circuit | 7 |
| | (b) Efficient impulse generator circuit | 7 |
| | (c) Laplace transform circuit | 7 |
| 2.4 | Impulse voltage wave and its components | 8 |
| 2.5 | A four stage impulse generator circuit | 10 |
| 3.1 | Field classification and different field configuration | 14 |
| 3.2 | Glow and streamer corona at point and rod electrodes | 17 |
| 3.3 | A typical positive and negative streamer discharge | 19 |
| 3.4 | Time required for the formation of breakdown with impulse voltage | 20 |
| 3.5 | Breakdown voltage time characteristics for impulse voltage | 21 |
| 4.1 | Experimental set up | 22 |
| 4.2 | Photograph of four stage impulse generator | 24 |
| 4.3 | Photograph of Control panel, Plotter and Oscilloscope | 24 |
| 4.4 | Photograph of impulse generator with Needle-Plane Electrodes | 25 |
| 5.1 | Breakdown characteristics of air in extremely non uniform field with si +190/1900 μ s | 32 |
| 5.2 | Breakdown characteristics of air in extremely non uniform field with si -190/1900 μ s | 32 |
| 5.3 | Breakdown characteristics of air in extremely non uniform field with si +250/2500 μ s | 37 |
| 5.4 | Breakdown characteristics of air in extremely non uniform field with si -250/2500 μ s | 37 |
| 5.5 | Breakdown field intensity characteristic for Needle-Plane electrodes with si 250/2500 μ s | 39 |
| 5.6 | Breakdown field intensity characteristic for Rod-Plane electrodes with si 250/2500 μ s | 39 |

| | | |
|------|---|----|
| 5.7 | Breakdown field intensity characteristic for Needle-Needle electrodes with si 250/2500 μ s | 40 |
| 5.8 | Comparison of si1 & si2 for Needle-Plane electrodes in air in extremely non Uniform field | 41 |
| 5.9 | Comparison of si1 & si2 for Rod-Plane electrodes in air in extremely non Uniform field | 42 |
| 5.10 | Comparison of si1 & si2 for Needle-Needle electrodes in air in extremely non Uniform field | 42 |
| 5.11 | Breakdown characteristics of air in extremely non uniform field with li +1.2/50 | 46 |
| 5.12 | Breakdown characteristics of air in extremely non uniform field with li -1.2/50 μ s | 46 |
| 5.13 | Breakdown characteristics for Needle-Plane electrodes of air in extremely non uniform field with li \pm 1.2/50 | 47 |
| 5.14 | Breakdown characteristics for Rod-Plane electrodes of air in extremely non uniform field with li \pm 1.2/50 | 47 |
| 5.15 | Breakdown characteristics for Needle-Needle electrodes of air in extremely non uniform field with li \pm 1.2/50 | 48 |
| 5.16 | Breakdown field intensity characteristic for Needle-Plane electrode with li 1.2/50 μ s | 50 |
| 5.17 | Breakdown field intensity characteristic for Rod-Plane electrode with li 1.2/50 μ s | 50 |
| 5.18 | Breakdown field intensity characteristic for Needle-Needle electrode with li 1.2/50 μ s | 51 |
| 5.19 | Comparison of si2 & li for Needle-Plane electrodes in air in extremely non Uniform field | 52 |
| 5.20 | Comparison of si2 & li for Rod-Plane electrodes in air in extremely non Uniform field | 53 |
| 5.21 | Comparison of si2 & li for Needle-Needle electrodes in air in extremely non Uniform field | 53 |
| 6.1 | Propagation characteristics of air breakdown channel for Needle-Plane electrodes with si \pm 250/2500 μ s | 56 |

| | | |
|-----|--|----|
| 6.2 | Propagation characteristics of air breakdown channel for Rod-Plane electrodes with si $\pm 250/2500 \mu\text{s}$ | 57 |
| 6.3 | Propagation characteristics of air breakdown channel for Needle-Needle electrodes with si $\pm 250/2500 \mu\text{s}$ | 57 |
| 6.4 | Propagation characteristics of air breakdown channel for Needle-Plane electrodes with li $\pm 1.2/50 \mu\text{s}$ | 74 |
| 6.5 | Propagation characteristics of air breakdown channel for Rod-Plane electrodes with li $\pm 1.2/50 \mu\text{s}$ | 74 |
| 6.6 | Propagation characteristics of air breakdown channel for Needle-Needle electrodes with li $\pm 1.2/50 \mu\text{s}$ | 75 |

List of Plots

| | | |
|---------|--|-------|
| P5.1 | Oscillograph showing si 190/1900 μs | 31 |
| P5.2 | Oscillograph showing si +250/2500 μs | 34 |
| P5.3 | Oscillograph showing si -250/2500 μs | 35 |
| P5.4 | Oscillograph showing li 1.2/50 μs | 44 |
| P5.5 | Oscillograph showing li -1.2/50 μs | 45 |
| P6.1-7 | Oscillograph showing U_{b50} 50 % breakdown voltage and propagation time for R-P Electrode with si 250/2500 μs with varying gap distances | 59-64 |
| P6.8-14 | Oscillograph showing U_{b50} 50 % breakdown voltage and propagation time for N-P Electrode with li -1.2/50 μs with varying gap distances | 65-72 |

List of Tables

| | | |
|-----|---|----|
| 4.1 | Specification of impulse generator | 23 |
| 5.1 | Data for breakdown voltage in extremely non uniform field with $si \pm 190/1900 \mu s$ | 30 |
| 5.2 | Data for breakdown voltage in extremely non uniform field with $si \pm 250/2500 \mu s$ | 36 |
| 5.3 | Data for breakdown field intensity in extremely non uniform field for $si \pm 250/2500 \mu s$ | 38 |
| 5.4 | Data for breakdown voltage in extremely non uniform field with $li \pm 1.2/50 \mu s$ | 43 |
| 5.5 | Data for breakdown field intensity in extremely non uniform field with $li \pm 1.2/50 \mu s$ | 49 |
| 6.1 | Propagation data of breakdown channel in air in extremely non uniform field with $si \pm 250/2500 \mu s$ | 55 |
| 6.2 | Propagation data of breakdown channel in air in extremely non uniform field with $li \pm 1.2/50 \mu s$ | 73 |

List of symbols

| | |
|-----------|--|
| U_{b50} | 50 % Breakdown voltage |
| li | 1.2/50 μ s : Lightning impulse |
| si1 | 190/1900 μ s : Switching impulse |
| si2 | 250/2500 μ s : Switching impulse |
| E | Electric field intensity |
| E_{max} | Maximum electric field intensity |
| E_{avg} | Average electric field intensity |
| d | Gap distance between electrodes |
| η | Degree of uniformity, Schwaiger factor |
| N-P | Needle-Plane electrode configuration |
| R-P | Rod-Plane electrode configuration |
| N-N | Needle-Needle electrode configuration |
| PD | Partial discharge |

Chapter 1

INTRODUCTION

Disturbances in electric power transmission and distribution systems are frequently caused by transient over voltages. Transient voltage waves are of magnitude greatly exceeding the peak value of the normal ac operating voltage. The transient voltages can be grouped under two categories viz. lightning and switching overvoltages.

The lightning overvoltages originated by lightning strokes hitting the phase wires of over-head lines or the bus bars of outdoor substations. The amplitudes of these is determined by the impulse current magnitude and the surge impedance of the line. Each stroke is then followed by a travelling wave, whose amplitude is limited by the maximum insulation strength of the over-head line. Travelling waves with steep wave fronts and even stepper wave tails reaching the substations may stress the insulation of power transformers and other high voltage equipment severely.

The amplitudes of switching transients are always related to the operating voltage and their shape is influenced by the impedance of the system as well as the switching conditions. Switching overvoltage waves contain larger energy compared to lightning waves. The rate of rise of these voltages is usually slower, still they are more dangerous to different insulation systems. These types of overvoltages are also affective in the low voltage distribution systems where they are produced either by current limiting switches or transmitted from the high voltage distribution systems and often cause breakdown of electronic equipment .

For the production of these overvoltages in our laboratory impulse voltage generator is used which can produce various types of switching and lightning impulses. In this work insulation breakdown characteristics of atmospheric air are studied in extremely non uniform field. This field configuration is of great technical importance as it is the most common and unfavorable condition of electric field faced by a dielectrics in the power systems. Extremely non uniform field is a sub classification of non-uniform field. Field is

classified according to the configuration of electric field prevalent in the space between the two electrodes. In uniform field, electric field intensity is constant but in non uniform fields it has non linear distribution between two electrodes. Behaviour of air in extremely non uniform fields is greatly influenced by the type of Partial Discharge (PD) which precede the breakdown. Stable glow discharge takes place for small gap distance with point electrodes. Stable streamer discharge take place for medium gap distance with rod or spherical electrodes while stable leader discharge occurs under much longer gap distances.

For producing extremely non uniform field, electrodes with sharp point or small curvature of rod are fabricated in the lab such as Needle-Plane, Needle-Needle and Rod-Plane. Characteristics of breakdown voltage and average field intensity are studied with varying gap distance between different electrode systems with three shapes of voltage impulses. These three type of waveshapes generated by impulse generator are 190/1900 μs , 250/2500 μs (switching impulse) and 1.2/50 μs (lightning impulse). The effect of shape of voltages and its polarity, wave front and wave tail on the breakdown characteristics are analysed. Leader propagation characteristics as propagation time and propagation velocity are also measured with the help of oscilloscope.

Objective of Thesis Work

- The choice of essential insulation level is impractical without the knowledge of its performance against overvoltages occurring in the power systems. The estimate of the danger presented by a given overvoltage and essential value to which it should be limited with the help of protective measures is possible with the knowledge of main electric characteristics of the insulation.
- The breakdown characteristics with either polarity impulse voltages are important for optimum design of insulation system and to know the behaviour of dielectric, the physical process of PD and the propagation of discharge leading to breakdown under different conditions of the dielectrics and the electrode systems.
- For design of the equipment, knowledge of the conditions under which a dielectric behaves weakest are more important. For positive polarity switching surges, the

breakdown of air is poorest. Hence it is important to study the behaviour of air with the different waveshapes of either polarity of impulse voltages.

- Breakdown characteristics studied here are for air as dielectric medium which is the most general insulation in the power system.
- Distinguishing of different type of PD is appreciated with different type of electrode configuration.

Organization of the thesis

- Chapter 2 presents the standard waveshapes and their generation by impulse generator. Single and multistage circuits of the impulse generator with impulse equations are described. Impulse generator design and operation is also considered briefly.
- Chapter 3 deals with the field classification and the theory of breakdown in extremely non uniform field with glow, streamer and leader discharge. Effect of polarity for impulse voltage and time phenomenon for breakdown are discussed.
- Chapter 4 presents the experiment set up and provide details about equipment used with impulse generator with their specification. Electrode configurations used are described with electrode dimension. The atmospheric conditions during experiments and set up photograph are also included.
- Chapter 5 presents the results and characteristics of breakdown voltage (U_{b50}) and average field intensity with varying gap distance between three electrode configurations for three type of impulse waveshapes of either polarity. First results of two switching impulses (si1 & si2) are discussed and compared for three electrode configuration and then with lightning impulse. Characteristics for si2 and li also compared. Chapter also provide detail analysis and comparisons of these characteristics.
- Chapter 6 presents the results of propagation characteristics as propagation time and propagation velocity with varying gap distance for three electrode configurations with switching impulse(si2) and lightning impulse(li).
- Chapter 7 includes the conclusions and scope for future works.

CHAPTER 2

Generation of Impulse Voltages

2.1 Standard Impulse Voltage waveshapes

Although the actual shape of switching impulses vary with operating voltage, impedance of the system and switching conditions, yet it becomes necessary to simulate these transient over voltages by simple means for testing purpose. Various national and international standards defined these impulse. An impulse voltage is defined as a unidirectional voltage which rises rapidly to peak value and then decays relatively slow to zero. The distinction between lightning and switching impulses is made depending upon their rate of rise and decay. Impulse voltages with a front duration varying from less than one and up to a few tens of microseconds are considered as lighting impulses. A typical lighting impulse is shown in Fig. 2.1. Time T_1 is the rise time and T_2 is the tail time required to decay to its 50 % magnitude. It is practice to define impulse voltages by their T_1/T_2 ratio. For a typical lightning impulse value of T_1/T_2 is 1.2/50 μ s. The specification permits a tolerance of upto $\pm 30\%$ for T_1 and $\pm 20\%$ for T_2 . Lightning impulses are of relatively shorter duration. Lightning overvoltages originated with the discharge of lightning into current carrying parts of an equipment or near it into the ground [7].

A typical value of T_1/T_2 for a switching impulse is $(250 \pm 20\%)/(2500 \pm 60\%)$. A switching impulse is shown in Fig. 2.2. Here T_1 is the time interval between the origin and the instant when voltage reaches its maximum value and T_2 is tail time. Switching overvoltages originate in the system itself by the connection and disconnection of circuit breaker contacts or due to initiation or interruption of faults. Another si type is 190/1900 μ s which is also generated by our laboratory impulse generator.

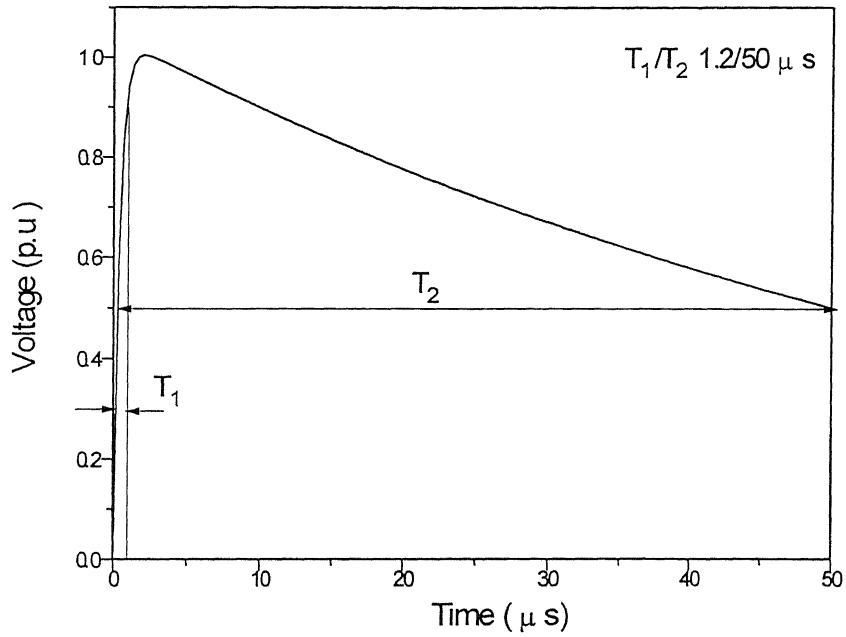


Fig 2.1 A Typical Lightning Impulse

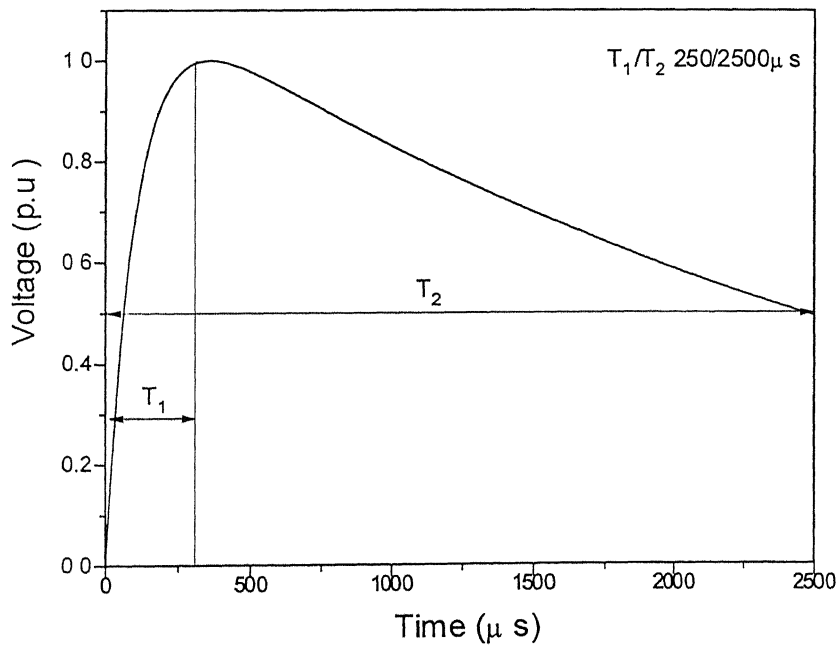


Fig 2.2 A Typical Switching Impulse

2.2 Theory of Impulse Generator

The two types of impulse voltages described in the previous section can be generated with two different charging and discharging circuits with two energy storage elements, as the wave shape is composed of the superposition of two exponential functions.

2.2.1 Single stage generator circuits

Two basic circuits for single stage impulse generators are shown in Fig. 2.3. the capacitor C_1 is charged by a dc source until the spark gap G breaks down. This spark gap acts as a voltage limiting and voltage sensitive switch. Its time for voltage breakdown is very short compared to rise time T_1 .

The resistors R_1 , R_2 and capacitor C_2 form the waveshaping network. R_1 primarily damps the circuit and controls the front time. R_2 will discharge the capacitors and therefore controls the wave tail. The capacitor C_2 represents the full load *i.e.* the loading capacitor and the object under test. The value of C_1 is very large compared to C_2 . C_1 mainly determines the cost of the generator.

The maximum energy stored in the discharge capacitor C_1 is

$$W = \frac{1}{2} C_1 (V_{o\max})^2 \quad (2.1)$$

For the analysis of the circuit in Fig. 2.3 . initially C_1 is charged to V_0 and for $t > 0$, the capacitor is connected to the waveshaping network.

Taking $V(s)$ to be the laplace transform of $V(t)$ and denoting the series connection of $R_1 R_2 C_1 C_2$ and C_1 as Z_1 and the parallel combination of R_1 and C_2 as Z_2 respectively, we obtain

$$V(s) = \frac{V_0}{s} \frac{Z_2}{Z_1 + Z_2} \quad (2.2)$$

$$Z_1 = \frac{1}{C_1 s} + R_1 \quad (2.3)$$

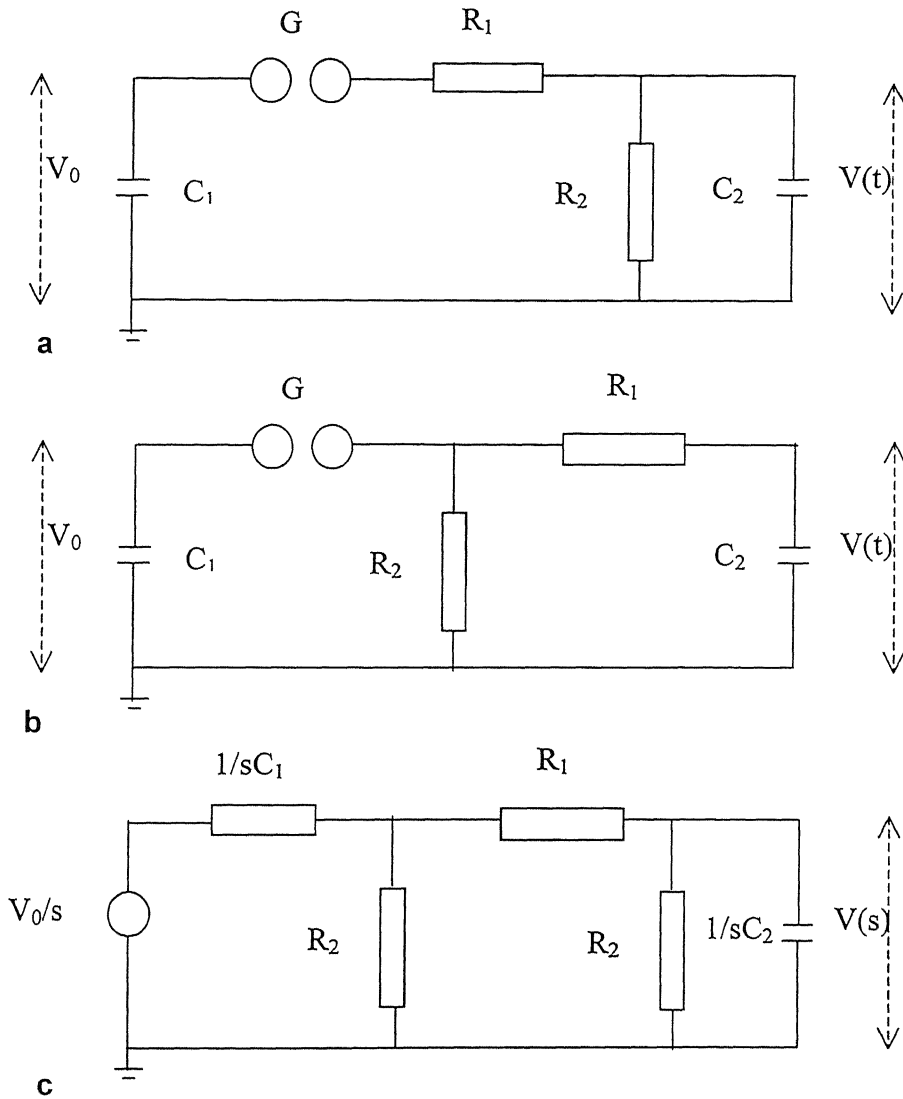


Fig. 2.3. (a) Single stage impulse generator circuit (b) More efficient impulse generator circuit (c) Laplace transform circuit [2]

$$Z_2 = \frac{R_2 / C_2 s}{R_2 + 1 / C_2 s} \quad (2.4)$$

$$V(s) = \frac{V_0}{k} \frac{1}{(s^2 + as + b)} \quad (2.5)$$

By substitution we get

$$a = \frac{1}{R_1 C_1} + \frac{1}{R_1 C_2} + \frac{1}{R_2 C_2} \quad (2.6)$$

$$b = \frac{1}{R_1 C_1 R_2 C_2} \quad (2.7)$$

$$k = R_1 C_2 \quad (2.8)$$

Hence in the time domain

$$V(t) = \frac{V_0}{k(\alpha_2 - \alpha_1)} [\exp(-\alpha_1 t) - \exp(-\alpha_2 t)] \quad (2.9)$$

where α_1 and α_2 are the roots of the equation $s^2 + as + b = 0$

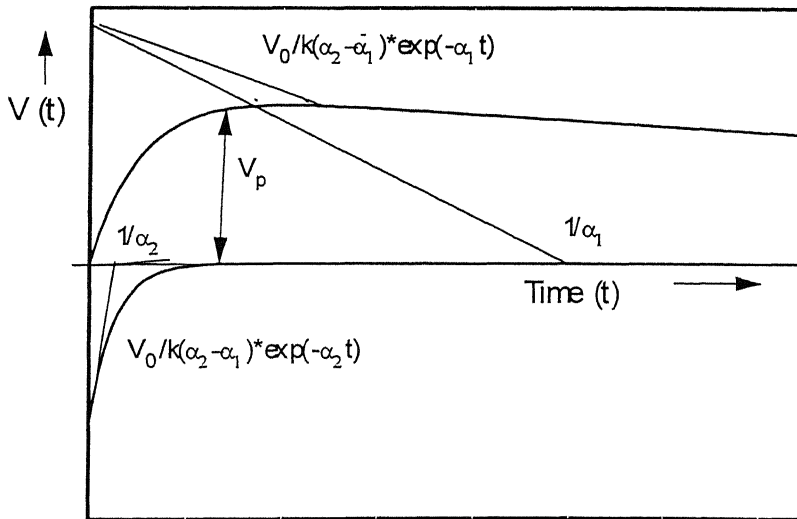


Fig. 2.4. Impulse voltage wave and its components

The voltage $V(t)$ is therefore produced by the superposition of two exponential functions of different signs. The negative root leads to a larger time constant compare to positive root. A graph of $V(t)$ is shown in Fig. 2.4.

The efficiency of the circuit is define as

$$\eta = \frac{V_p}{V_0} \quad (2.10)$$

where V_p is the peak value of the impulse voltage. It is calculated by finding t_{\max} from

$$\frac{d(V(t))}{dt} = 0;$$

$$t_{\max} = \frac{\ln(\alpha_2/\alpha_1)}{(\alpha_2 - \alpha_1)} \quad (2.11)$$

By using equation 2.11 and conditions $C_2 \ll C_1$ and $\alpha_2 \gg \alpha_1$ we get

$$\eta = \frac{C_1}{C_1 + C_2} \quad (2.12)$$

This equation indicates the reasons why the discharge capacitance C_1 should be much larger than the load C_2 .

2.2.2 Multistage Impulse Generator Circuit

Single stage Impulse Generator is inconvenient for producing higher impulse voltages due to problem of spark gap, physical size of circuit elements and difficulties in suppressing corona limit and requirement of high dc charging voltage. To circumvent these difficulties an arrangement where a number of condensers are charged in parallel through high ohmic resistances and then discharged in series through spark gaps. A four stage Impulse Generator is shown in Fig. 2.5.

R = Single stage charging resistor

R_1 = Internal front resistor

R_2 = Discharge resistor

R_1' = External front resistor

C_1 = Single stage charging capacitor

C_2 = Load capacitance

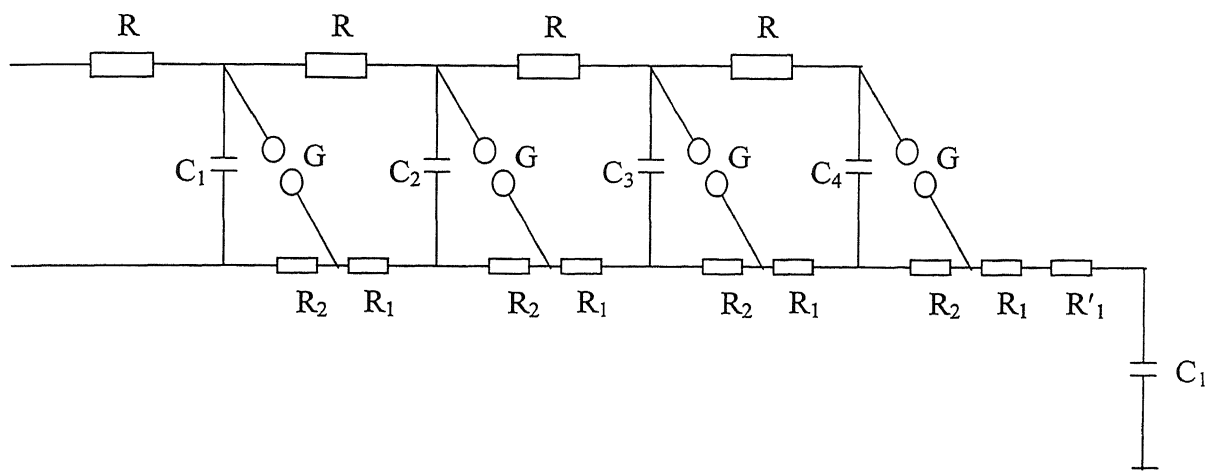


Fig. 2.5. A four stage impulse generator circuit [2]

For consistent operation it is necessary to set the distance of the spark gap G_1 only slightly below that of the second and further gaps for earliest breakdown. The axes of the gaps are set in a same vertical plane, so that the ultraviolet illumination from the spark in the first gap irradiates the other gap. This ensures a supply of electron released from the gap to initiates breakdown during the short period when the gaps are subjected to overvoltages. An arrangement of four stage Impulse Generator is made by combining circuits of Fig. 2.3 a & b so provide both profit of space economy and damping of oscillations. This circuit can be reduced to single stage Impulse Generator circuit shown in Fig. 2.3 (b). Here

$$1/C_{eq} = \sum 1/C_1$$

$$R_{1eq} = R_1' + \sum R_1$$

$$R_{2eq} = n R_2 = \sum R_2$$

Where n is the number of stages [2].

2.2.3 Design and Operation of Impulse Generator

An Impulse Generator requires a dc power supply for charging the capacitor C_1 . The supply consist of a step up transformer and rectifier, non inductive wire wound resistors are used. Resistors are placed as convenience of replace and exchange.

The layout of the Impulse Generator is mainly decided by the type of capacitors used. Generator consists of oil impregnated, paper dielectric capacitors arranged one above the other with center tapping and ohmic resistors connected in parallel. The

coupling sphere gaps are arranged one above the other on horizontal arms and the settings of the gaps is adjusted by a remotely controlled motor in conjunction with an indicator.

The charging voltage is applied to the system. The stage capacitors charge through the charging resistors. When fully charged, either the lowest gap is allowed to breakdown from overvoltage or it is triggered by an external source (if the gap spacing is set greater than the charging voltage breakdown spacing). This effectively puts the bottom two capacitors in series, overvoltageing the next gap up, which then puts the bottom three capacitors in series, which overvoltagees the next gap, and so forth. This process is referred to as "erecting". A common specification is the erected capacitance of the bank, equal to the stage capacitance divided by the number of stages [10].

Impulse Generator is operated in conjunction with CRO for measurement and analysis of waves. As the impulses are of shorter duration, so it is necessary that the operation of generator and the oscillograph should be synchronize accurately. The time sweep circuit of the oscillograph is initiated at time slightly before the impulse wave reaches to the deflecting plates.

Trigatron is a device used for producing initiating electrons for breakdown of the spark gap. The trigatron consists of a three electrode gap. The main electrodes which are high voltage and ground electrode are sphere or semi sphere electrode configurations. A small hole is drilled into the earthed electrode into which a metal rod is projected. The annular gap between the rod and the surrounding sphere is typically about 1 mm. The metal rod or trigger electrode forms the third electrode. It is connected to earthed electrode through a high resistance. A tripping pulse is given between these two electrodes. A glass tube is fitted across the rod and is surrounded by a metal foil connected to the potential of the main electrode. The function of this tube is to promote corona surface discharge around the rod as this causes photoionisation of the pilot gap, if a tripping pulse is applied to the rod. Due to this photoionisation enough primary electron are available in the annular gap which breaks down without appreciable time delay. The glass tube also fill the annular the gap so that rod as well as tube with its face is flush with the outside surface of the sphere. Thus a surface discharge is caused by a tripping pulse. Trigatron requires a pulse of 5 kV of the both polarity [5].

CHAPTER 3

Field Classification and Theory of Breakdown in Extremely Non Uniform Field

3.1 Field Classification

The electric stress between two electrodes mainly depends upon the shape of the electrodes. The electric field is classified depending upon the electrode configuration and the extent of the field distortion. The field is classified into following types :-

- (a) Uniform field
- (b) Non uniform field

In a '**uniform field**', the potential is linearly distributed and the electric field intensity is constant throughout the space between the two electrodes. In '**non uniform field**' distribution of potential is non linear between the electrodes, leading to non uniformity in electric field intensity.

Whenever the field intensity becomes greater than the strength of the air, the air or the medium breaks down at these locations. This local breakdown of the medium is called '**Partial Discharge**' (PD). PD are localized electric discharges within an insulation system, restricted to only a certain part of the dielectric system, *i.e.* PD are discharges which do not bridge the two electrodes. Stable PD in air or any other gaseous dielectric are known as **Corona**. When such PD occur on the boundary surface of some solid and liquid dielectrics with air or any other gaseous medium, these are known as '*surface discharge*' or '*tracking*' which is basically a corona. In uniform field insulation breakdown takes place without any PD preceding the breakdown but in non uniform field, the insulation breakdown takes place after stable PD are set. Hence non uniform fields are sub classified taking into account the aspect of PD. The sub classification is :-

- (1) Weakly non uniform field
- (2) Extremely non uniform field

As in uniform field, PD inception voltage is equal to the breakdown voltage in weakly non uniform field also, hence no stable PD takes place in this configuration.

$$U_b \cong U_i$$

In extremely non uniform fields stable PD takes place before the breakdown, thus,

$$U_b \gg U_i$$

Another factor of classification is Schwaiger factor ,discussed in next section.

3.2 Degree of Uniformity of Electric Field

The degree of uniformity η introduced by Schwaiger in 1922, as a measure of uniformity of electric field is defined as follows :

$$\eta = \frac{E_{\text{mean}}}{E_{\text{max}}} = \frac{U}{d \times E_{\text{max}}}$$

$$U = \eta E_{\text{max}} d$$

where E_{mean} and E_{max} are the peak values of the mean and maximum field intensities respectively. U is the peak value of potential applied between the electrodes at 'd' distance apart. As the difference between the maximum and mean field intensity increases (smaller η), the field characteristic becomes more non uniform [1]. Consequently , a poorer utilization of the insulating properties of the insulation takes place. For a uniform field η equals to unity and it approaches zero for a extremely non uniform field. Typical value of η and various field classification are shown in Fig. 3.1.

3.3 Theory of Breakdown of Air under Impulse Voltage

Breakdown of air is a complicated phenomenon which not only depends upon its atmospheric conditions but also upon field configuration determined by the shape and size of the electrodes and gap distance. Besides breakdown strength also depend upon the type of voltage applied and its polarity. Breakdown strength when measured with

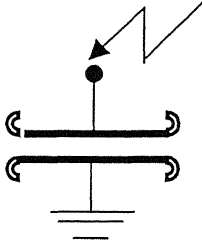
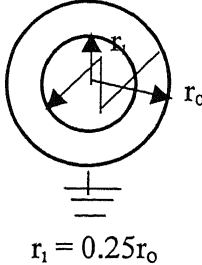
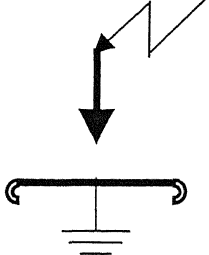
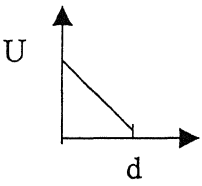
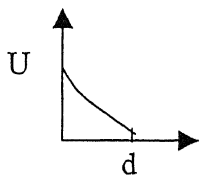
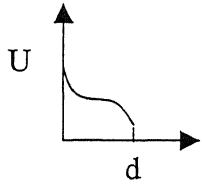
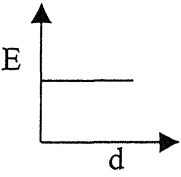
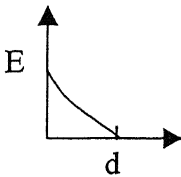
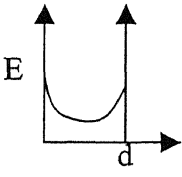
| Field Classification | Uniform | Weakly Non-uniform | Extremely Non-uniform |
|-------------------------|---|--|---|
| Electrode Configuration | Parallel plate  | Concentric spheres  $r_i = 0.25r_o$ | Needle-plane  |
| Potential Distribution |  |  |  |
| Field Intensity |  |  |  |
| U_I vs U_b | $U_I = U_b$ | $U_I = U_b$ | $U_I \ll U_b$ |
| η | $\cong 1$ | $0.2 < \eta < 1$ | $\eta < 0.2$ |

Fig 3.1 Field Classification and different Field Configuration

impulse voltage depends upon the type of voltage and the extent of stable PD which precedes the breakdown. The quasi continuous partial discharge process in air is basically characterized by the three distinguished stages of its development. These essential stages are avalanche, streamer and leader discharges. For a stable PD process to be able to establish a fairly good conductive path between the electrodes, it requires to extend itself sufficiently in the gap. When this is accomplished, the discharge process is rendered '*instable*', leading to '*spark breakdown*' of the dielectric between the two electrodes. Breakdown depends upon the electrode configuration, gap distance, gas pressure, voltage polarity and nature of the gas and accordingly main type of stable PD are :-

1. A stable avalanche or glow discharge, leading to spark over by forming an instable leader towards its advance stage, and finally the arc.
2. An avalanche discharge continued with stable streamer or bunch discharge, followed by a spark breakdown producing an instable leader in the last stage and ultimately an arc.
3. A dense filamentary streamer corona is followed by stembunch discharge. Stable leader channels are then formed accomplishing the spark breakdown with an arc.

In all cases it is '*instable leader*' which ultimately give rise to the required conductivity of the breakdown channel and develop finally into an arc. Among many parameters, the magnitude of the breakdown voltage depends strongly upon the type of stable discharge that precede the spark breakdown. There is significant effect of the type and polarity of the applied voltage on the breakdown strength of a dielectric . In case of impulse voltage not only the polarity but also the time required to reach the crest affects the breakdown voltage. Higher voltage of negative polarity is needed to achieve breakdown compared to positive polarity in extremely non uniform fields [1].

3.3.1 Breakdown in extremely non uniform field

Electrode configurations having extremely non uniform fields are more common in practice than with uniform and weakly non uniform fields because :-

1. to achieve a uniform field considerable efforts are needed.

2. majority of the high voltage equipment electrode systems are installed in open air where the ground and the atmospheric conditions lead to extremely non uniform fields.
3. Presence of undesirable foreign particles in dielectrics and electrode projections also lead to field distortion.

As the field characteristic becomes more non uniform a poorer utilization of the insulating properties of the dielectric takes place. In extremely non uniform fields at voltages much below the breakdown, a stable ionization process in the gas confined locally to the region of extreme field intensity is maintained. The value of η is quite small and the maximum field intensity rises considerably, so at voltage much below the breakdown voltage a stable PD process confined locally in the region of high electric field intensity occur. Breakdown strength of gas depends upon the type of stable corona preceding the complete breakdown of the dielectric. Discharge in this field is described on the basis of the avalanche and streamer and leader processes. The most suitable electrode combinations for this purpose are Needle-Plane, Rod-Plane, Needle-Needle electrode configurations, as they have a highly localized region of extreme field intensity.

GLOW CORONA:

At sharp point electrodes a very steep fall in field intensity occur in the medium so the depth through which the required field intensity for impact ionization (E_I) exists is very small. This restricts the impact ionization to take place at the very close proximity of the tip of the electrode. Such phenomenon extends only a few mm in the gap length and avalanche discharge of below critical amplification (10^8) are able to take place. The optical impression of glow corona is a weak, bluish Glow seen adjacent to the electrode like a feable star in the dark and hissing sound is produced. Average field intensity in the electrode gap acquires comparatively higher values of the order of 15 to 20 kV/cm for both polarity of voltages in this case [1].

STREAMER CORONA:

In case of the electrodes like Rod-Plane, the depth in which field intensity higher than the minimum required for impact ionization (E_I) prevails is much longer .

Although the inception of PD takes place at considerably higher voltage compared to glow corona, but the depth in which the partial discharge activity extends is in cm range depending upon the curvature of the electrode. This facilitates avalanche discharge of above critical amplification to take place, a required condition for streamer discharge.

Streamer corona is like a shower of discharge in number of streamer trajectories spreading in to the gap from surface of the electrode in to the main field region. Streamer trajectories do not intersect each other and branch off like a tree. The streamer corona appears much weaker light intensity and produces flutter noise which can be heard much before the streamer corona is visible. The average potential gradient across streamer channel is reduces to about 5 kV/cm for the positive and 15 kV/cm for negative polarity voltages.

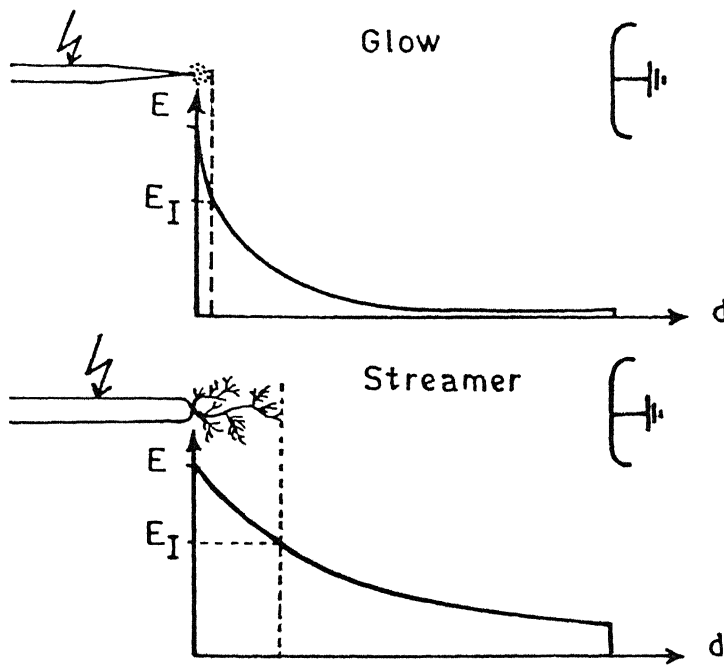


Fig. 3.2. Glow and Streamer corona at point and rod electrodes

LEADER CORONA:

If the electrodes producing streamer corona are placed at longer distance, it enables higher magnitude of voltage which can be applied without complete breakdown of the gap. Thus the streamer trajectories would be able to extend themselves more deep in the gap and develop stronger constricting in to brighter channels less in number. The extended streamer phenomenon thus produced is known as '**Leader**' discharge. The

discharge current trajectories increases such that it leads even thermal ionization in this case only. The leader corona channels are the brightest of all and produce a cracking noise.

The spatial propagation of the leader channel is in a narrow irregular path, often in a direction at an angle to the field. So termed as '*Stepped Leader*'. The leader channels extend themselves due to injection of discharge current in channels by the streamer corona at their tips. As the current density in the leader channels increase, it brings down the potential gradient across them producing a suitable condition for their propagation. The average field intensity reduces further to about 1 kV/cm for positive and 3 kV/cm for negative polarity voltages [1].

Depending upon the electrode shape and gap length the streamer and leader corona both may occur in a gap simultaneously at different extends before the breakdown. As the polarity affects the breakdown voltage in extremely non uniform field strongly ,it is considered in next section.

3.3.2 Effect of polarity in extremely non uniform field

Effect of polarity is easily appreciable in extremely non uniform field with Rod or Needle-Plane electrodes. For positive polarity the discharge originates in intense ionisation of air molecules at the anode electrode. Due to space charge, avalanche grows successively into the space. The positive charge carriers, being heavier particles, do not move themselves much. The process is comparable to the movement of a wave. Numerous avalanches begin together as shown in fig. 3.3 and the whole process is a continuous development of a large number of streamer trajectories which grow exponentially with increasing gap length and bridges the gap on satisfying the critical amplification development of streamer discharge at each point.

In case of negative polarity, the development of a streamer discharge begins like in positive polarity with avalanche which acquire critical amplification. The direction of the avalanche is opposite, *i.e.* their heads are directed towards anode. The high basic field in this case due to space charge enables the impact and the photo ionization to continue further and scattering of negative space charge takes place by radial diffusion, because of the high mobility of electrons. The field intensity which is affected by the

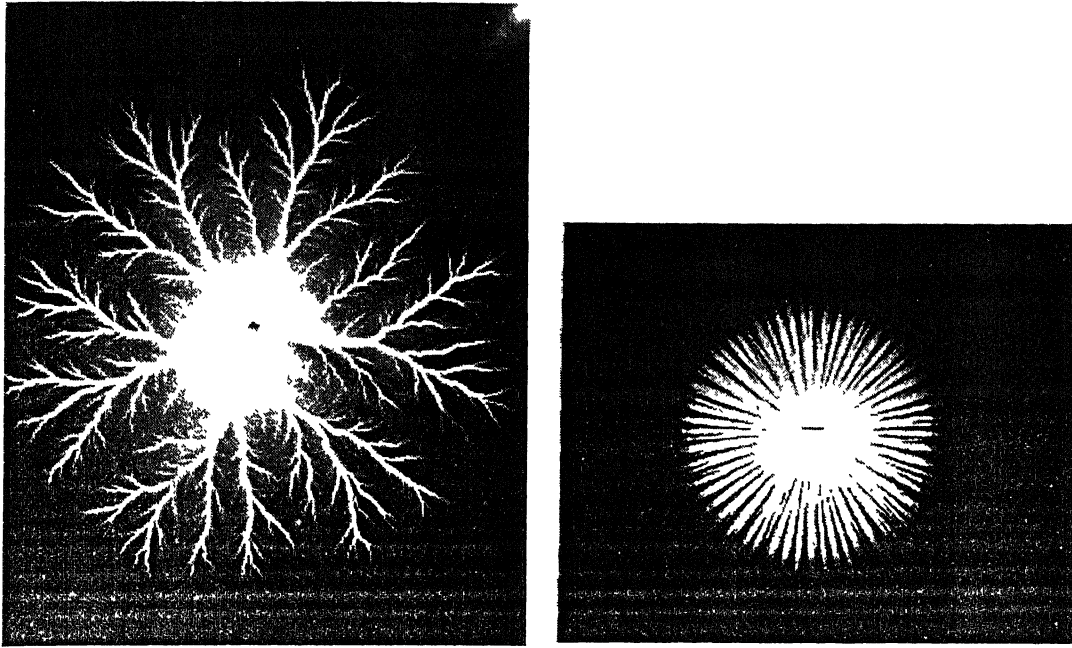


Fig. 3.3. A typical positive and negative streamer discharge [9]

concentration of the space charge, increases near the electrode but reduces away from it. Due to this space charge effect on the field, the negative discharge does not grow in the gap to that extent compared to positive discharge at the same potential as shown in Fig 3.3 known as **Lichtenberg figures**. The radial diffusion of electrons is also responsible for a comparatively lesser number of distinct trajectories of streamer discharge. Therefore breakdown strength with negative polarity is considerably higher than with positive polarity.

3.4 Propagation of Breakdown Channel

With switching and lightning impulses, it is possible that breakdown may not occur even when the peak voltage magnitude exceeds the lowest breakdown voltage, unless the presence of sufficient number of initiatory electrons is ensured. The delay in beginning of the discharge process is called '**Statistical time lag**' t_s . The statistical time lag depends upon the area of electrode, the gap distance and magnitude of radiation producing primary electrons.

Once the discharge process begins, it requires a certain finite time called '**Propagation time**' to reach the opposite side electrode. The total propagation time (t_p)

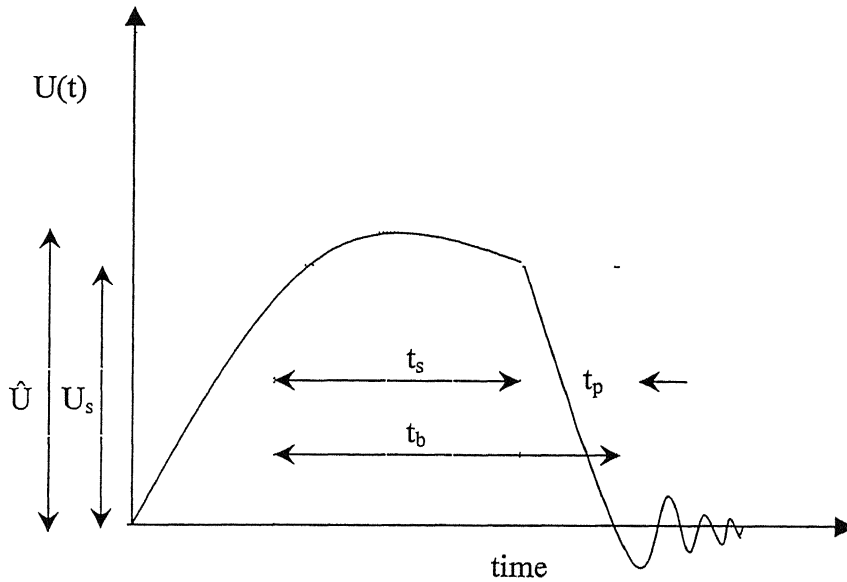


Fig. 3.4. Time required for the formation of breakdown with impulse voltage

in a gap depends upon the individual type of PD and their extent in the gap just before the breakdown. The extents of the PD depend upon the field distribution and the magnitude of applied voltage. For streamer discharge the propagation velocity is about $100 \text{ cm}/\mu\text{s}$ and for leader discharge it is around $10 \text{ cm}/\mu\text{s}$. Since breakdown in very long gap is achieved when a stable leader bridges the gap, the transient time required for propagation is mainly by the leader propagation velocity in case of impulse voltages.

Total time required for formation of breakdown t_b is

$$t_b = t_s + t_p$$

t_s = Statistical time lag

t_p = Propagation time

U_s = Lowest breakdown voltage

\hat{U} = Peak magnitude applied

When an impulse voltage of peak value greater than U_s is applied to a gap, a certain probability, but no certainty exists that a spark breakdown will take place. The occurrence of breakdown is conditional. The duration of applied voltage magnitude above U_s must prevail longer than the minimum time required for the formation of breakdown. The probability of breakdown for a given impulse voltage is estimated experimentally. A large number of identical impulses are applied on a gap and the ratio

of number of pulses accomplishing breakdown to the total number of pulses applied gives the probability of breakdown. $U_{b\ 100}$ represents the 100% breakdown. $U_{b\ 50}$ is the 50% breakdown voltage, *i.e.* only half the number of applied impulses of this magnitude accomplish breakdown.

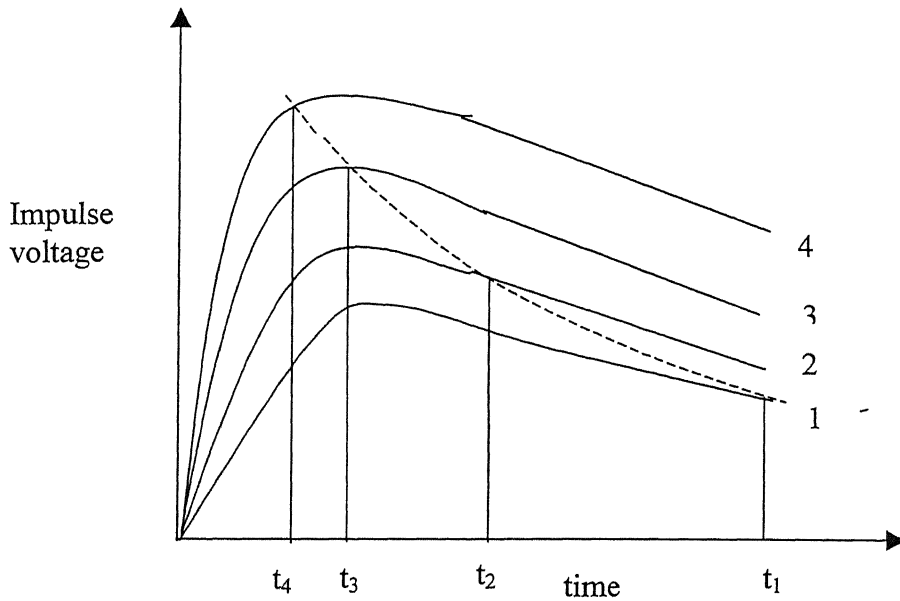


Fig. 3.5. Breakdown voltage time characteristics for impulse voltage

Let impulse voltage of the same wave shape but different peak value is applied across a gap. For the impulse voltage 1 (as shown in Fig 3.5), the breakdown occurs at the time t_1 . As the voltage magnitude is increased, it is observed that the instant of breakdown shifts towards left and breakdown occurs in a lesser time at t_2 . If the voltage is increased further as in impulse 3 the breakdown occurs at even smaller time t_3 at the peak of the impulse voltage. If voltage higher than impulse 3 is applied then breakdown will occur on the front region of the impulse as in impulse 4. It is a practice to perform experiments with the breakdown taking place in the wave tail region.

CHAPTER 4

Experimental Set-Up

4.1 Experimental Set-Up

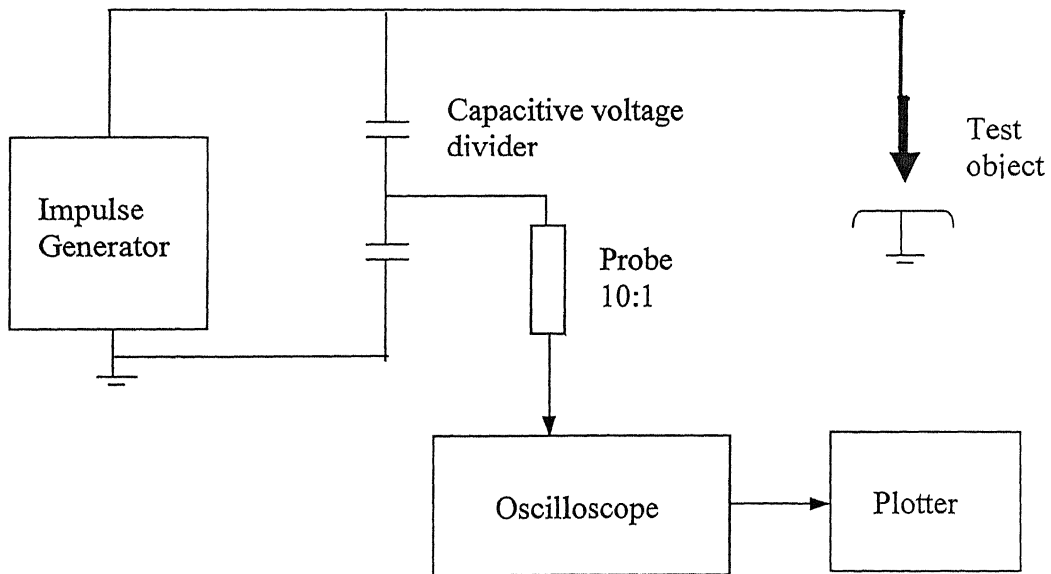


Fig. 4.1. Schematic diagram for experiment set up

4.1.1 Impulse Generator

A four stage 500 kV impulse generator was used for this experimental work. The specifications are given in Table 4.1. The output of the impulse generator was connected to a capacitive voltage divider having ratio of 750:1. The impulse generator could be triggered with the help of a trigatron circuit, which produced pulse of 10 kV at an interval of 5-30 seconds. The duration between successive impulses could be set automatically or they

could be provided manually also. Impulse generator front and side view with capacitive voltage divider are shown in photographs in fig. 4.2 and 4.4 respectively.

Table 4.1 : Specification of impulse generator

| Specification | Value |
|-----------------------------|------------------------------------|
| Max. charging voltage | 500 kV |
| Max. no load output voltage | 450 kV |
| Rated energy | 4.4 kJ |
| Number of stages | 4 |
| Input voltage | 440 V, 3 ϕ |
| Capacitor per stage | 140 nF, 125 kV |
| Wave shape of li | 1.2/50 μ s |
| Wave shapes of si | 190/1900 μ s; 250/2500 μ s |
| Make | TUR, Germany |

4.1.2 Load Unit

The load unit consist of oil impregnated, paper dielectric capacitors arranged one above the other with center tapping and ohmic resistors connected thereto in parallel. Load unit also work as capacitive voltage divider of ratio 750:1. The rating of capacitor is 1.5nF, 600 kV.

4.1.3 DC Generator

In a sheet steel tank displaceable on rollers and filled with transformer oil, DC generator is used to produced a high dc voltage to earth which serves as charging voltage for the generator . HT transformer, HT capacitor, HT rectifier and HT measuring resistor are fixed

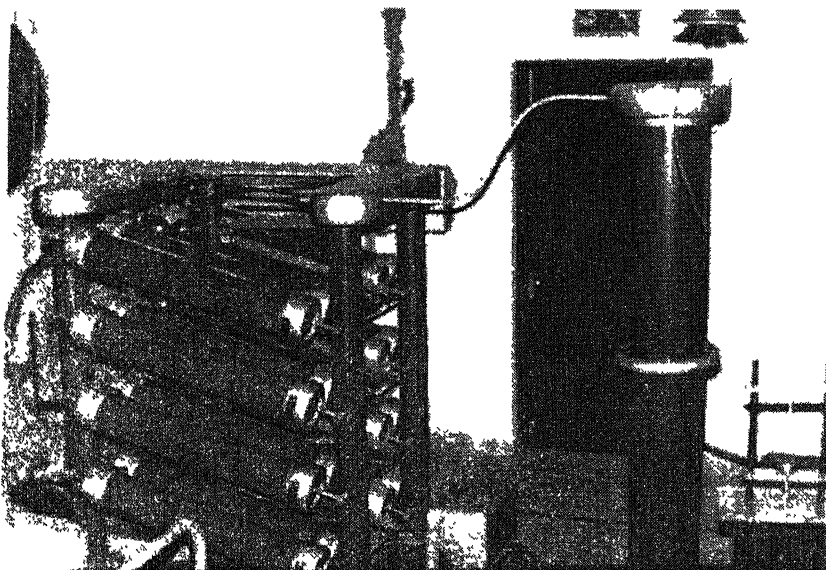


Fig 4.2 Photograph of four stage Impulse Generator

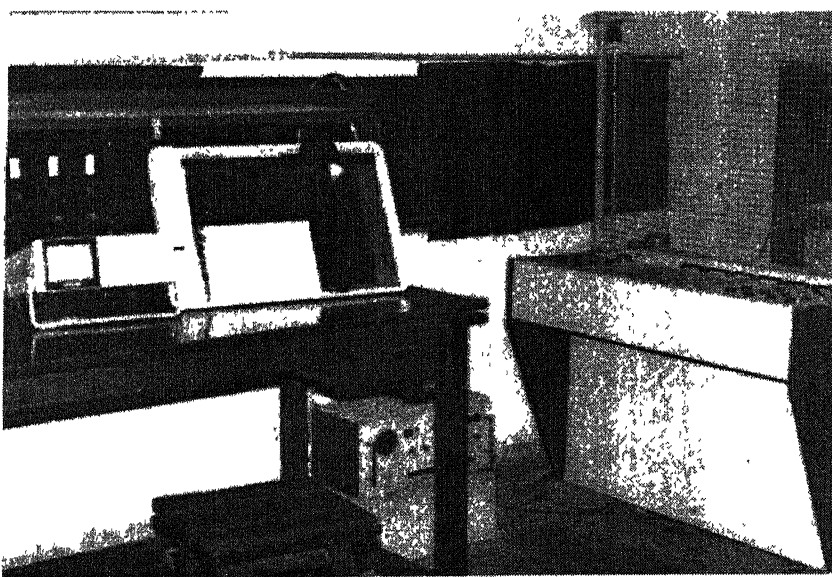


Fig 4.3 Photograph of Control Panel, Plotter and Oscilloscope

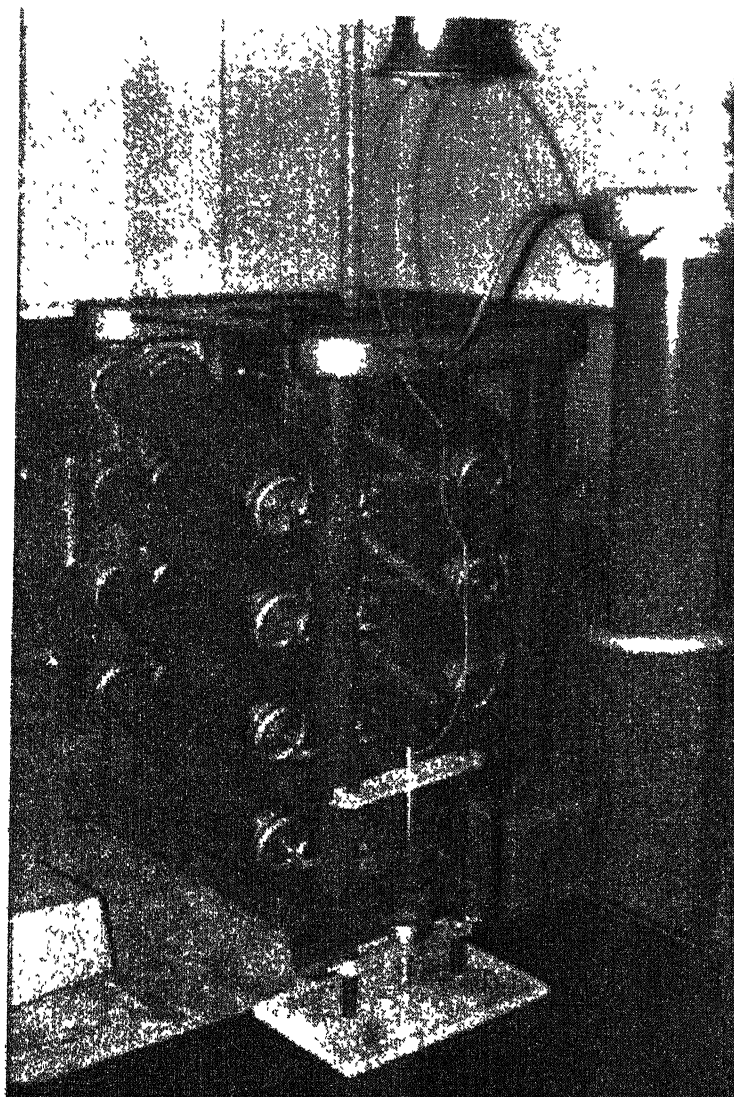


Fig 4.4 Photograph of impulse Generator with Needle-Plane Electrodes

connected to the cover. Other components of impulse generator are discharge switch, control cubicle, control panel.

4.2 Oscilloscope

A digital storage oscilloscope of KIKUSUI (COR 5502U) 100 MHz is used to measure the magnitude of impulse voltage and propagation time. Output from the capacitive voltage divider is fed to oscilloscope through a probe of ratio 10:1. Therefore the total reduction factor between the actual applied voltage to test object voltage to oscilloscope is 7500:1. Thus voltage reading of oscilloscope multiplied by a factor of 7.5 directly gave the value in kV. A digital plotter is connected to oscilloscope to obtain the wave shape plot through RS 232 serial interface. Control Panel, Oscilloscope and Plotter are shown by photograph in fig. 4.3.

4.3 Electrode Preparation

The shape and size of the electrodes fabricated for the experiments are as follows :-

- (a) Needle 1 Total length=18 cm, Taper length=9.5 cm, Taper angle=6°, Diameter=0.12cm
- (b) Needle 2 Total length=10 cm, Taper length=4 cm, Taper angle=6°, Diameter=0.12 cm
- (c) Rod Total length=10.5 cm, Diameter=0.08 cm
- (d) Plane Diameter=7.7 cm, Height=2.1 cm

Electrode configurations used to create extremely non uniform field are as follows

- 1 Needle1-Plane
- 2 Rod-Plane
- 3 Needle1-Needle2

To hold the electrodes a stand of Perspex ebonite is used which also have arrangement to change the gap between the electrodes. .Before starting the experiments, the electrodes were first cleaned with Acetone and then dried with a soft cloth. The electrode arrangements were protected from dust.

4.4 Atmospheric conditions

Atmospheric conditions during experiments are :-

Temperature range : 20-30 °C

Pressure range : 760-770 mm Hg

Humidity : 60-70 %

Chapter 5

Investigations

5.1 Introduction

Experiments in this work were performed to study insulation breakdown of atmospheric air in extremely non uniform field with switching (si) and lightning (li) impulse waveshapes. Waveshapes generated by impulse generator in our lab are switching impulse of 190/1900 μ s & 250/2500 μ s and lightning impulse of 1.2/50 μ s of either polarity. These waveshapes can be obtained by changing the values of internal front resistor R_1 and discharge resistor R_2 in each stage of four stage impulse generator.

Experiment electrode set up is connected to output of impulse generator. Measurement of output voltage of impulse generator is accomplished by CRO connected through capacitive voltage divider. Impulse generator and electrode setup are locked behind the safety fence. Safety door is locked and whole set up is controlled through control panel and control cubicle from outside. Control panel contains various meters for reading of voltage(input & output), current and spark gap distance. It have also mechanism for controlling voltage magnitudes & its polarity and spark gap distance. Triggering pulse can be applied externally from control panel or it can also be set automatically for an known regular interval from control cubicle. Control cubicle is also having option for counting number of pulses with help of counter, generated repetitively for triggering .

5.2 Experimental Procedure

First desire electrode configuration (Needle-Plane , Rod-Plane or Needle-Needle) is set with a particular impulse voltage. Impulse generator must be set ON for around half an hour in order to heating of trigatron circuits. Then desire polarity of voltage is chosen and safety door is closed. After closing the main service contactor, discharge rod is

automatically lifted. Now the voltage level is raised gradually not exceeding the limit 1 kV/sec. from the control panel.

Gap distance between stage spark gap is set according to electrode configuration and polarity of impulse voltage. Stage spark gap configuration of sphere-sphere has breakdown strength around 20 kV/cm. For test object of Needle or Rod - Plane, the breakdown strength of the gap is around 5 kV/cm and 12 kV/cm for positive and negative switching impulse. With lightning impulse it is 7 kV/cm and 15 kV/cm for positive and negative polarity.

For Needle-Plane electrodes having gap distance of 10 cm with negative lightning impulse, estimation of stage gap distance is as follows:- the approximate breakdown voltage for this case is expected to be 150kV and voltage to be generated per stage of impulse generator will be $150/4 = 37.5$ kV. Hence stage spark gap distance should be set at $37.5/20 = 1.875$ cm. It is preferable to set stage spark gap distance to some what lower value of 18 mm and voltage level is increased slowly until first breakdown takes place.

5.2.1 Determination of 50 % breakdown voltage (U_{b50})

After first breakdown takes place , the magnitude of the impulse voltage is kept constant and the pulses are applied at regular interval of 30 seconds. Total 20 shots of a particular voltage level are applied and the number of shots at which breakdown occurred is counted . The percentage breakdown voltage for a particular gap is obtained by dividing the number of shots at which breakdown occurred with the total number of shot applied. Then the voltage is increased slightly and the above procedure is repeated till 50 % breakdown voltage (U_{b50}) is obtained i.e. breakdown take place for 10 pulses out of total 20 pulses.

In this experimental work three electrode configurations (N-P, R-P & N-N) were used. For each configuration gap distance between electrodes was varied from 3 to 15 cm and U_{b50} was measured at each gap distance set for all three shapes (si1, si2 & li) of voltages of either polarity. Important precaution while setting the voltage level is that the breakdown should take place among all the four stage of the impulse generator and applied voltage is not greater than U_{b100} .

5.3 Results with Switching Impulse

5.3.1 Results with $\pm 190/1900 \mu\text{s}$ switching impulse

The switching impulse of $190/1900 \mu\text{s}$ is obtained by using front resistor $R_1 = 20.4 \text{ k}\Omega$ and discharge resistance $R_2 = 27.2 \text{ k}\Omega$, single stage charging capacitance is 140 nF . The load capacitance used is 1.5 nF , 600 kV . Experimental set up is as shown in Fig 4.1. Oscillograph plot of $si1$ is showing in P5.1 taken from plotter interfaced with CRO.

Voltage level is raised gradually not exceeding the limit 1 kV/sec . U_{b50} is measured as described in experimental procedure for all three electrode configurations with either polarity of voltage varying gap distance 3 to 15 cm between the electrodes. For each final reading at least 10 pulses are applied at an interval of 30 seconds.

Table 5.1 Data for breakdown voltage in extremely non uniform field with $si \pm 190/1900 \mu\text{s}$

| Gap distance (cm) | Breakdown voltage in kV for $si + 190/1900 \mu\text{s}$ | | | Breakdown voltage in kV for $si - 190/1900 \mu\text{s}$ | | |
|----------------------|--|--------------------|----------------|--|--------------------|----------------|
| | Needle - Plane | Needle - Needle | Rod - Plane | Needle - Plane | Needle - Needle | Rod - Plane |
| 0 | 0 | 0 | 0 | 0 | 0 | 0 |
| 3 | - | 33.90 | - | 62.55 | 35.10 | 51.00 |
| 4 | 33.00 | 35.40 | 35.55 | 92.55 | 42.00 | 85.95 |
| 5 | 36.75 | 40.05 | 39.60 | 117.38 | 53.55 | 114.38 |
| 6 | 42.75 | 45.90 | 45.00 | 130.50 | 56.70 | 124.13 |
| 7 | 46.20 | 51.90 | 50.55 | 144.38 | 62.85 | 139.13 |
| 8 | 49.95 | 56.40 | 54.55 | 146.63 | 70.35 | 143.25 |
| 9 | 57.15 | 60.75 | 60.30 | 150.00 | 75.30 | 144.75 |
| 10 | 60.75 | 65.40 | 66.75 | 156.00 | 83.40 | 151.50 |
| 11 | 67.13 | 71.25 | 71.25 | 159.00 | 85.88 | 159.00 |
| 12 | 72.75 | 78.15 | 77.10 | 165.00 | 90.75 | 160.50 |
| 13 | 78.30 | 82.50 | 82.35 | 171.00 | 99.75 | 166.50 |
| 14 | 82.35 | 88.05 | 86.55 | 177.00 | 108.38 | 174.00 |
| 15 | 88.95 | 97.13 | 92.70 | 183.00 | 117.00 | 179.25 |

KIKUSUI COR 5502U

NORM TP1

MEM1 2V 0.2ms

SI 190/1900 μ S

NEEDLE PLANE

MEM1

C1 2V A 0.2ms

CH1

P 5.1 Oscillograph showing si 190/1900 μ s

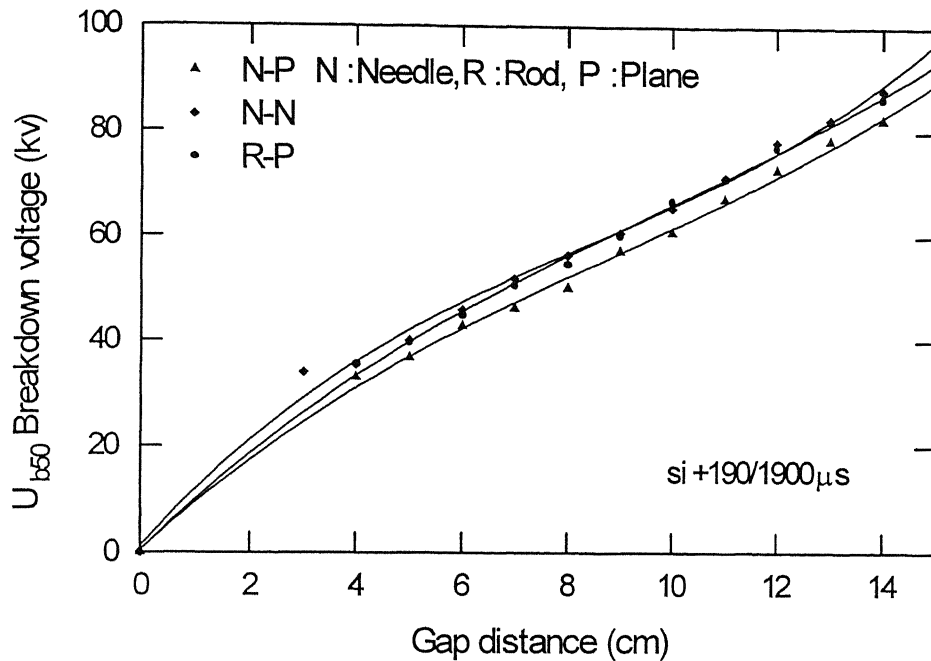


Fig 5.1 Breakdown characteristics of air in extremely non uniform field with $si +190/1900 \mu s$

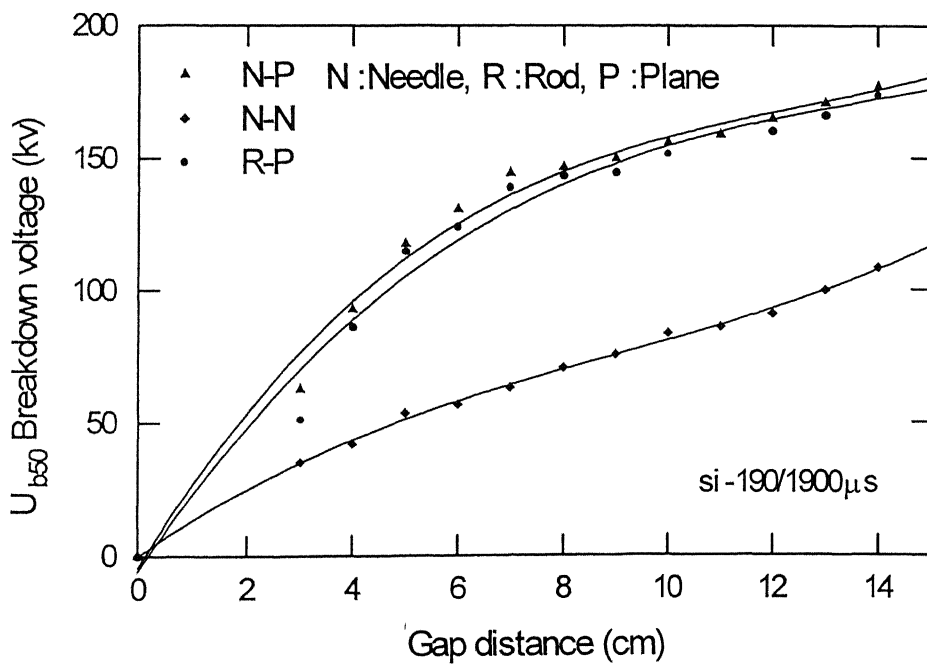


Fig 5.2 Breakdown characteristics of air in extremely non uniform field with $si -190/1900 \mu s$

Breakdown voltage(U_{b50}) vs gap distance characteristics for all three configurations with positive and negative polarity switching impulse are shown in fig 5.1.and 5.2 respectively. From these figures it can be observed that effect of polarity of the voltage is conspicuous in case of Needle-Plane and Rod-Plane electrodes. The breakdown strength with negative polarity voltage is measured to be almost 3 times for smaller gap distances and about 2 times for longer gap distances compared to positive polarity voltage. However, polarity effect is marginal in case of identical Needle-Needle electrode system. It can be concluded that for identical electrode system effect of polarity is not there. This is because identical electrode system is a mirror image with respect to each other. When positive polarity voltage is applied, the negative polarity is induced on the ground electrode and vice versa, resulting into identical conditions in the two cases.

With positive polarity si there is no significant difference in breakdown voltage characteristics for all the three electrode configurations. It can be concluded that breakdown strength in this range of gap distance is independent of the electrode configurations for positive polarity voltage. In case of Needle-Plane and Rod-Plane electrodes remarkable increase in breakdown strength of air with negative polarity of voltage is explained by the theory of development of negative polarity streamer. Because of the space charge effects, negative polarity streamer do not extend in the gap so much as the positive polarity streamer (Lichtenberg figure) [9], resulting into higher breakdown voltage.

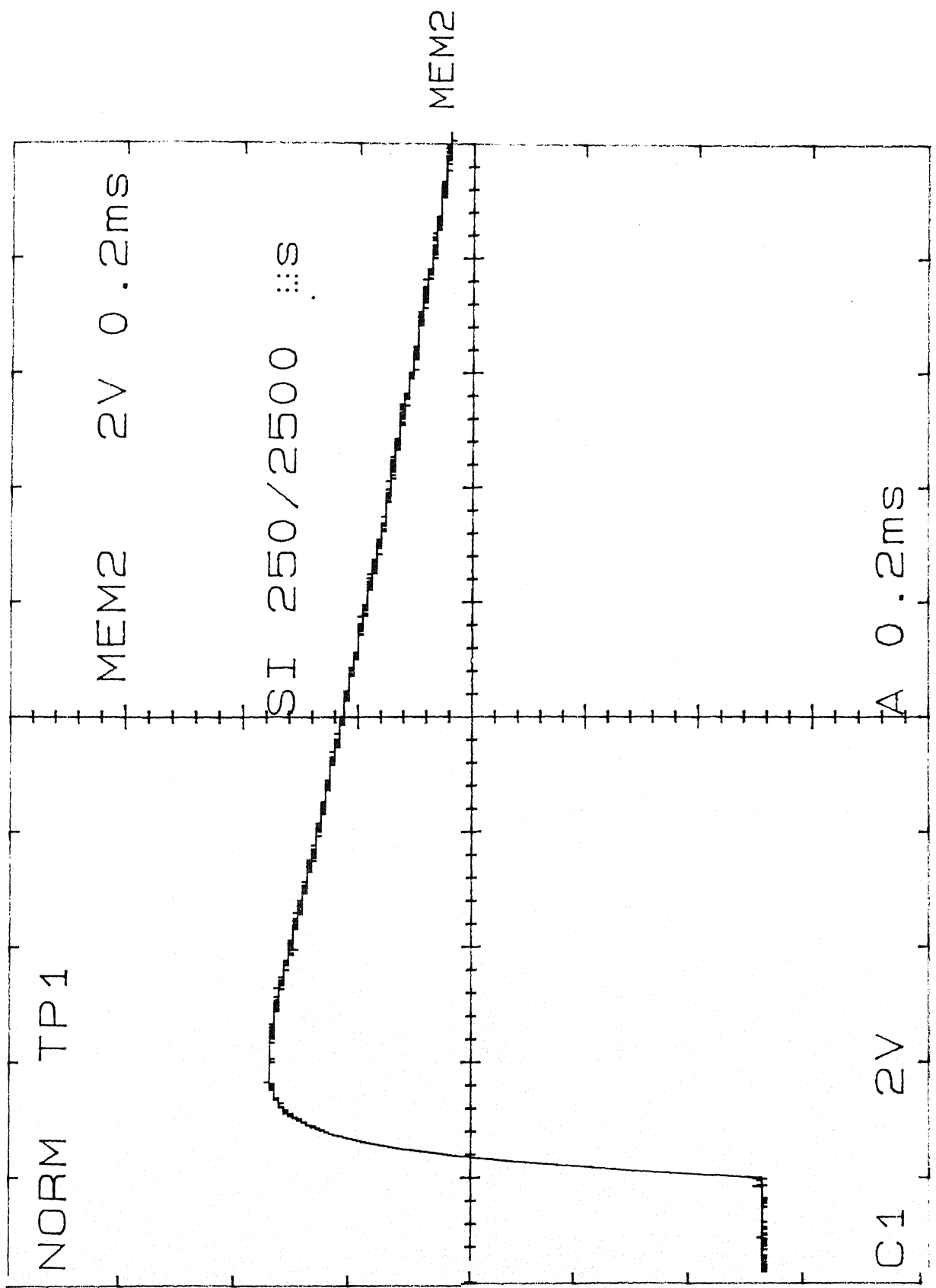
5.3.2 Results with $\pm 250/2500 \mu s$ switching impulse

(a) U_{b50} characteristics

The switching impulse of $250/2500 \mu s$ is obtained by using front resistor $R_1 = 20.4 \text{ k}\Omega$ and discharge resistance $R_2 = 54.4 \text{ k}\Omega$, single stage charging capacitance is 140 nF . The load capacitance used is 1.5 nF , 600 kV . Experimental set up is as shown in Fig 4.1. Oscillograph plot of si2 is showing in P5.2-3 taken from plotter interfaced with CRO.

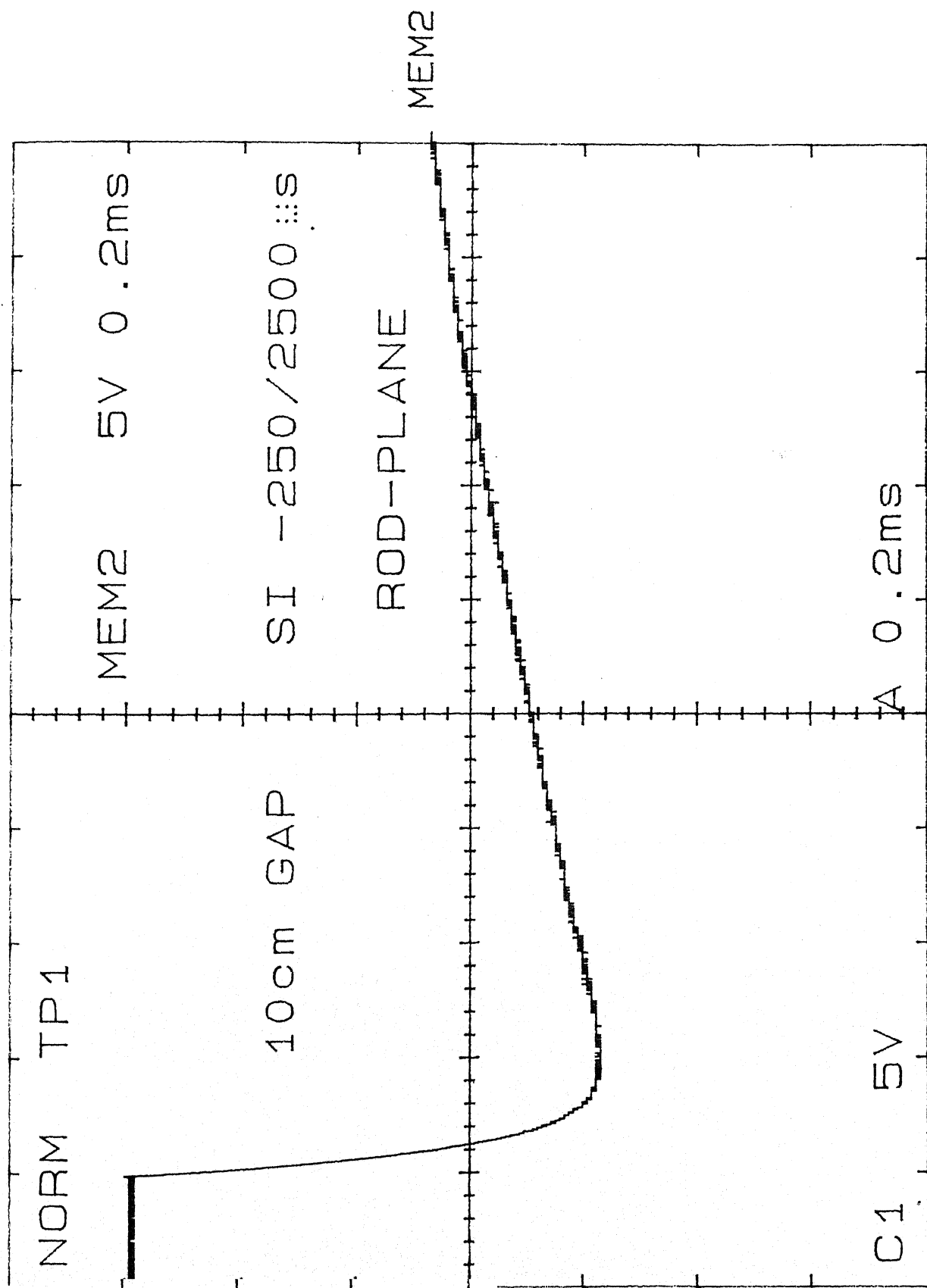
Voltage level is raised gradually not exceeding the limit 1 kV/sec . U_{b50} is measured as described in experimental procedure for all three electrode configuration with both polarities of voltage varying gap distance 3 to 15 cm between the electrodes. For each final reading at least 10 pulses are applied at an interval of 30 seconds.

CH1



P 5.2 Oscilloscope showing si 250/2500 μ s

CH1



P 5.3 Oscilloscope showing si -250/2500 μs

Table 5.2 Data for breakdown voltage in extremely non uniform field with $si \pm 250/2500 \mu s$

| Gap distance (cm) | Breakdown voltage in kV for $si + 250/2500 \mu s$ | | | Breakdown voltage in kV for $si - 250/2500 \mu s$ | | |
|-------------------|---|-----------------|-------------|---|-----------------|-------------|
| | Needle - Plane | Needle - Needle | Rod - Plane | Needle - Plane | Needle - Needle | Rod - Plane |
| 3 | 31.05 | 33.15 | 38.70 | 67.05 | 36.00 | 46.50 |
| 4 | 32.25 | 34.20 | 41.10 | 92.10 | 46.50 | 66.00 |
| 5 | 36.45 | 42.45 | 47.10 | 114.75 | 51.60 | 108.38 |
| 6 | 44.85 | 47.85 | 50.25 | 127.50 | 54.15 | 120.00 |
| 7 | 47.70 | 55.50 | 56.55 | 139.50 | 60.45 | 136.13 |
| 8 | 54.30 | 57.75 | 61.65 | 144.38 | 68.55 | 141.38 |
| 9 | 61.50 | 64.20 | 67.35 | 150.75 | 76.05 | 145.88 |
| 10 | 63.15 | 67.20 | 71.25 | 156.75 | 84.30 | 151.50 |
| 11 | 65.85 | 70.50 | 78.75 | 160.13 | 89.25 | 157.13 |
| 12 | 71.25 | 77.25 | 83.85 | 163.88 | 96.00 | 160.13 |
| 13 | 76.65 | 84.00 | 85.88 | 171.00 | 105.00 | 166.88 |
| 14 | 82.05 | 89.25 | 90.75 | 174.38 | 108.75 | 172.88 |
| 15 | 87.00 | 94.88 | 98.25 | 180.00 | 118.50 | 181.13 |

Breakdown voltage(U_{b50}) vs gap distance for all three configuration with positive and negative polarity switching impulse(si_2) is shown in fig 5.3.and 5.4 respectively. From fig 5.3 and 5.4 , it can be observed that characteristics obtain in this case with si_2 does not much differ to si_1 . Distinguish characteristic of Needle-Needle can be explained by same reasoning as in si_1 . Effect of polarity is same as before for three electrode configuration

Here positive polarity characteristics showing clearly different curve for three electrode configuration. Breakdown voltage for particular gap distance is in increasing order of Needle-Plane (N-P), Needle-Needle (N-N) and Rod-Plane (R-P).but for negative polarity characteristic this order is N-N, R-P and N-P.

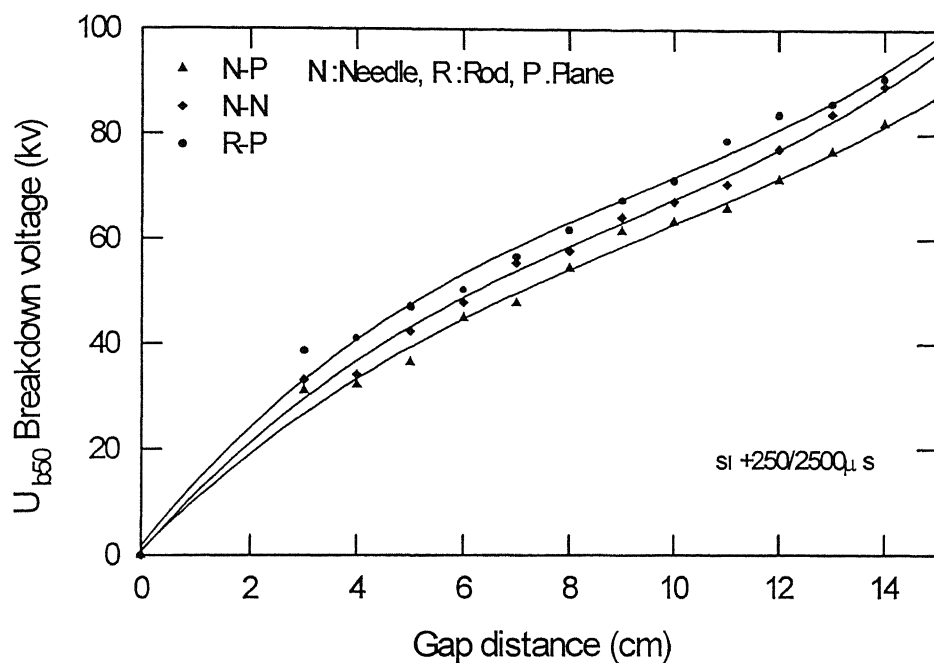


Fig 5.3 Breakdown characteristics of air in extremely non uniform field with si +250/2500 μ s

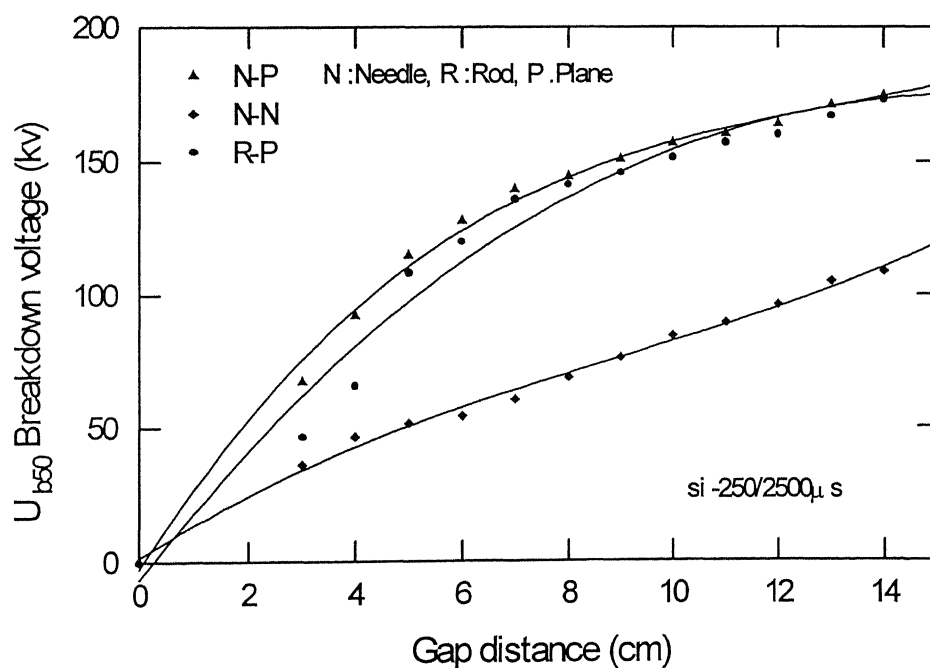


Fig 5.4 Breakdown characteristics of air in extremely non uniform field with si -250/2500 μ s

5.3.2 (b) Average field intensity characteristics

Average field intensity is determined by the ratio of breakdown voltage(U_{b50}) to corresponding gap distance. Significance of average field intensity is in assessment of uniformity of field and type of corona preceding the breakdown.

If the breakdown takes place following the stable glow corona, the average potential gradient which may be required in the gap for the breakdown to take place is 15 to 20 kV/cm for the positive and negative polarity voltages respectively. The requirement of average potential gradient reduces to about 5 for the positive and 15 for the negative polarity voltages if the breakdown is preceded with stable streamer corona [1].

Table 5.3. Data for breakdown field intensity in extremely non uniform field for si \pm 250/2500 μ s

| Gap distance (cm) | Breakdown field intensity in kV/cm for si + 250/2500 μ s | | | Breakdown field intensity in kV/cm for si - 250/2500 μ s | | |
|-----------------------|---|----------------|--------------------|---|----------------|--------------------|
| | Needle - Plane | Rod - Plane | Needle - Needle | Needle - Plane | Rod - Plane | Needle - Needle |
| 3 | 10.35 | 12.90 | 11.05 | 22 35 | 15.50 | 12.00 |
| 4 | 8.06 | 10.28 | 8.55 | 23.03 | 16.50 | 11.63 |
| 5 | 7.29 | 9.42 | 8.49 | 22.95 | 21.68 | 10.32 |
| 6 | 7.48 | 8.38 | 7.98 | 21.25 | 20.00 | 9.02 |
| 7 | 6.81 | 8.08 | 7.93 | 19.93 | 19.45 | 8.64 |
| 8 | 6.79 | 7.71 | 7.22 | 18 05 | 17.68 | 8.57 |
| 9 | 6.83 | 7.48 | 7.13 | 16.75 | 16.21 | 8.45 |
| 10 | 6.32 | 7.13 | 6.72 | 15.68 | 15.15 | 8.43 |
| 11 | 5 99 | 7.16 | 6.41 | 14 56 | 14.29 | 8.11 |
| 12 | 5.94 | 6.99 | 6.44 | 13.66 | 13.34 | 8.00 |
| 13 | 5.90 | 6.61 | 6.46 | 13 15 | 12.84 | 8.08 |
| 14 | 5.86 | 6.48 | 6.38 | 12.46 | 12.35 | 7 77 |
| 15 | 5.80 | 6.55 | 6.33 | 12.00 | 12.08 | 7.90 |

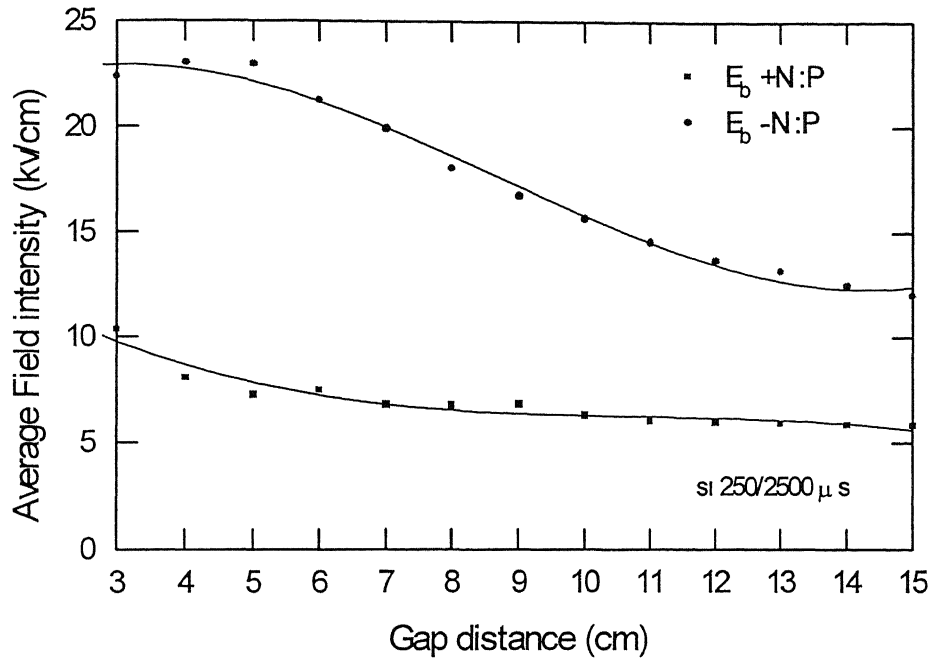


Fig 5.5 Breakdown field intensity characteristic for Needle-Plane electrodes with si 250/2500 μ s

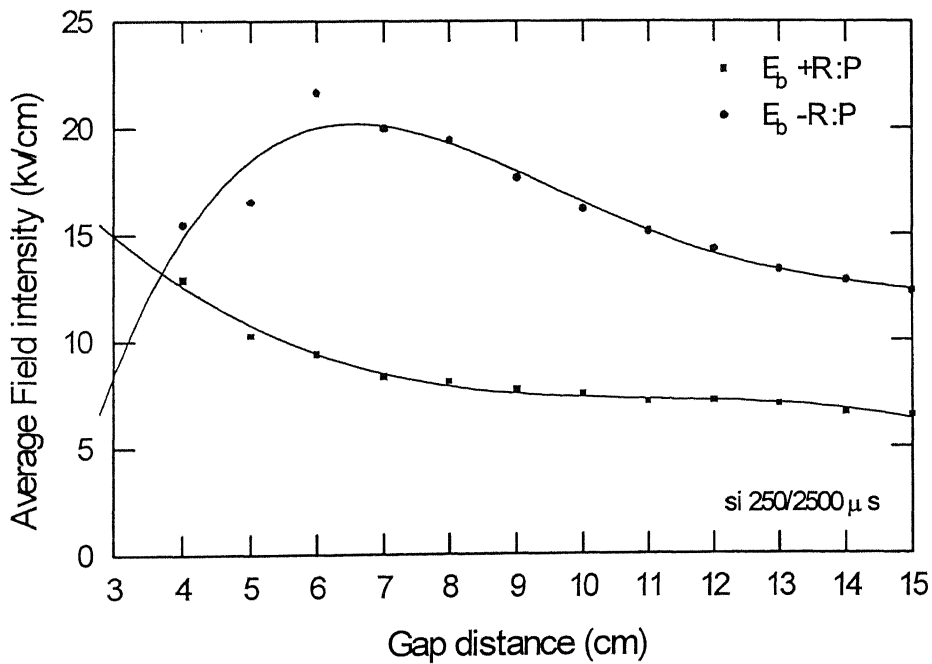


Fig 5.6 Breakdown field intensity characteristic for Rod-Plane electrodes with si 250/2500 μ s

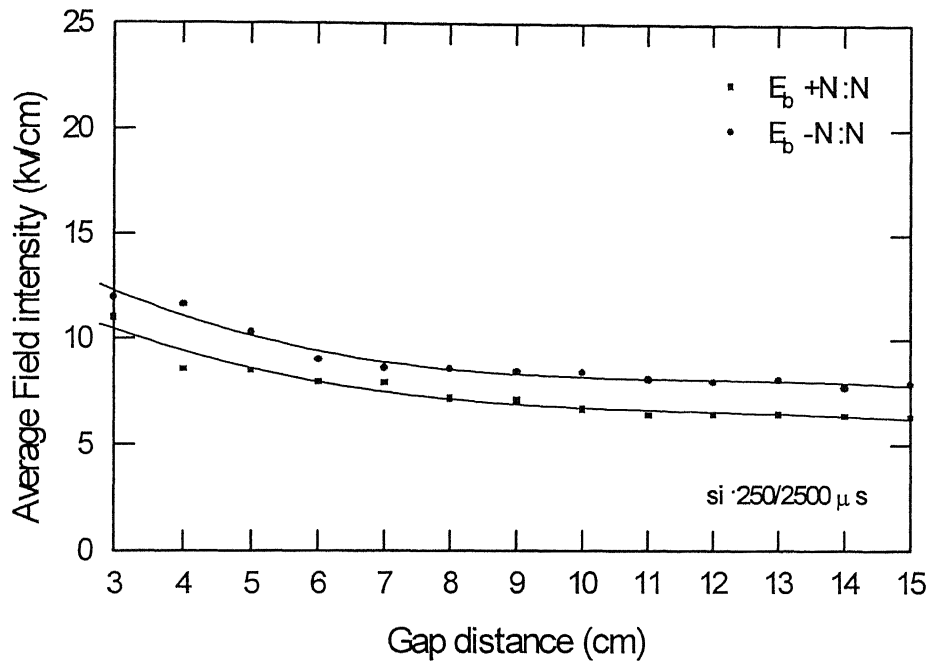


Fig 5.7 Breakdown field intensity characteristic for Needle-Needle electrodes with si 250/2500 μ s

Fig 5.5-7 exhibits the characteristics of Average field intensity with gap distance for three electrode configuration with both polarity of switching impulse (si2). Fig 5.6 & 5.7 showing similar nature of curve for average field intensity with N-P and R-P electrodes. For small gap distances for R-P electrodes average field intensity is comparable suggesting stable corona phenomenon. But for long gap distances (≥ 10 cm) average field intensity for N-P & R-P electrodes with positive polarity is 6 kV/cm and for negative is around 12 kV/cm, that is in the range of average potential gradient across positive and negative stable streamer.

Average field intensity characteristics (Fig 5.7) for Needle-Needle electrodes shows not much difference for positive and negative curves as it is identical electrode configuration. In this case for long gap distances Average field intensity is in range of 6-8 kV/cm, implying stable streamer precedes the breakdown.

5.3.3 Comparison of two switching impulse

In fig 5.8 to 5.10 result obtain with two switching impulses are brought together. We can conclude that effect of polarity is same for both cases for each electrode configuration and there is not much difference in breakdown characteristic with two switching impulses. Curves overlap each other for si1 and si2 shows that effect of wave shape of either polarity on breakdown voltage is insignificant.

How ever a typical characteristic for negative polarity voltage applied on Rod-Plane electrodes is observed in fig 5.9. This characteristic curve is showing a typical transition. For smaller gap distance in this case Glow corona precedes the breakdown resulting into average breakdown strength of 15-23 kV/cm , after the transition a straight line curve shows that stable streamer corona precedes the breakdown in the gap bringing down the average breakdown strength of 12 kV/cm. Such average breakdown strength for negative polarity voltage are conformed from [1].Such phenomena is not appearing in characteristic of N-P and N-N electrodes as it occurs for long gap distances (≥ 15 cm).

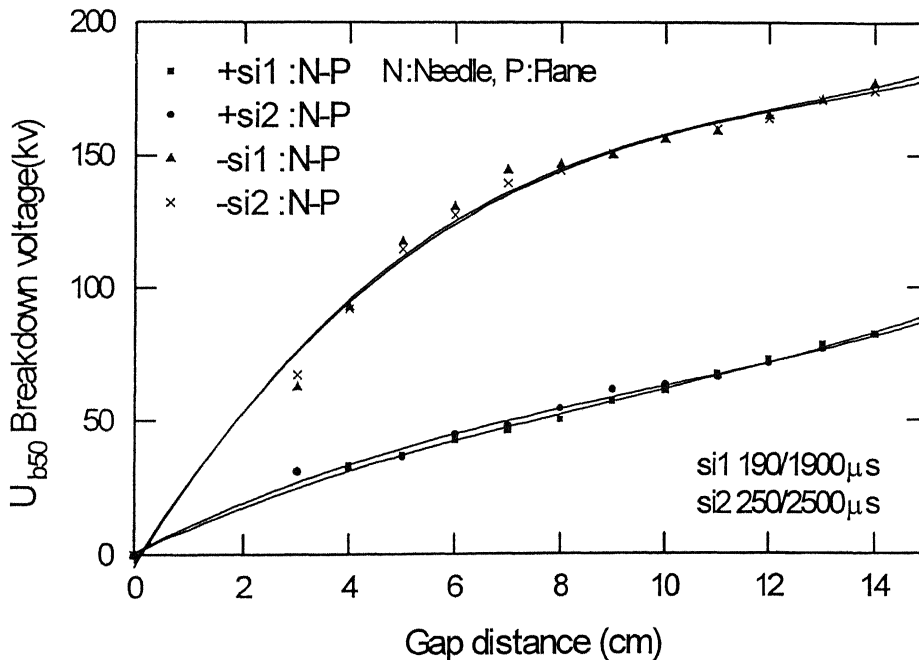


Fig 5.8 Comparison of si1 & si2 for Needle-Plane electrodes in air in extremely non Uniform field

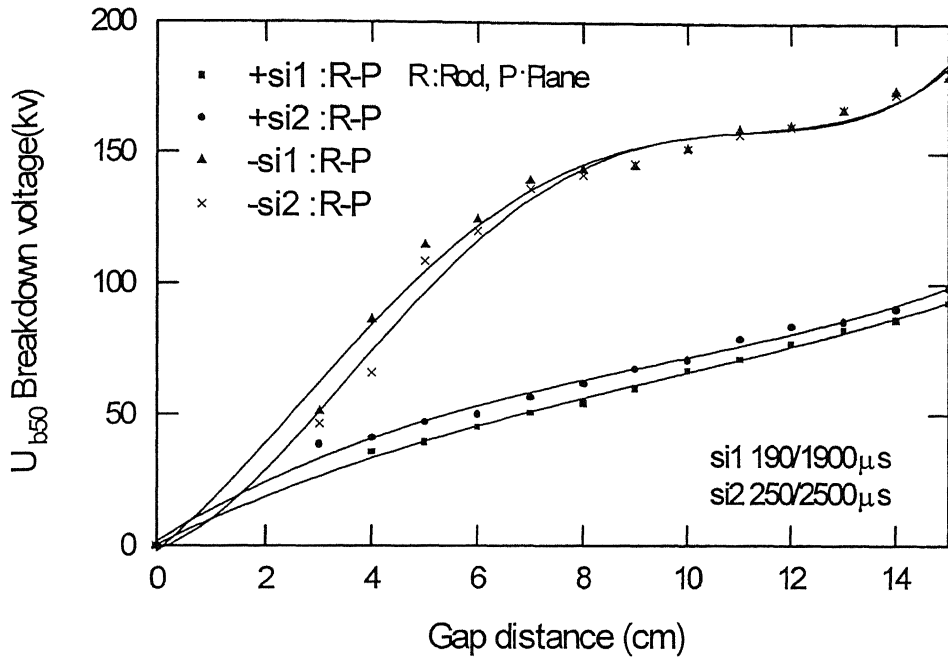


Fig 5.9 Comparison of si1 & si2 for Rod-Plane electrodes in air in extremely non Uniform field

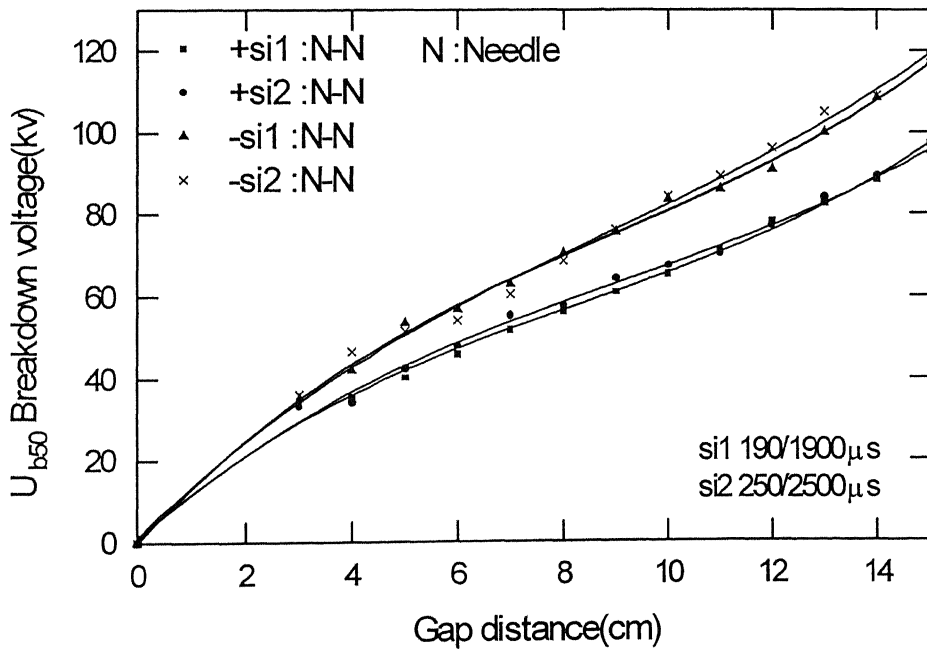


Fig 5.10 Comparison of si1 & si2 for Needle-Needle electrodes in air in extremely non Uniform field

5.4 Result with Lightning Impulse

5.4.1 U_{b50} characteristics with $\pm 1.2/50 \mu s$ lightning impulse

The lightning impulse of T_1/T_2 ratio $1.2/50 \mu s$ is obtained by using internal front resistor $R_1 = 244 \Omega$ and discharge resistance $R_2 = 22 k\Omega$, single stage charging capacitance is $140 nF$. The load capacitance used is $1.5 nF$, $600 kV$. Oscillograph plot of lightning impulse is shown in P5.4 & 5 for positive and negative polarity respectively.

Voltage level is raised gradually not exceeding the limit $1 kV/sec$. U_{b50} is measured as described in experimental procedure for all three electrode configurations with both polarity of voltage varying gap distance from 3 to 15 cm between the electrodes. For each final reading at least 10 pulses are applied at an interval of 30 seconds.

Table 5.4 Data for breakdown voltage in extremely non uniform field with li $\pm 1.2/50 \mu s$

| Gap distance (cm) | Breakdown voltage in kV for li $+1.2/50 \mu s$ | | | Breakdown voltage in kV for li $-1.2/50 \mu s$ | | |
|-------------------|--|-----------------|-------------|--|-----------------|-------------|
| | Needle - Plane | Needle - Needle | Rod - Plane | Needle - Plane | Needle - Needle | Rod - Plane |
| 0 | 0 | 0 | 0 | 0 | 0 | 0 |
| 3 | 43.80 | 48.75 | 44.25 | 63.75 | 39.15 | 59.25 |
| 4 | 44.70 | 52.80 | 49.05 | 84.00 | 47.25 | 78.45 |
| 5 | 50.25 | 62.25 | 54.90 | 101.63 | 56.55 | 95.10 |
| 6 | 59.85 | 72.75 | 60.15 | 120 00 | 67.50 | 122 25 |
| 7 | 68.40 | 81.75 | 64.50 | 140 63 | 82 50 | 133.13 |
| 8 | 74.10 | 85.80 | 72 75 | 157 50 | 91.13 | 142.50 |
| 9 | 79.80 | 90.75 | 79.05 | 167.25 | 102.00 | 157.50 |
| 10 | 82.50 | 93.75 | 87.75 | 182.25 | 108.00 | 162.00 |
| 11 | 85.50 | 97.88 | 92.25 | 185.25 | 117.00 | 170.25 |
| 12 | 93.60 | 104.25 | 100.13 | 197.63 | 121.13 | 181 88 |
| 13 | 95.25 | 110.25 | 112.50 | 214.50 | 146.25 | 190.13 |
| 14 | 102.00 | 116.63 | 118.88 | 216.00 | 149.25 | 217 50 |
| 15 | 104.25 | 120.75 | 125.25 | 225.75 | 156.75 | 220.88 |

KIKUSUI COR 5502U

NORM MP1

LI 1.2/50 μ s

CH1

5 μ s

2V

C1

P 5 4 Oscilloscope showing li 1.2/50 μ s

KIKUSUI cor 5502U

NORM MP1

LI -1.2/50 :S

CH1

C1 2V

5 :S

A

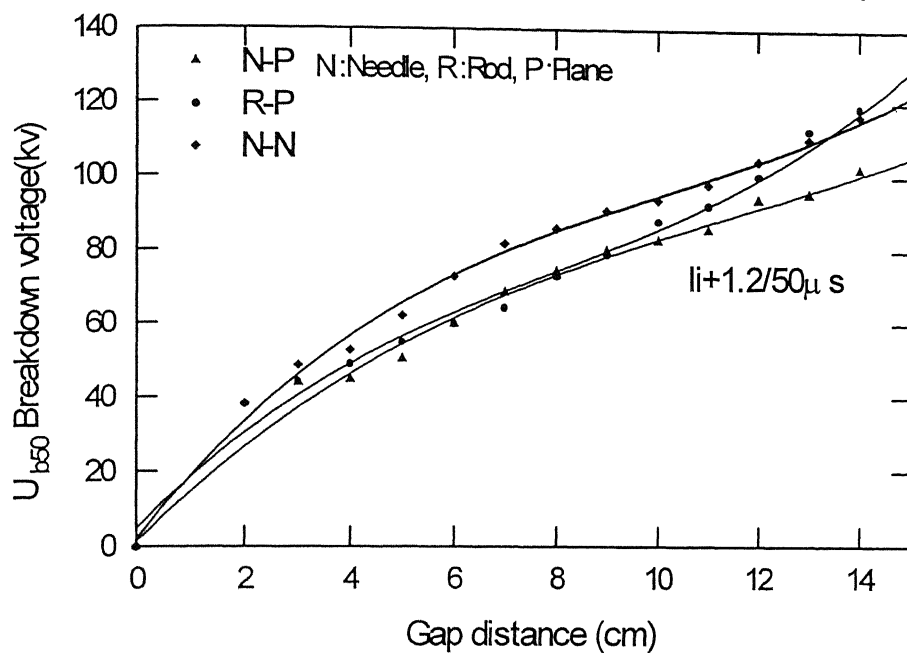


Fig 5.11 Breakdown characteristics of air in extremely non uniform field with $li + 1.2/50$

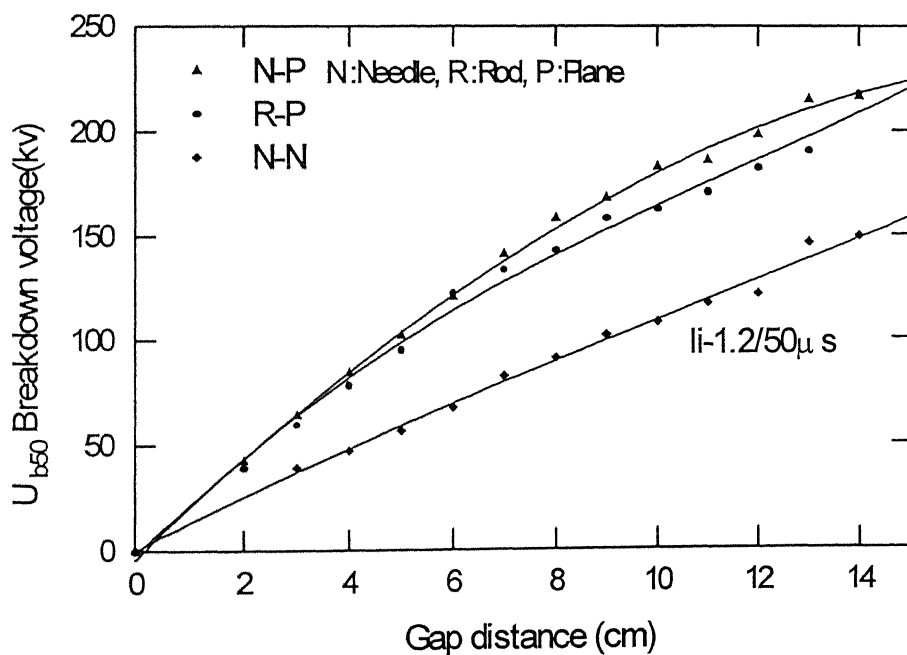


Fig 5.12 Breakdown characteristics of air in extremely non uniform field with $li - 1.2/50 \mu s$

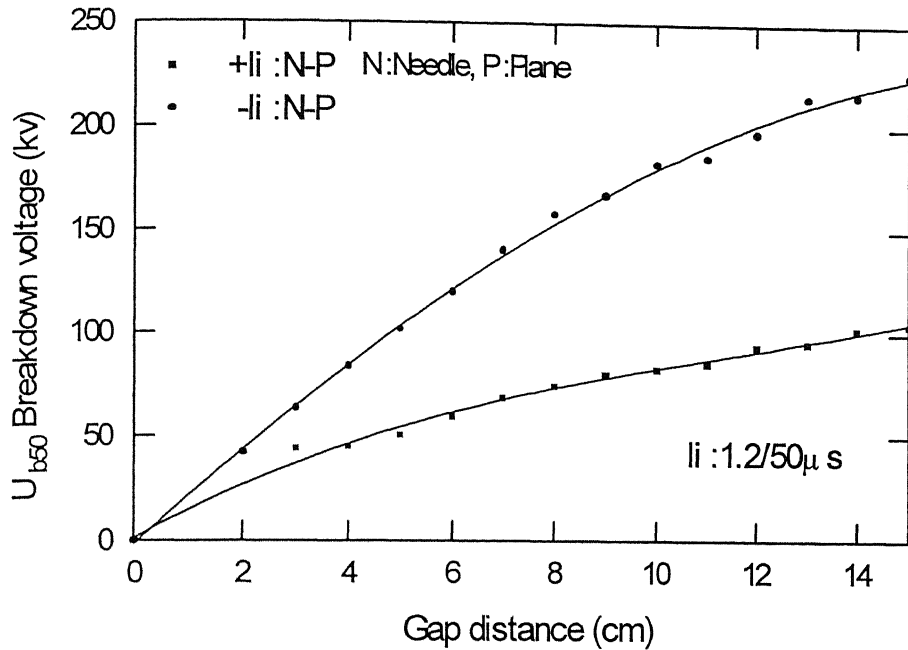


Fig 5.13 Breakdown characteristics for Needle-Plane electrodes of air in extremely non uniform field with $li \pm 1.2/50$

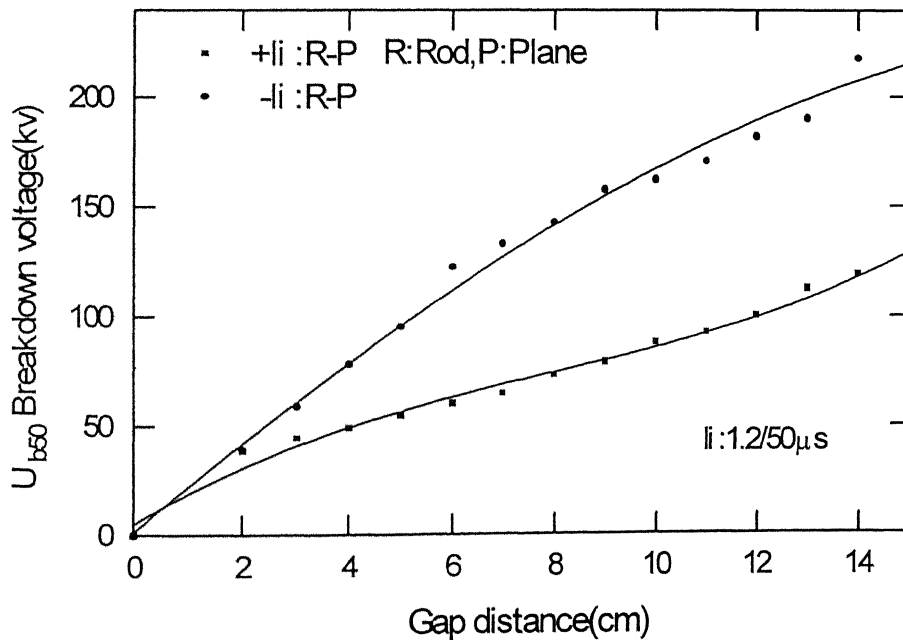


Fig 5.14 Breakdown characteristics for Rod-Plane electrodes of air in extremely non uniform field with $li \pm 1.2/50$

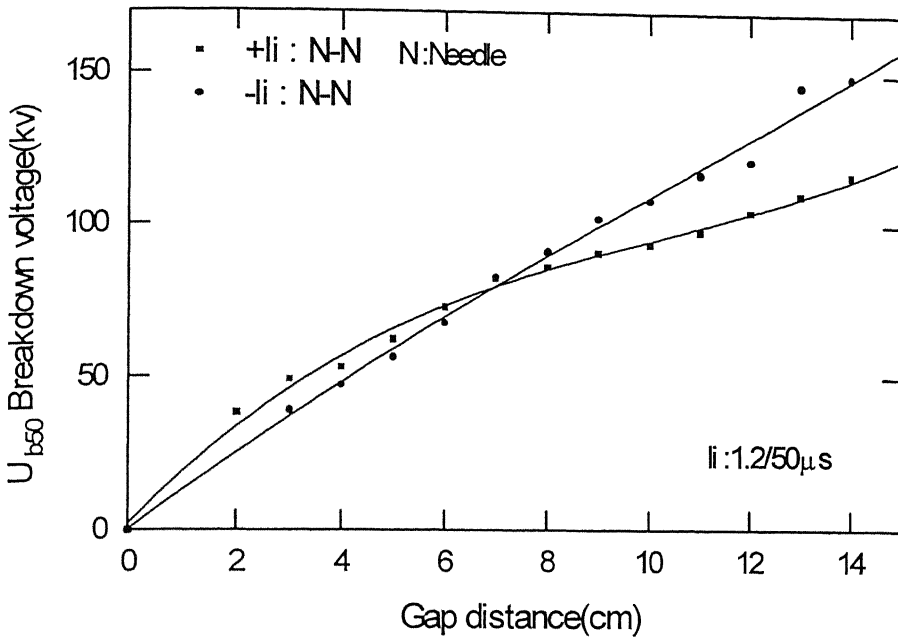


Fig 5.15 Breakdown characteristics for Needle-Needle electrodes of air in extremely non uniform field with $li \pm 1.2/50$

From Fig 5.11-12 it can be observed that U_{b50} breakdown voltage characteristics with positive and negative polarity are of similar nature as obtain with both switching impulses for three type of electric field configurations, however the magnitude of breakdown voltage is comparably higher with either polarity of li . As it is obvious that lightning impulse which have shorter duration compared to switching impulse require, higher breakdown voltage as no stable PD are able to precede the breakdown.

Breakdown characteristics with each electrode system are also shown for comparison in Fig 5.13-15. The polarity effect is conspicuous here for N-P and R-P electrode configurations but it is marginal in case of N-N electrode configuration. The reason can be explained in similar manner as symmetric electrode configuration for N-N. The more important observation is that as the field is becoming more non uniform on increasing the gap distance the difference between the breakdown strength for positive and negative polarities is also increasing. In case of uniform field, breakdown strength for positive and negative polarity would have remained the same. The effect is more prominent in case of extremely non uniform field as the space charge distorts the field.

5.4.2 Average field intensity characteristics

Average field intensity with lightning impulse is determined same as with switching impulse by the ratio of breakdown voltage(U_{b50}) to corresponding gap distance. Significance of average field intensity is in assessment of uniformity of field and type of corona preceding the breakdown.

If the breakdown takes place following the stable glow corona, the average potential gradient which may be required in the gap for the breakdown to take place is 15 to 20 kV/cm for the positive and negative polarity voltages respectively. The requirement of average potential gradient reduces to about 5 for the positive and 15 for the negative polarity voltages if the breakdown is preceded with stable streamer corona.

Table 5.5 Data for breakdown field intensity in extremely non uniform field with $li \pm 1.2/50 \mu s$

| Gap distance (cm) | Breakdown field intensity in kV/cm for $li + 1.2/50 \mu s$ | | | Breakdown field intensity in kV/cm for $li - 1.2/50 \mu s$ | | |
|------------------------|---|----------------|--------------------|---|----------------|--------------------|
| | Needle - Plane | Rod - Plane | Needle - Needle | Needle - Plane | Rod - Plane | Needle - Needle |
| 3 | 14.60 | 14.75 | 16.25 | 21.25 | 19.75 | 13.05 |
| 4 | 11.18 | 12.26 | 13.20 | 21.00 | 19.613 | 11.81 |
| 5 | 10.05 | 10.98 | 12.45 | 20.33 | 19.02 | 11.31 |
| 6 | 9.98 | 10.03 | 12.13 | 20.00 | 20.38 | 11.25 |
| 7 | 9.77 | 9.21 | 11.68 | 20.09 | 19.02 | 11.79 |
| 8 | 9.26 | 9.09 | 10.73 | 19.69 | 17.81 | 11.39 |
| 9 | 8.87 | 8.78 | 10.08 | 18.58 | 17.50 | 11.33 |
| 10 | 8.25 | 8.78 | 9.38 | 18.23 | 16.20 | 10.80 |
| 11 | 7.77 | 8.38 | 8.90 | 16.84 | 15.48 | 10.64 |
| 12 | 7.80 | 8.34 | 8.69 | 16.47 | 15.16 | 10.09 |
| 13 | 7.33 | 8.65 | 8.48 | 16.50 | 14.63 | 11.25 |
| 14 | 7.29 | 8.49 | 8.33 | 15.43 | 15.54 | 10.66 |
| 15 | 6.95 | 8.35 | 8.05 | 15.05 | 14.73 | 10.45 |

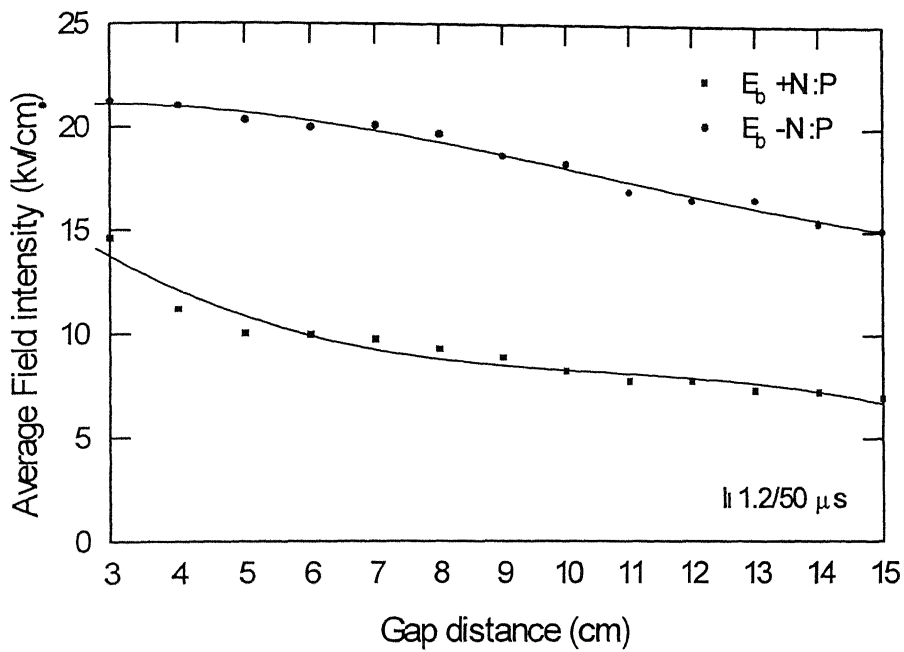


Fig 5.16 Breakdown field intensity characteristic for Needle-Plane electrode with $li\ 1.2/50\ \mu s$

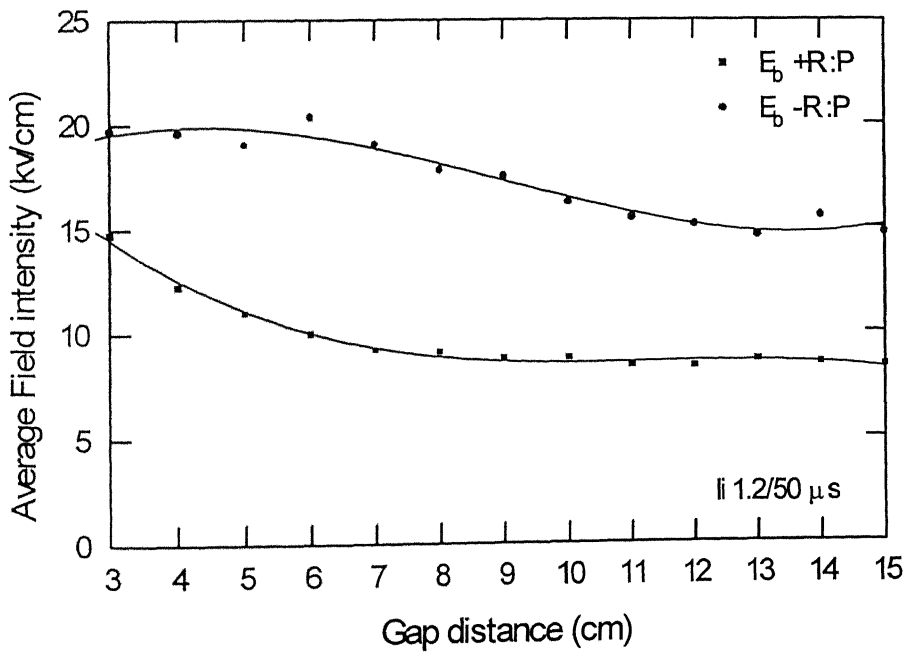


Fig 5.17 Breakdown field intensity characteristic for Rod-Plane electrode with $li\ 1.2/50\ \mu s$

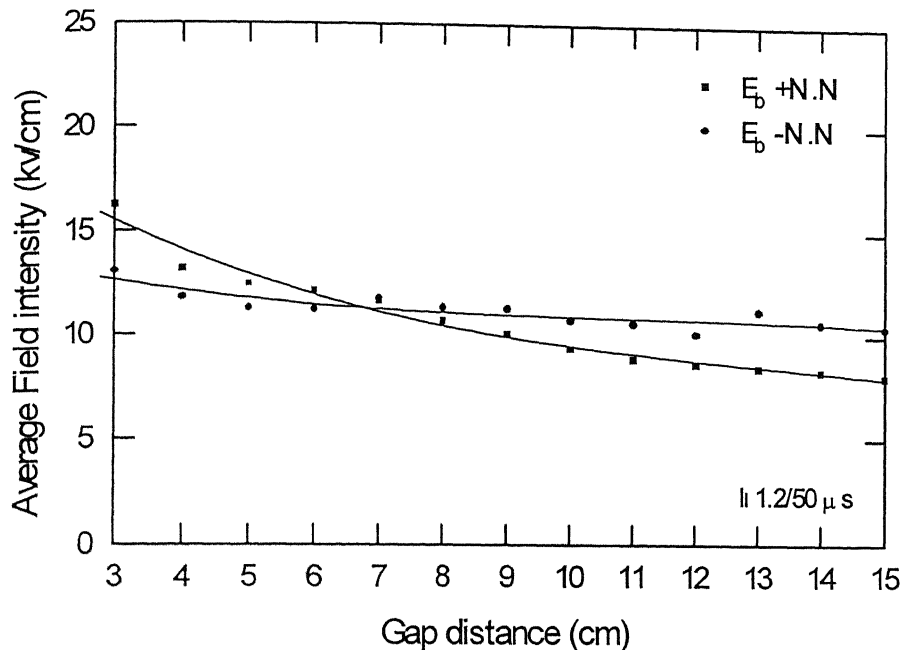


Fig 5.18 Breakdown field intensity characteristic for Needle-Needle electrode with li 1.2/50 μ s

Figures 5.16-18 exhibit the characteristics of average breakdown field intensity with increasing gap distance for three electrode configurations with both polarities of lightning impulse. These characteristics measured for N-P and R-P electrode system show similar nature of curves for average breakdown field intensity. For small gap distances (3-5 cm) average breakdown field intensity is in the range of 15-20 kV/cm for either polarity. On increasing the gap distance a transition in measured characteristics take place and it saturates a two distinct values for the respective polarities. for gap distances (≥ 10 cm). The average field intensity for positive polarity is calculated to be around 8 kV/cm and for negative it is around 15 kV/cm. These values agree to the breakdown strength of air under the given conditions as given in (1).

Average breakdown field intensity characteristics (Fig 5.18) for Needle-Needle electrodes shows not much difference for positive and negative curves as it is identical electrode configuration. In this case for long gap distances average field intensity is in range of 8-11 kV/cm.

5.5 Comparison of Switching Impulse and Lightning Impulse

In case of lightning since duration of pulse is very short, it can be taken for granted that no stable partial discharge are able to take place, whereas in the case of much slower switching impulse stable partial discharge precede the breakdown which affects the breakdown strength considerably. Hence the breakdown voltage is larger with li than si with both polarities.

Nature of the curve for each configuration is same for both type of impulse voltages. Polarity effect is conspicuous in the case of N-P and R-P electrode configuration, but it is marginal in case of N-N electrode configuration with both si and li. For switching impulse average breakdown field intensity characteristics show the intensity with long gap distances is around 5 & 12 kV/cm for positive and negative polarity respectively, but for li it is around 8 & 15 kV/cm. Due to short duration of the li,, the development of stable PD are difficult before the breakdown. This is also confirm from the average breakdown field intensity values, which are higher compared to the condition when stable PD precede the breakdown.

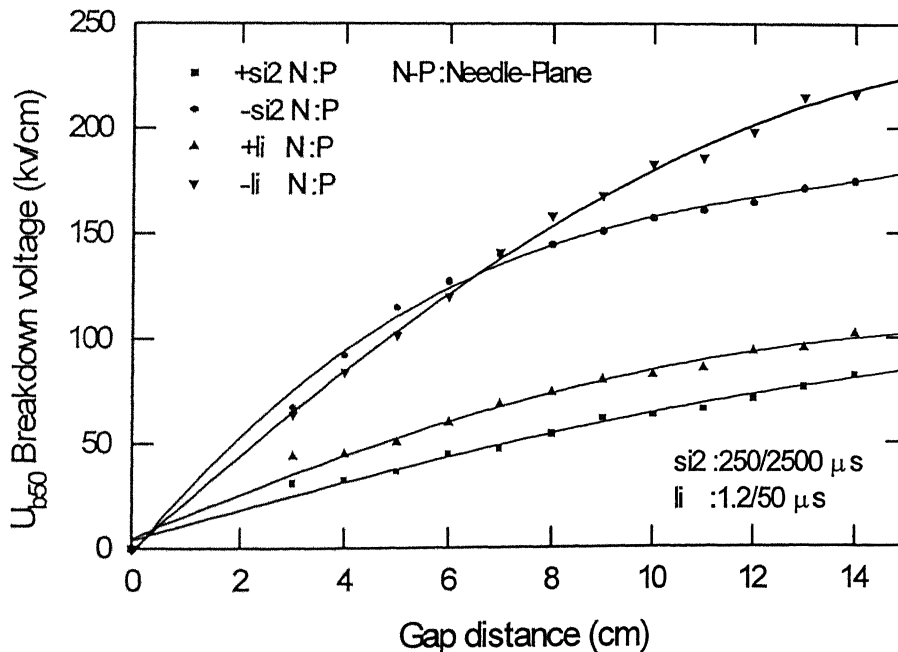


Fig 5.19 Comparison of si2 & li for Needle-Plane electrodes in air in extremely non uniform field

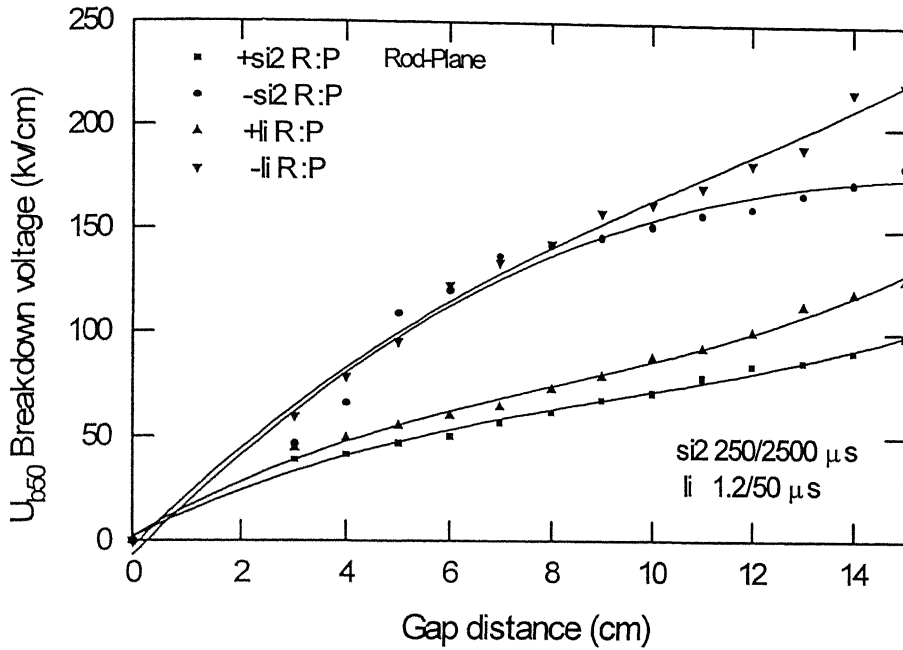


Fig 5.20 Comparison of si2 & li for Rod-Plane electrodes of air in extremely non Uniform field

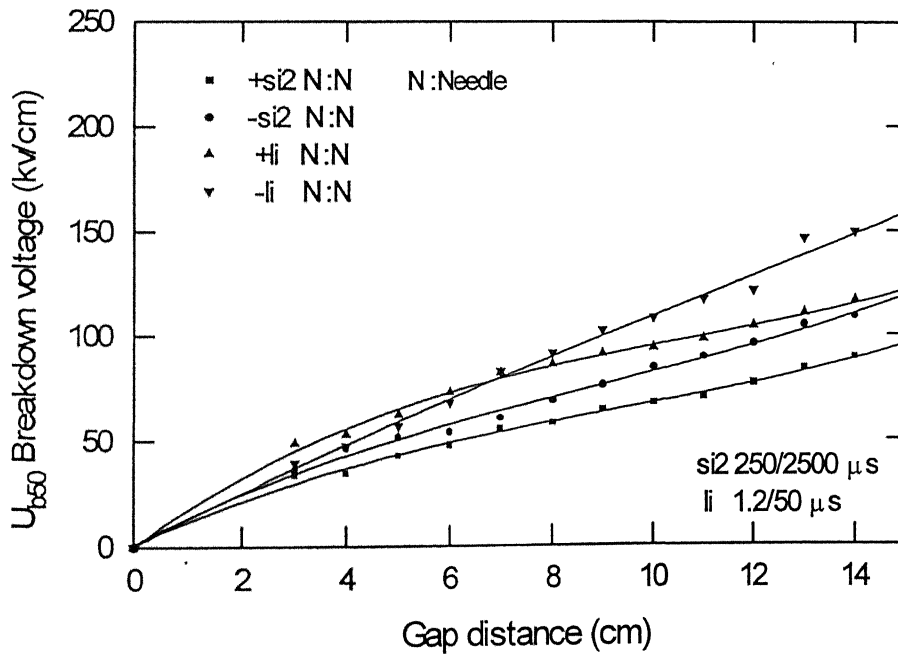


Fig 5.21 Comparison of si2 & li for Needle-Needle electrodes of air in extremely non Uniform field

Chapter 6

Investigations of Propagation Time and Propagation Velocity of Leader

The leader propagation time with impulse voltages can be considered to be from the instant the applied voltage begins to collapse to the instant when it reaches to zero. Actually this is the time required for the discharge in the event of breakdown to travel through the gap distance between the electrodes. Propagation time in a gap depends upon the individual types of PD and their extent in the gap just before the breakdown. The extents of PD are affected by the field distribution and the magnitude of the applied voltage. Propagation time is measured accurately with the help of storage oscilloscope. Propagation velocity is calculated assuming that the leader takes the path through the shortest gap distance between electrodes.

$$\text{Propagation Velocity} = \frac{\text{Gap Distance}}{\text{Propagation Time}}$$

The propagation velocity for instable leader is reported to be a few tens of cm/ μ s and for streamer discharge about 100 cm/ μ s. Leader propagation velocity depends upon the electrode configuration and shape of the applied impulse voltage.

6.1 Investigations with 250/2500 μ s Switching Impulse

Experimental set up and electrode configurations for these investigations were the same as mentioned in chapter 5. Propagation time was measured for U_{b50} and when the breakdown took place in wave tail region. Readings were taken when the breakdown occurred approximate at the same instant on the wave tail region of the impulse voltage.

Table 6.1 shows the measured values of the propagation time from CRO and corresponding calculated propagation velocity for all the three electrode configurations with switching impulse wave shape of 250/2500 μs for both polarities.

Table 6.1 Propagation data of breakdown channel in air in extremely non uniform field with si \pm 250/2500 μs

| Gap distance (cm) | Needle - Plane | | | | Rod - Plane | | | | Needle - Needle | | | |
|-------------------|------------------------------------|------|---|-------|------------------------------------|------|---|-------|------------------------------------|------|---|-------|
| | Propagation time (μs) | | Propagation velocity (cm/ μs) | | Propagation time (μs) | | Propagation velocity (cm/ μs) | | Propagation time (μs) | | Propagation velocity (cm/ μs) | |
| | +si | -si | +si | -si | +si | -si | +si | -si | +si | -si | +si | -si |
| 3 | 0.78 | 1.00 | 3.85 | 3.00 | 0.84 | 1.00 | 3.58 | 3.00 | 0.74 | 0.80 | 4.06 | 3.75 |
| 4 | 0.70 | 0.80 | 5.71 | 5.00 | 1.00 | 1.00 | 4.00 | 4.00 | 0.82 | 0.80 | 4.88 | 5.00 |
| 5 | 0.84 | 0.80 | 5.95 | 6.25 | 1.00 | 2.00 | 5.00 | 2.50 | 0.90 | 1.00 | 5.56 | 5.00 |
| 6 | 0.82 | 0.80 | 7.32 | 7.50 | 0.90 | 1.00 | 6.67 | 6.00 | 0.90 | 0.90 | 6.67 | 6.67 |
| 7 | 0.90 | 0.80 | 7.78 | 8.75 | 0.80 | 1.00 | 8.75 | 7.00 | 1.10 | 0.80 | 6.36 | 8.75 |
| 8 | 0.70 | 0.80 | 11.43 | 10.00 | 1.00 | 1.20 | 8.00 | 6.67 | 0.90 | 0.80 | 8.89 | 10.00 |
| 9 | 0.80 | 1.50 | 11.25 | 6.00 | 0.75 | 1.25 | 12.00 | 7.20 | 0.80 | 0.80 | 11.25 | 11.25 |
| 10 | 0.94 | 2.00 | 10.63 | 5.00 | 0.80 | 0.75 | 12.50 | 13.33 | 0.90 | 0.80 | 11.11 | 12.50 |
| 11 | 0.80 | 1.00 | 13.75 | 11.00 | 1.00 | 0.80 | 11.00 | 13.75 | 1.00 | 1.00 | 11.00 | 11.00 |
| 12 | 0.80 | 1.80 | 15.00 | 6.67 | 0.80 | 0.80 | 15.00 | 15.00 | 0.70 | 1.10 | 17.14 | 10.91 |
| 13 | 0.80 | 1.80 | 16.25 | 7.22 | 0.90 | 1.00 | 14.44 | 13.00 | 0.70 | 1.20 | 18.57 | 10.83 |
| 14 | 0.80 | 0.88 | 17.50 | 15.91 | 0.92 | 0.80 | 15.22 | 17.50 | 0.75 | 1.20 | 18.67 | 11.67 |
| 15 | 0.80 | 0.80 | 18.75 | 18.75 | 1.00 | 0.95 | 15.00 | 15.79 | 0.80 | 1.20 | 18.75 | 12.50 |

It has been reported in the literature that on applying a positive impulse voltage, first a dense filamentary corona discharge occurs. This discharge is described as the 'first corona' which extends in the gap for small gap distance. Initial velocity of propagation of leader channel was approximately $5 \text{ cm}/\mu\text{s}$, but it increases to the value $15\text{-}20 \text{ cm}/\mu\text{s}$ for long gap distances. When a leader developed to about 50 % of the gap distance, it had a discontinuous stepped structure. Beyond this length it underwent a sudden increase in velocity, losing the stepped structure.

The spatial propagation characteristic of a leader channels are those of a narrow irregular path, often in a direction at an angle to the field. The streamer discharge at the leader tip, also having a weak filamentary structure ionizes the air ahead of the leader channel. Leader corona which is actually a streamer discharge at the tip of leader, is responsible for maintaining the current flow in the propagating discharge and modifying the field distribution in the gap by developing space charge [1]. Fig 6.1-3 show propagation characteristics of atmospheric air breakdown channel for all the three electrode configurations with $si \pm 250/2500 \mu\text{s}$

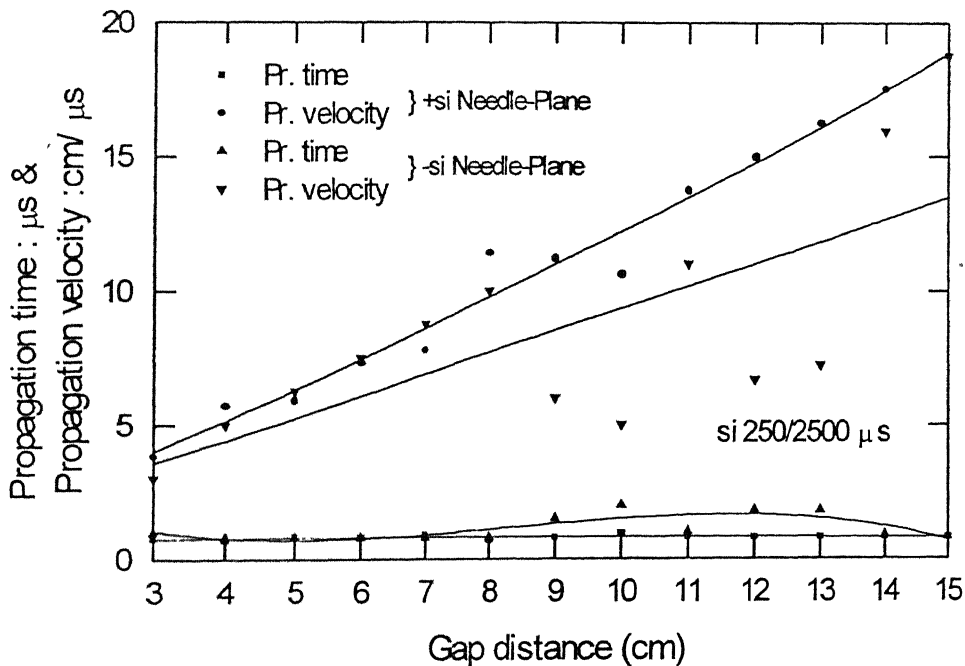


Fig 6.1 Propagation characteristics of air breakdown channel for Needle-Plane electrodes with $si \pm 250/2500 \mu\text{s}$

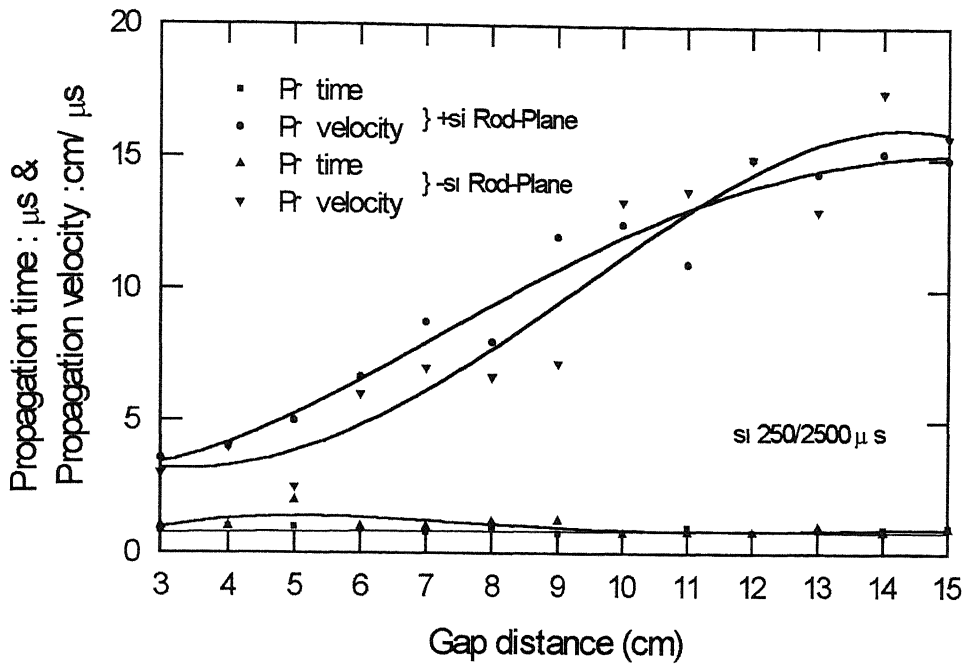


Fig 6.2 Propagation characteristics of air breakdown channel for Rod-Plane electrodes with si $\pm 250/2500 \mu s$

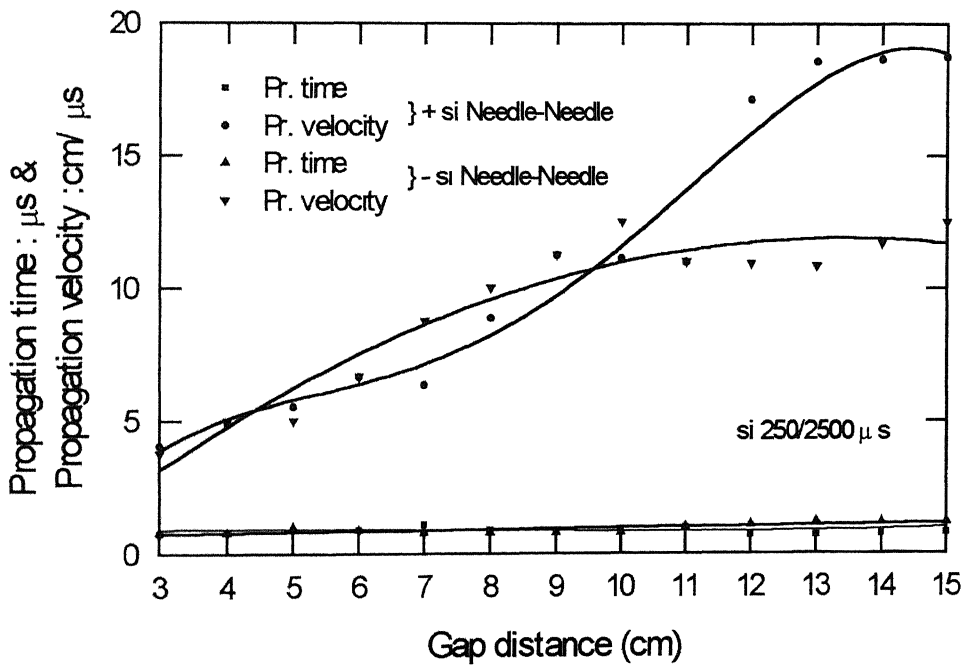
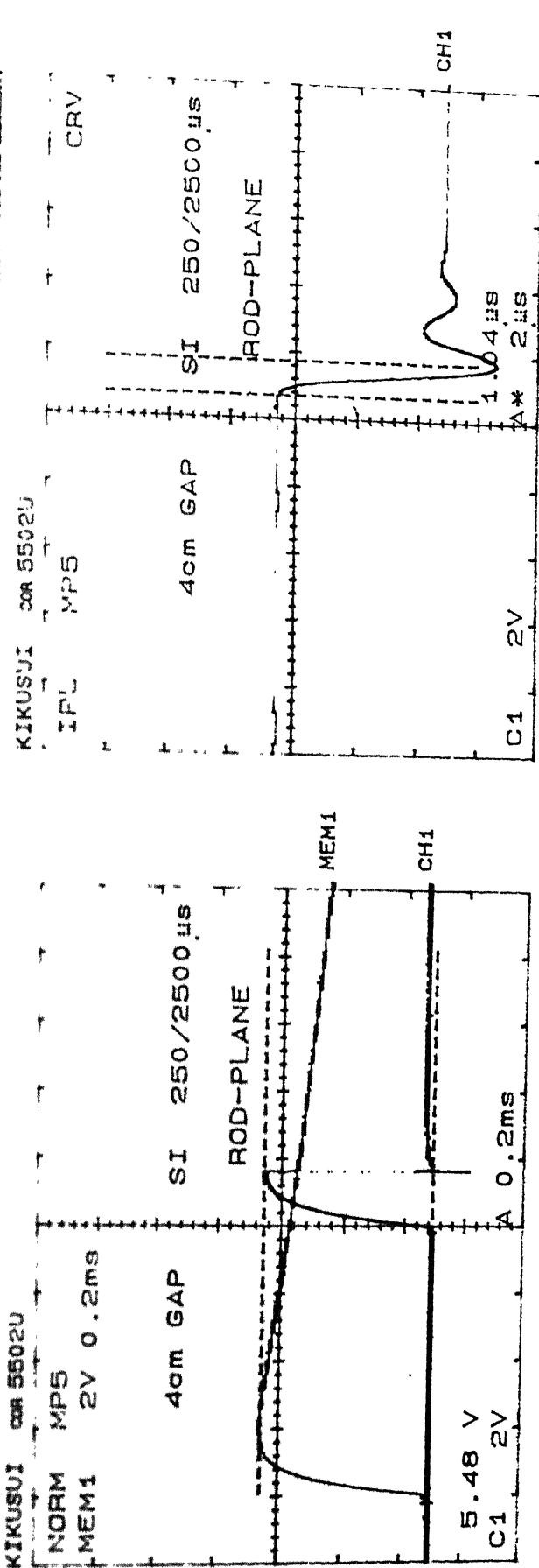
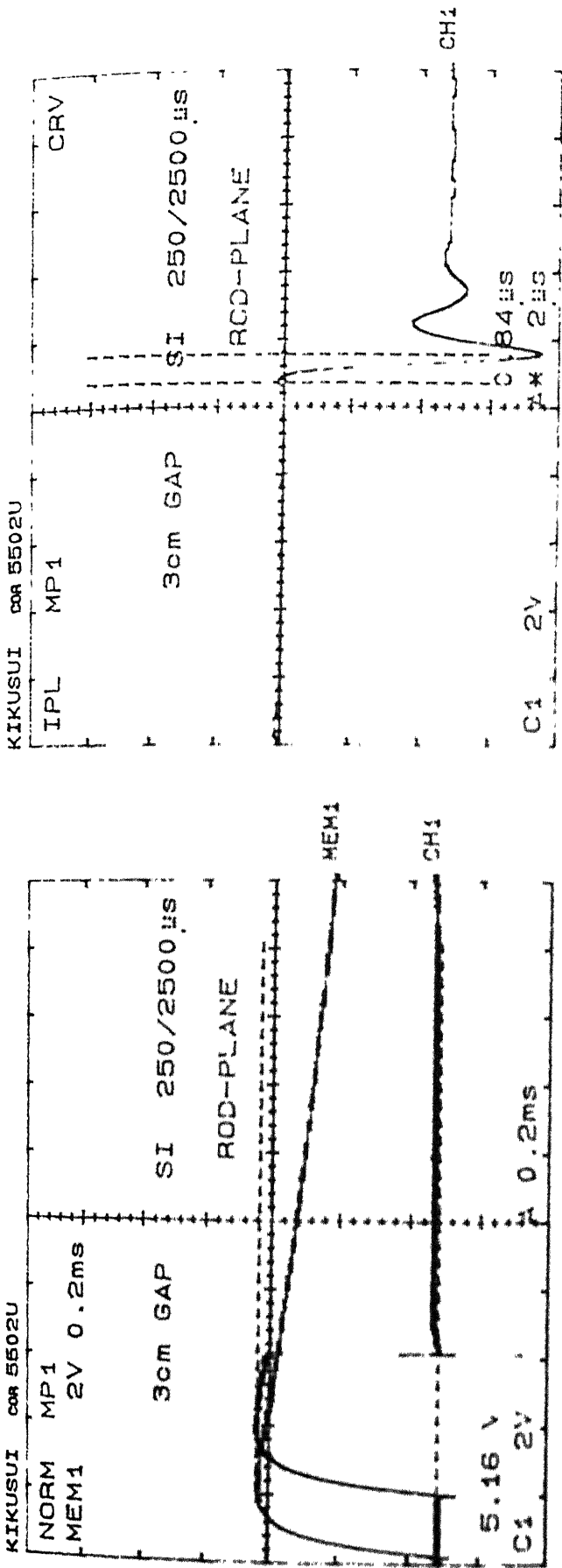


Fig 6.3 Propagation characteristics of air breakdown channel for Needle-Needle electrodes with si $\pm 250/2500 \mu s$

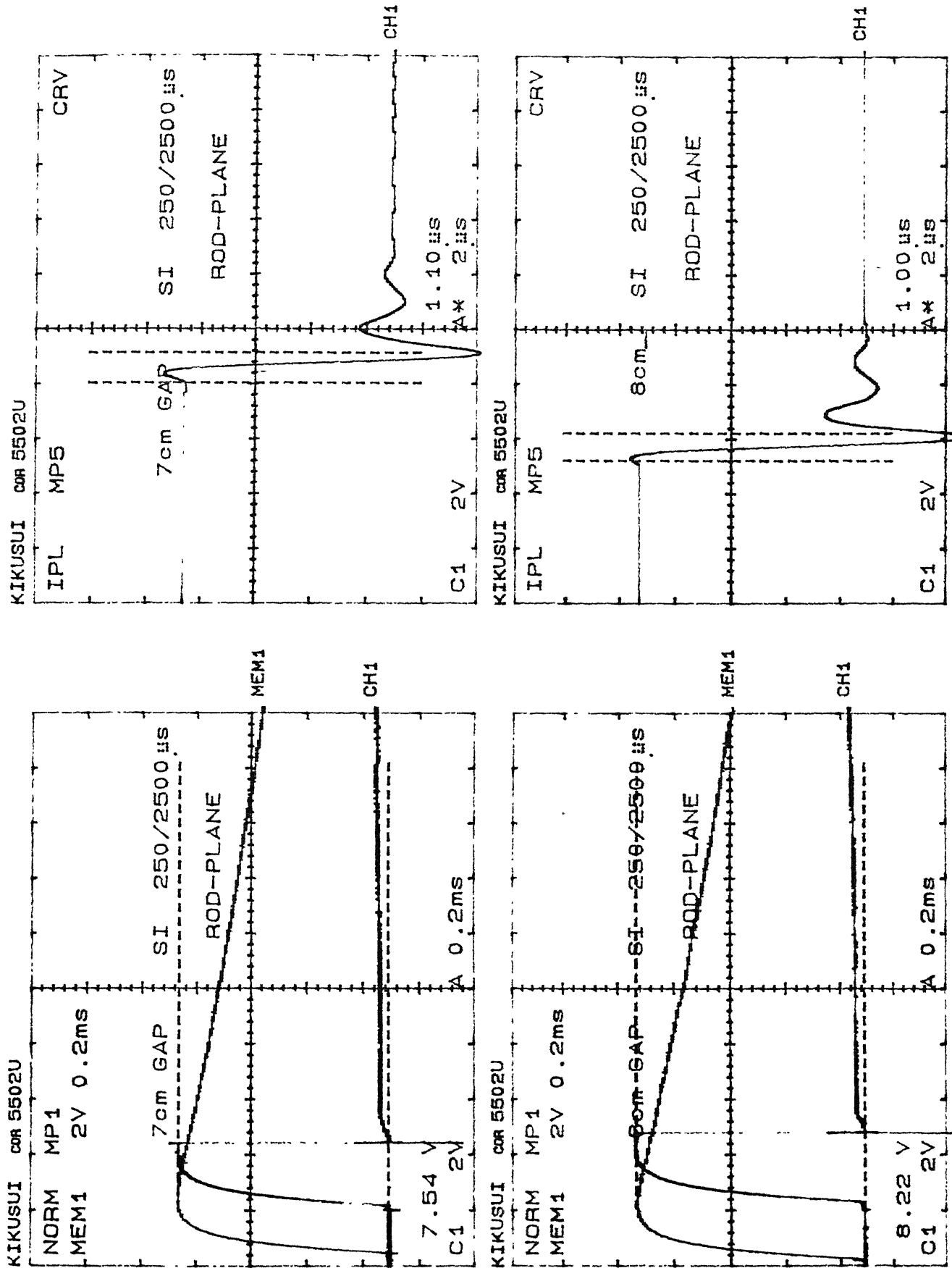
From these figures it can be observed that propagation time remains nearly constant, but propagation velocity increases linearly with gap distance. As there is variation in propagation time measured for the same gap distance which is due to its dependence on voltage magnitude and the instant of breakdown. We see from figures that the propagation velocities calculated are deviating from the fitted linear curve.

From figures it is also observed that there is no effect of polarity of voltage on propagation time and propagation velocity in case of electrode system where grounded electrode is a plane. However, effect of polarity of the applied voltage can be seen for both propagation time and propagation velocity in case of N-N electrode system.

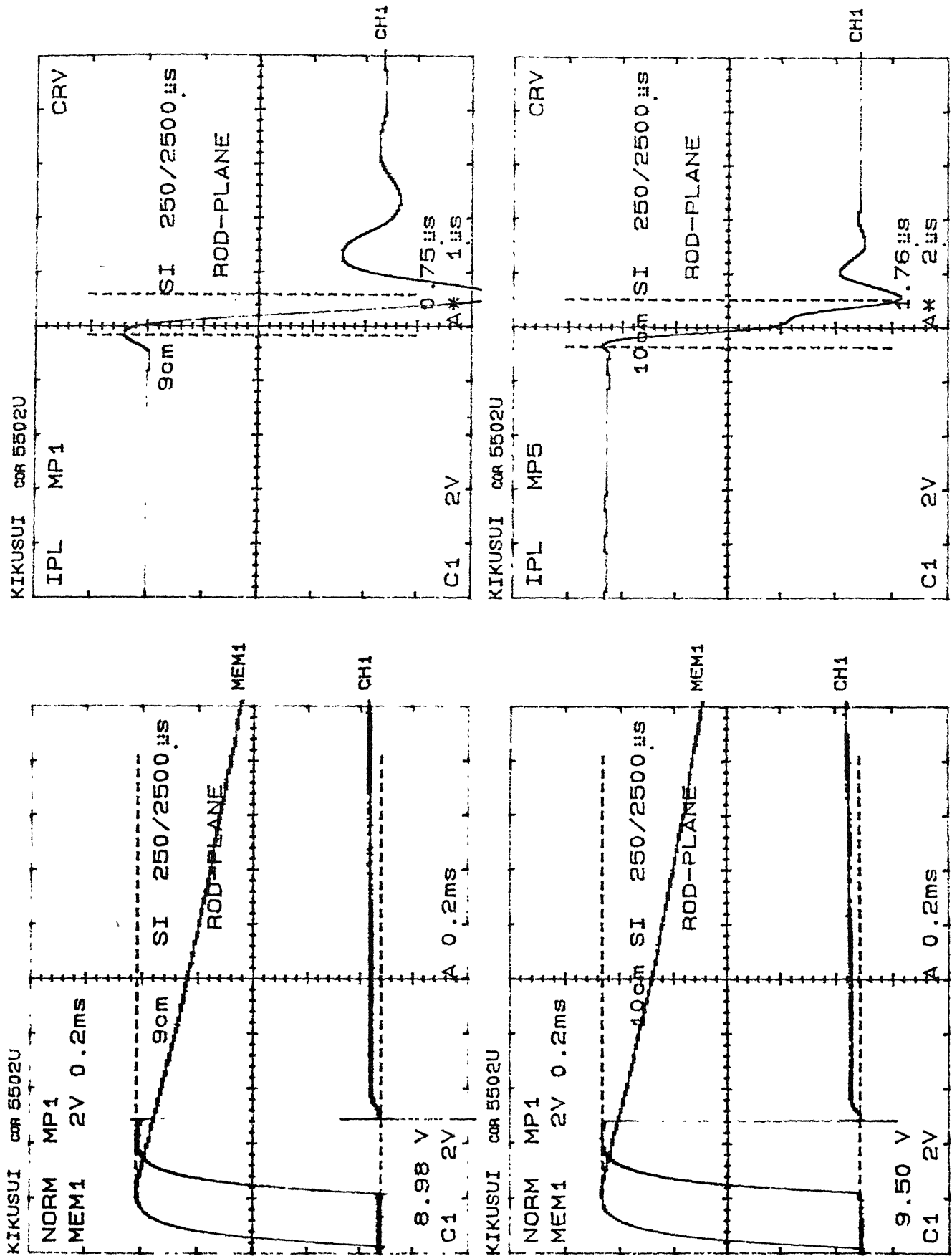
Oscillograph plot obtained from plotter interfaced with CRO for 50 % breakdown voltage U_{b50} and Propagation time, are shown in following pages for si 250/2500 μs and li.1.2/50 μs .



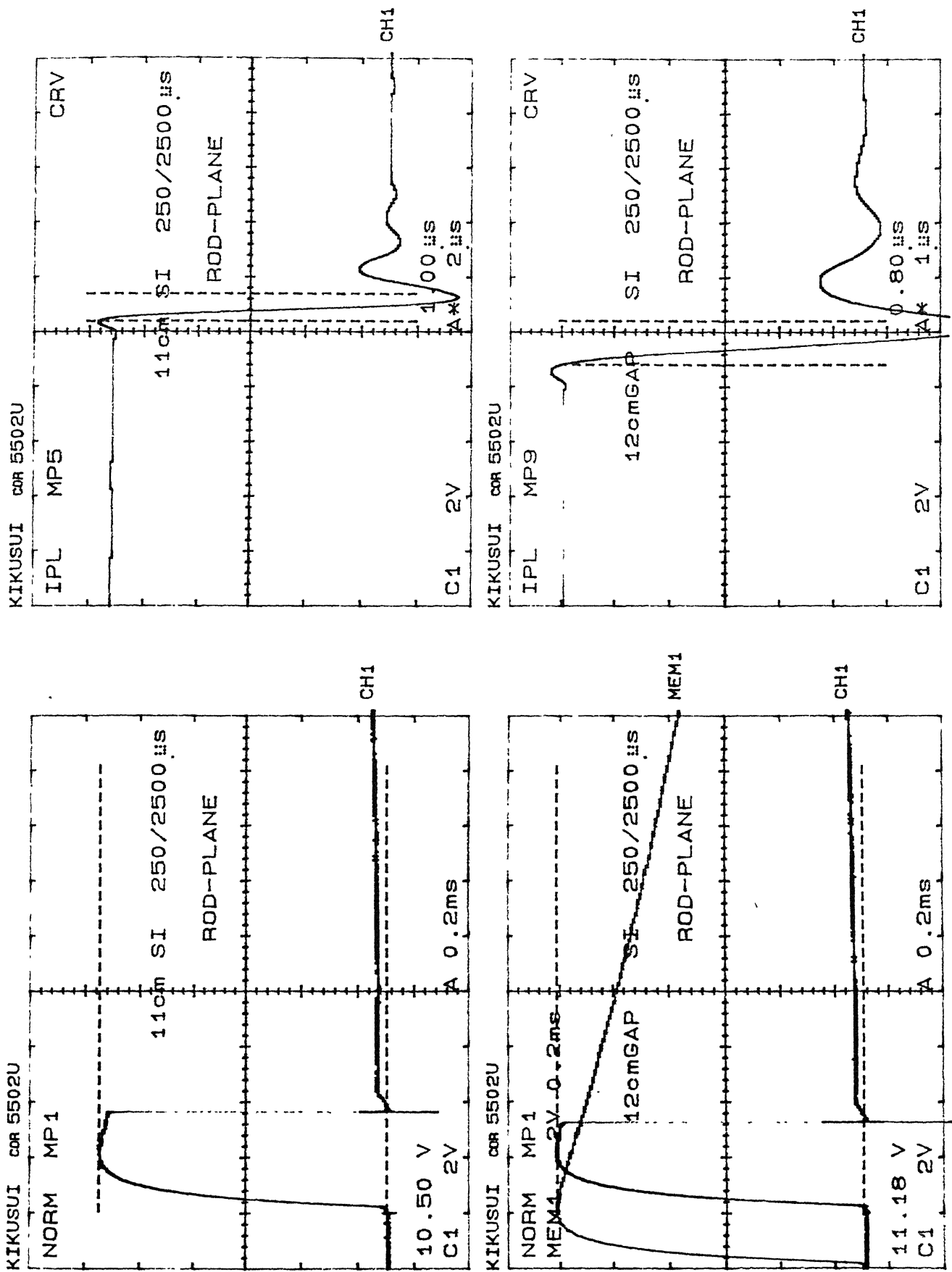
P 6.1 Oscilloscope showing U_{50} 50 % breakdown voltage and propagation time for R-P Electrode with si 250/2500 μ s with varying gap distance



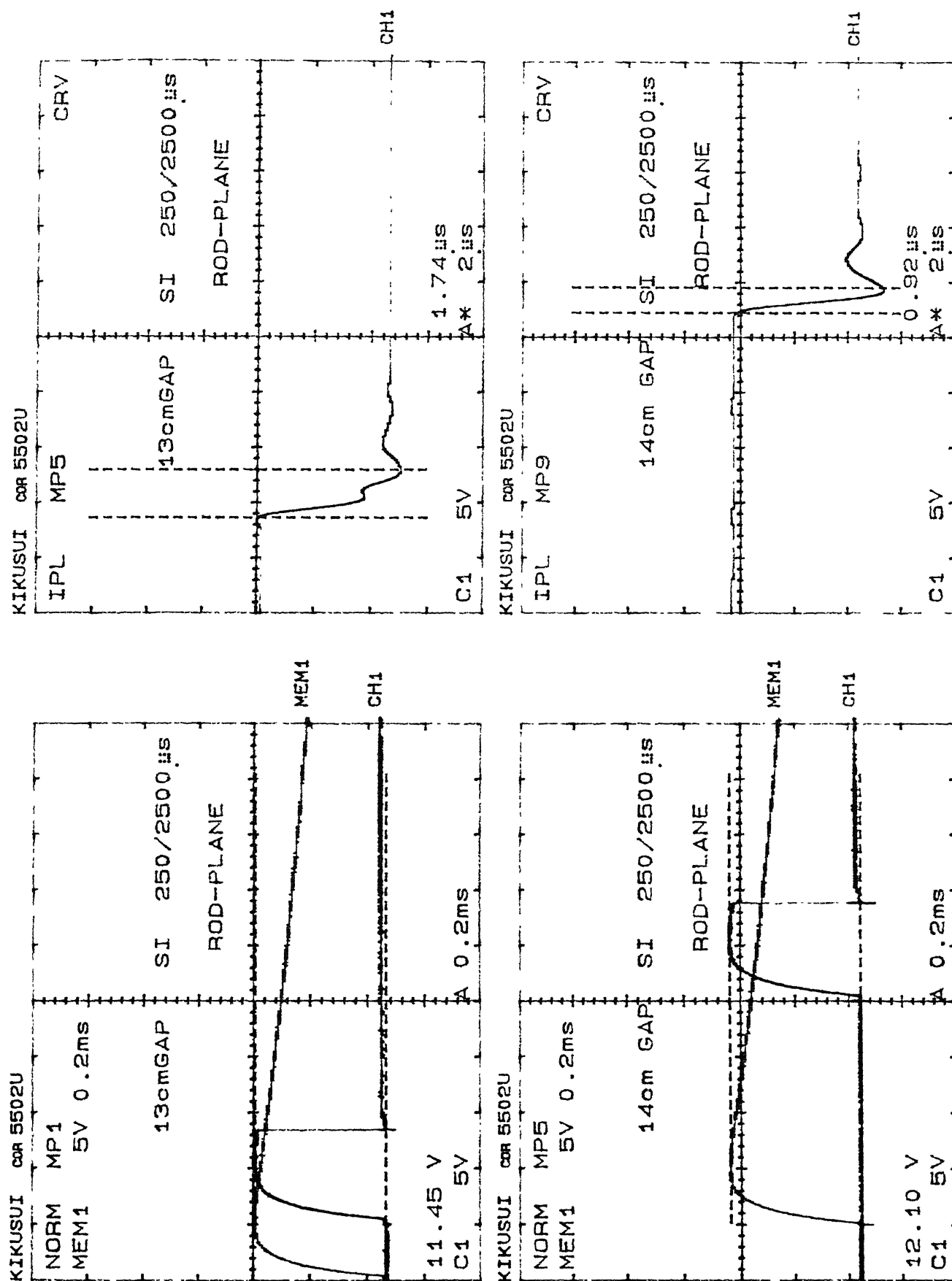
P 6.3 Oscillograph showing U_{b50} 50 % breakdown voltage and propagation time for R-P Electrode with si 250/2500 μ s with varying gap distance



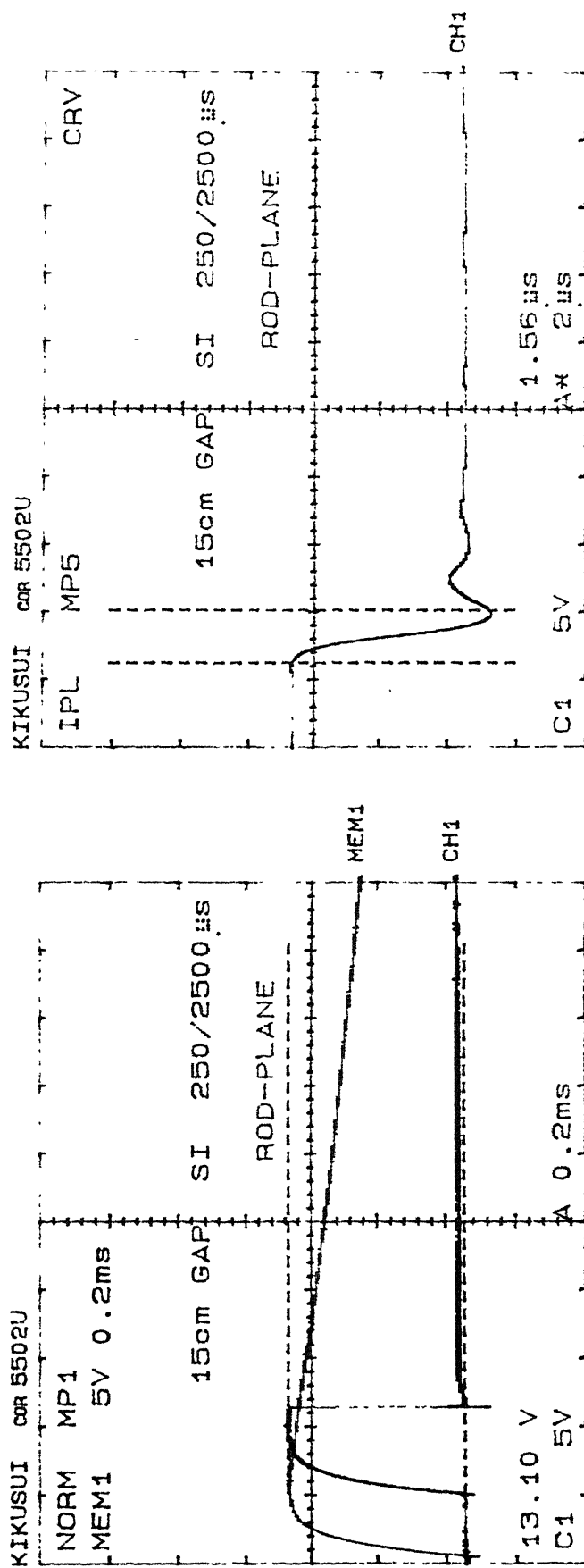
P 6.4 Oscilloscope showing U_{b50} 50 % breakdown voltage and propagation time for R-P Electrode with si 250/2500 μs with varying gap distance



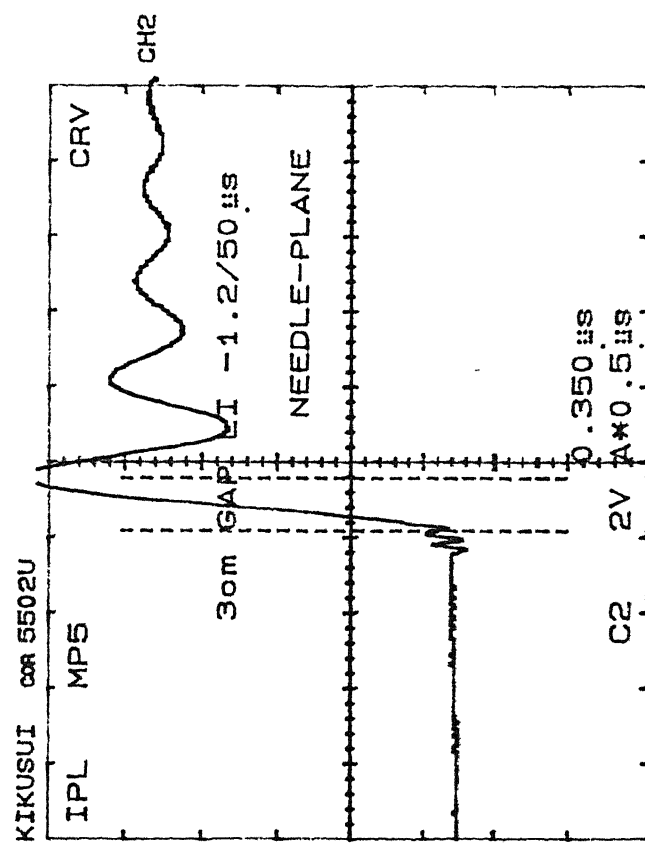
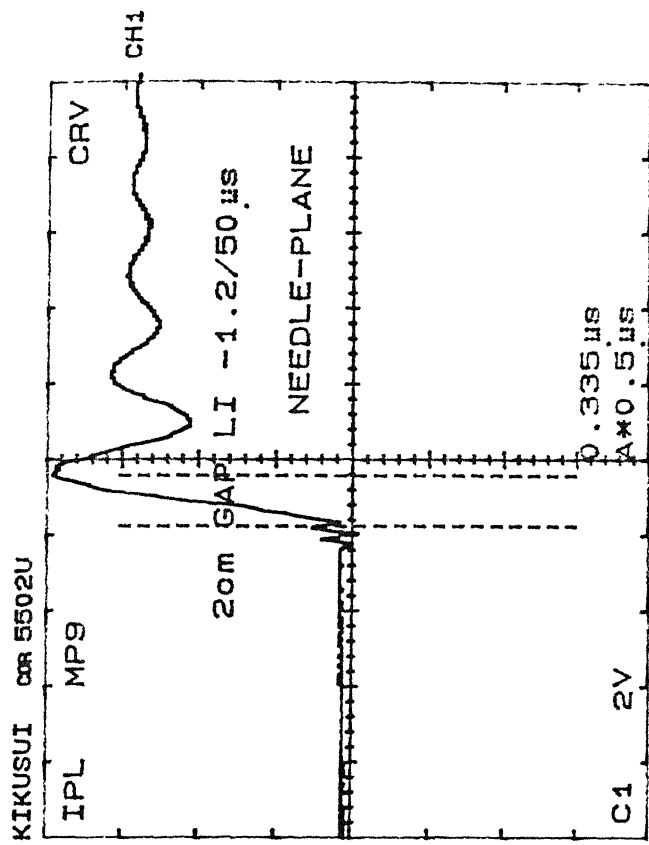
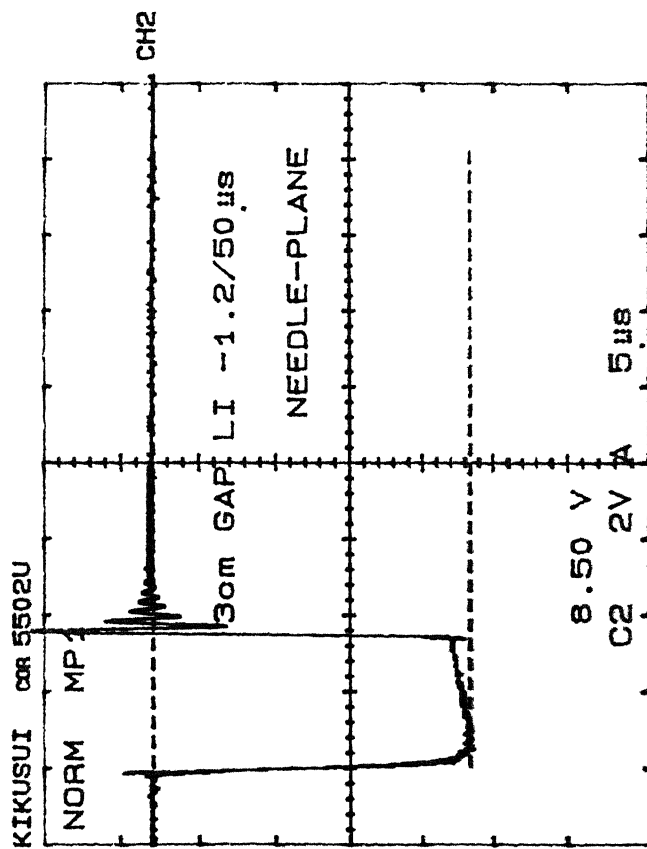
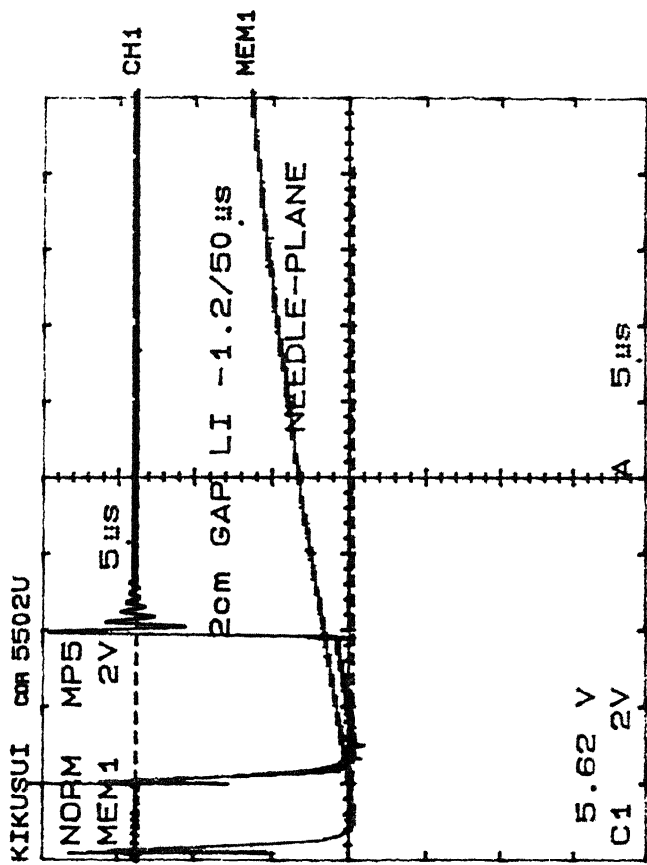
P 6.5 Oscillograph showing U_{b50} 50 % breakdown voltage and propagation time for R-P Electrode with si 250/2500 μs with varying gap distance



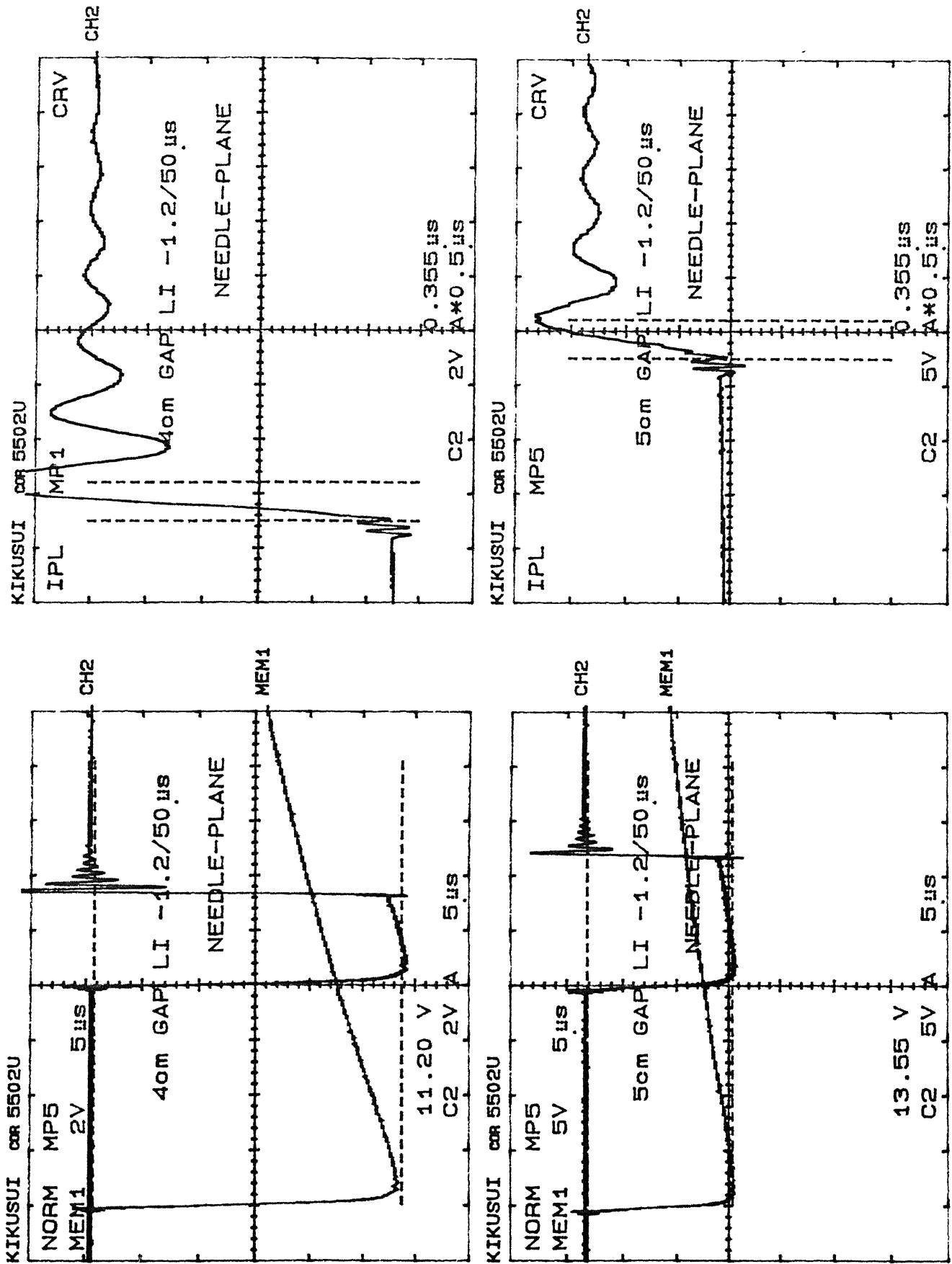
P 6.6 Oscilloscope showing U_{50} 50 % breakdown voltage and propagation time for R-P Electrode with si 250/2500 μ s with varying gap distance



P 6.7 Oscillograph showing U_{b50} 50 % breakdown voltage and propagation time for R-P Electrode with si 250/2500 μ s with varying gap distance

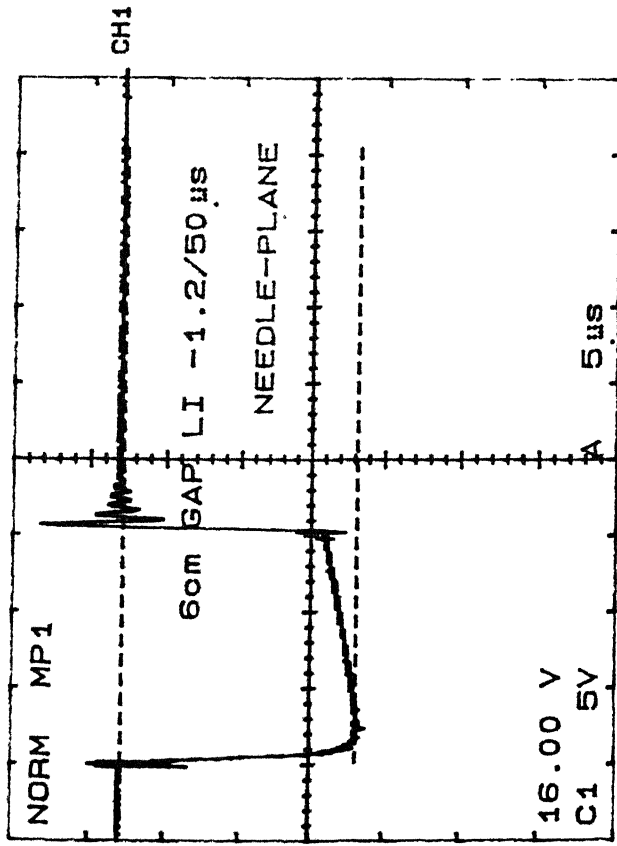


P 6.8 Oscillograph showing U_{b50} 50 % breakdown voltage and propagation time for N-P Electrode with li -1.2/50 μ s with varying gap distance

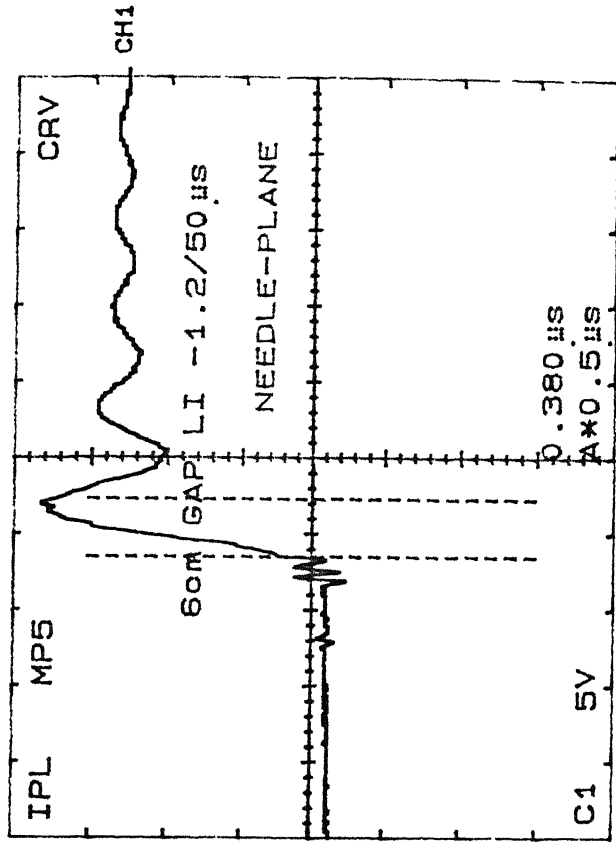


P 6.9 Oscilloscope showing U_{50} 50 % breakdown voltage and propagation time for N-P Electrode with li -1.2/50 μ s with varying gap distance

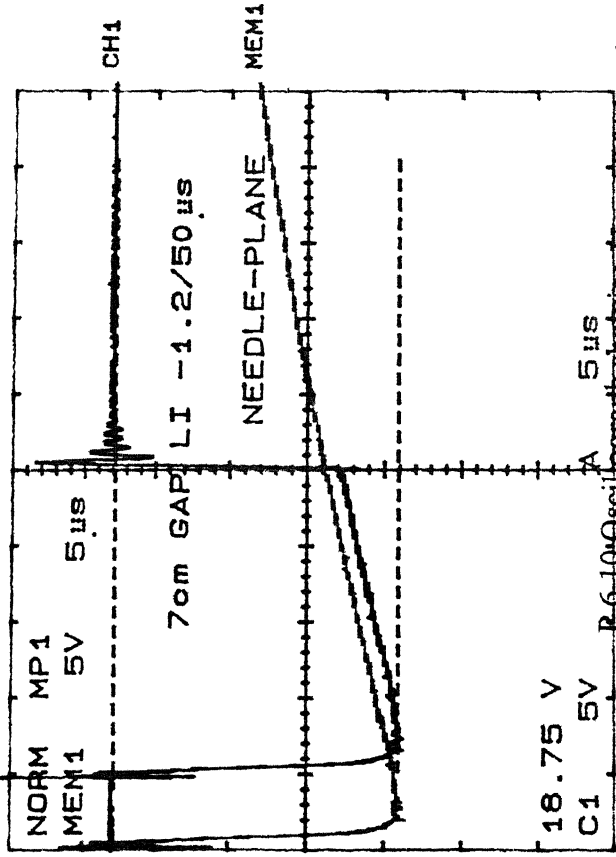
KIKUSUI CR 5502U



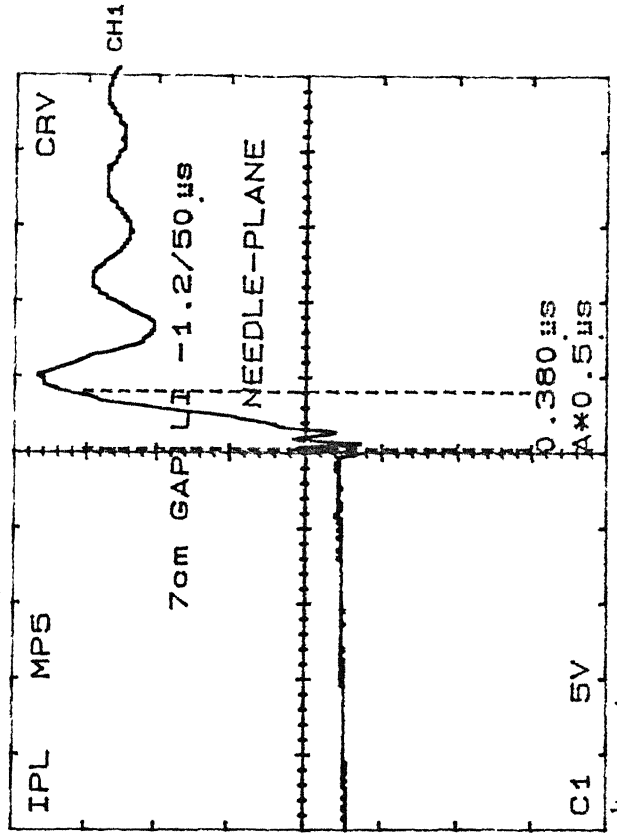
KIKUSUI CR 5502U



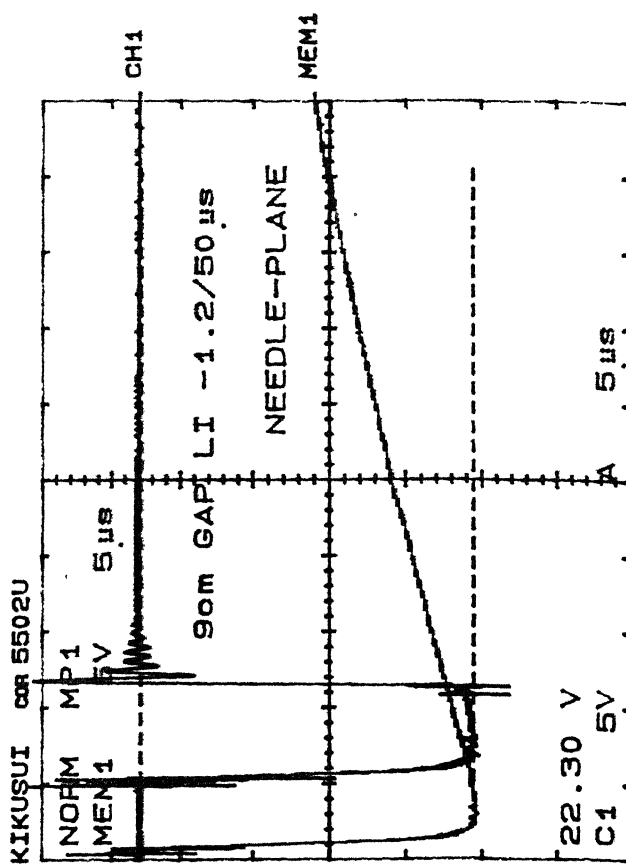
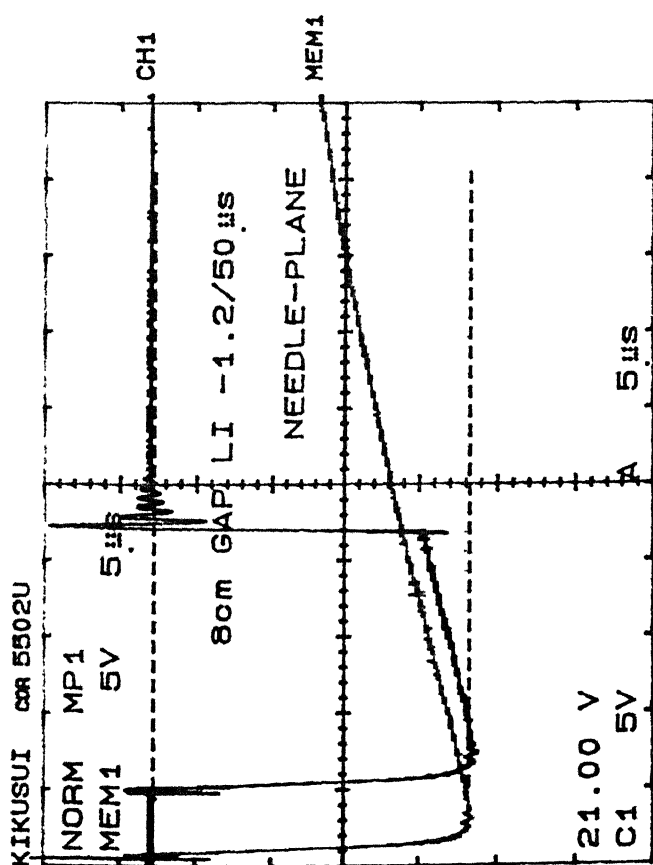
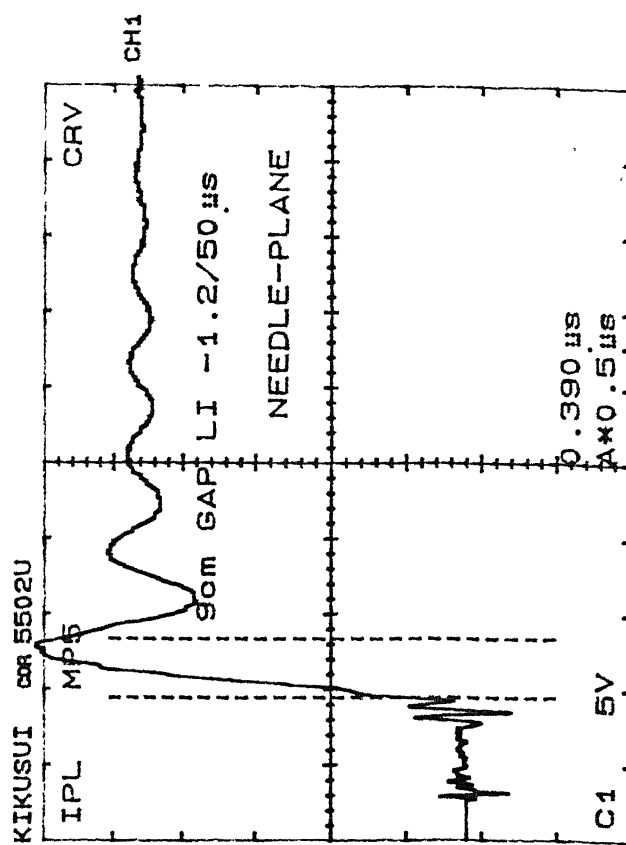
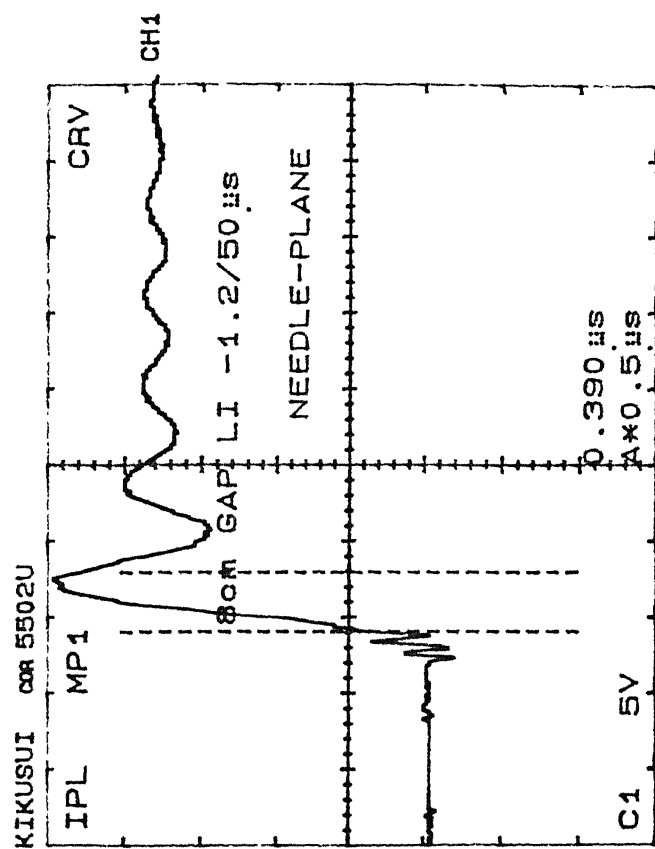
KIKUSUI CR 5502U



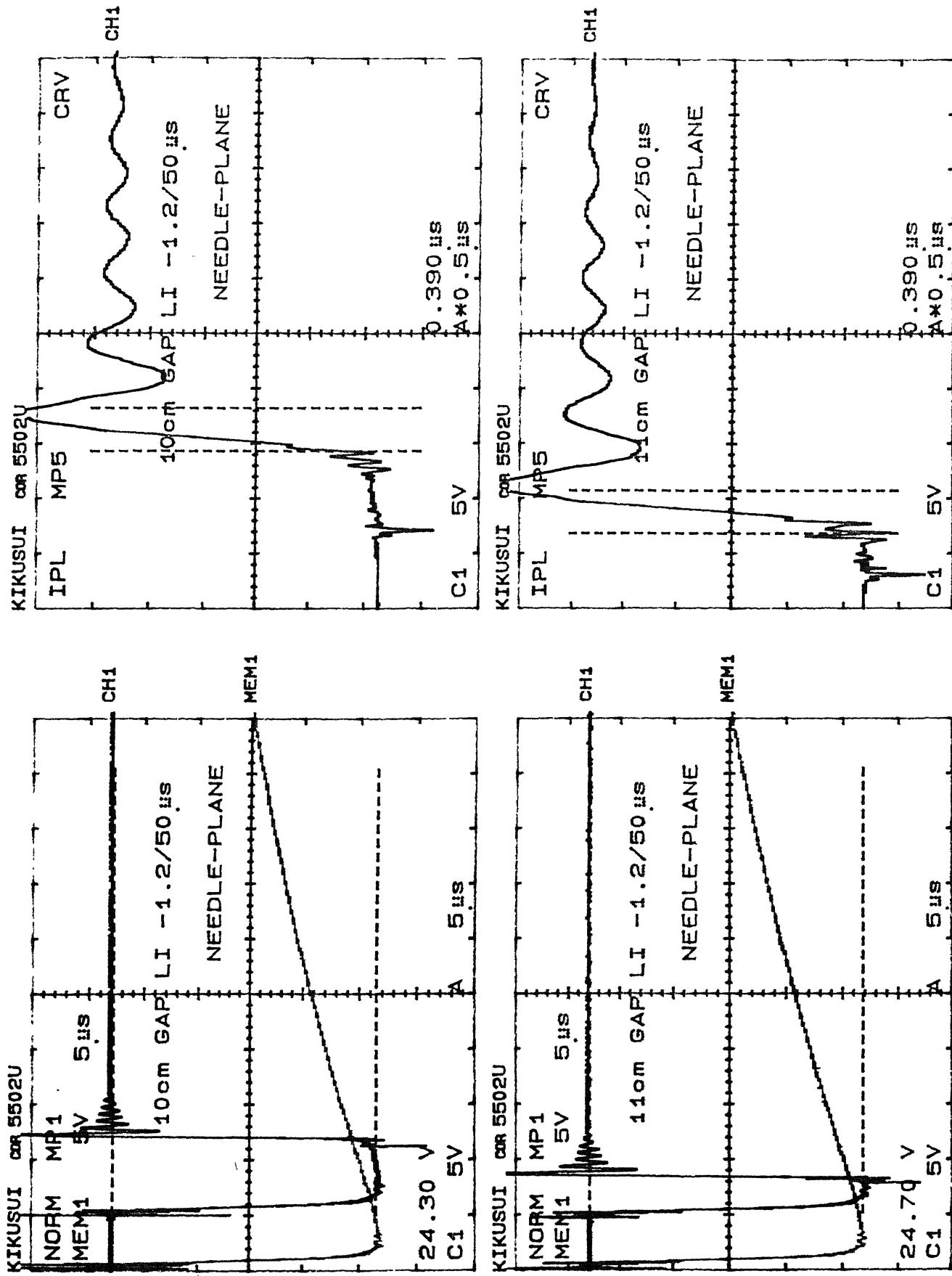
KIKUSUI CR 5502U



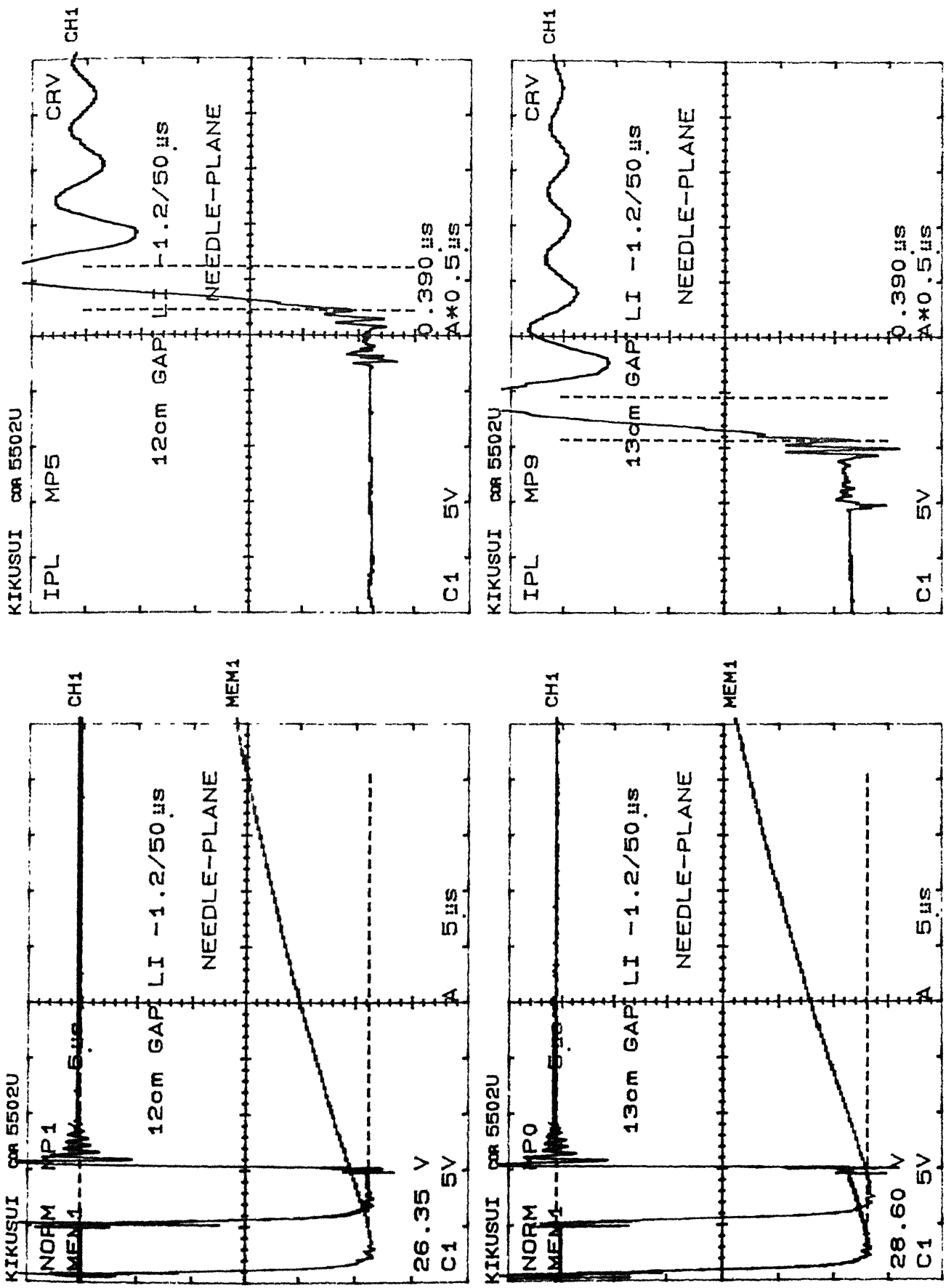
P-6-10 Oscillograph showing U_{h50} 50% breakdown voltage and propagation time for N-P Electrode with li -1.2/50 μ s with varying gap distance



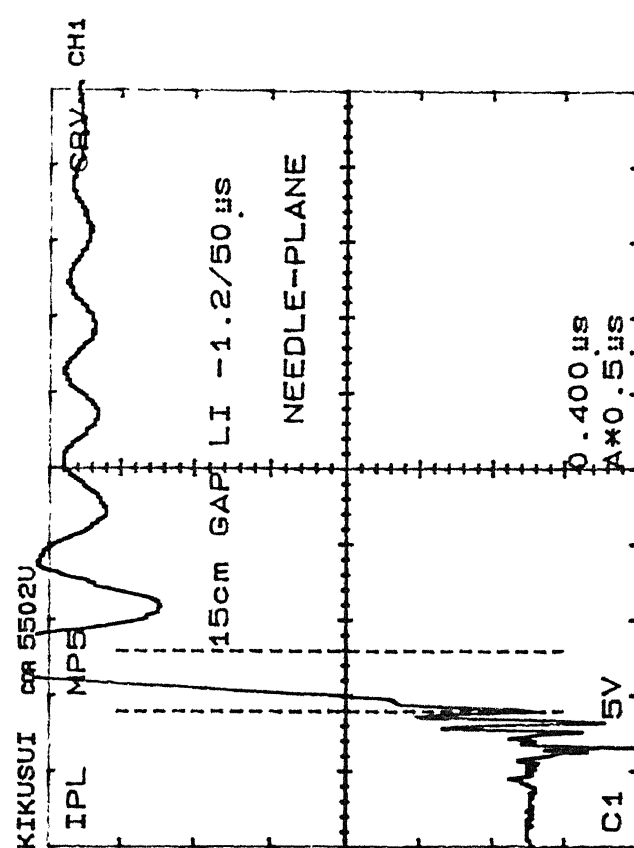
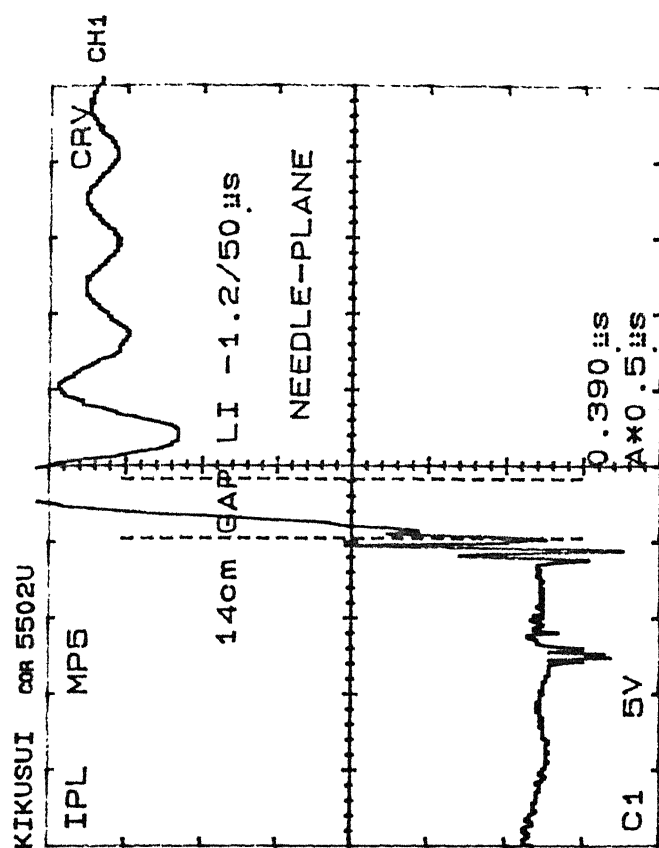
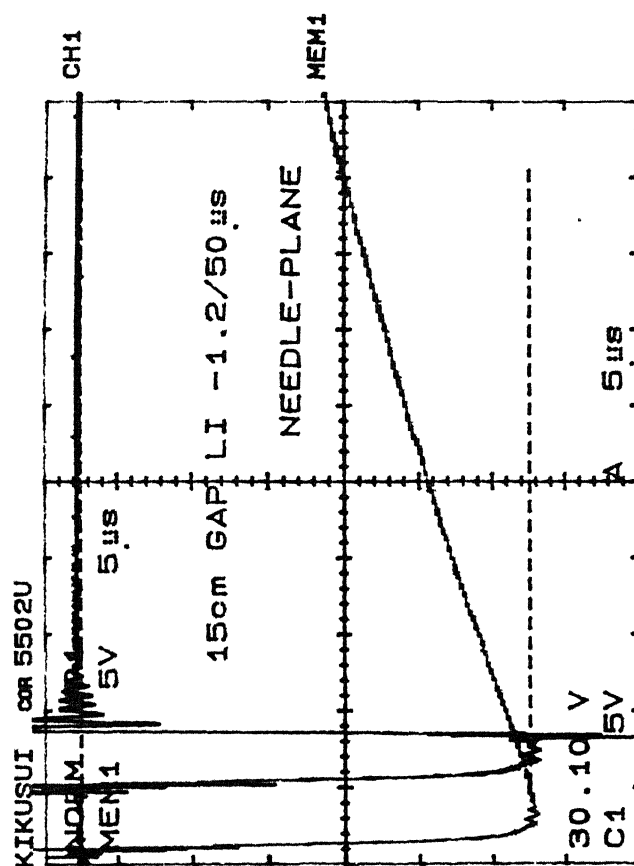
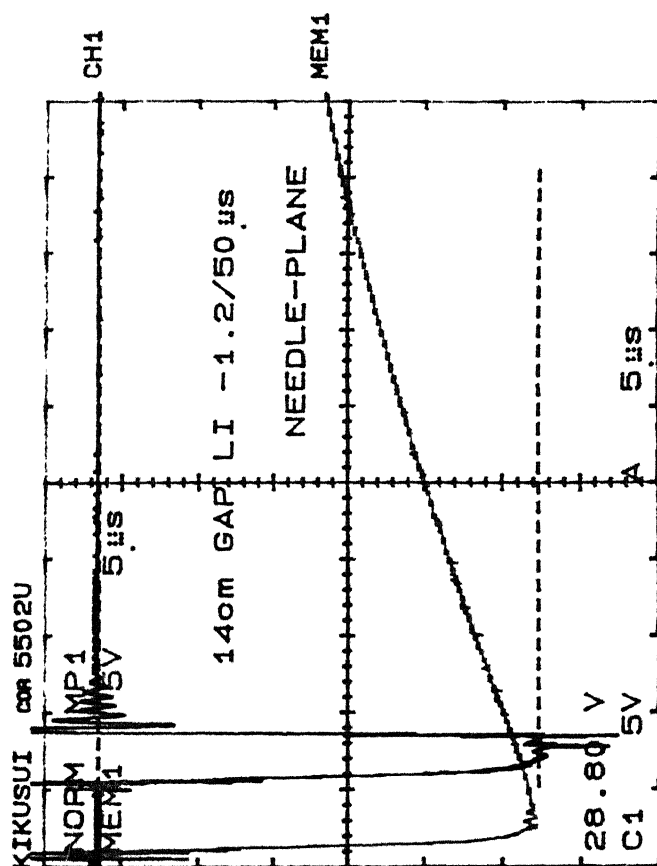
P 6.11 Oscillograph showing U_{b50} 50 % breakdown voltage and propagation time for N-P Electrode with li -1.2/50 μ s with varying gap distance



P 6.12 Oscilloscope showing U_{b50} 50 % breakdown voltage and propagation time for N-P Electrode with li -1.2/50 μ s with varying gap distance



P 6.13 Oscillograph showing U_{b50} 50 % breakdown voltage and propagation time for N-P Electrode with li -1.2/50 μ s with varying gap distance



P 6.14 Oscillograph showing U_{b50} 50 % breakdown voltage and propagation time for N-P Electrode with li -1.2/50 μ s with varying gap distance

6.2 Investigations with 1.2/50 μs Lightning Impulse

Experimental set up and electrode configurations were same as mentioned in chapter 5. Propagation time is measured when the breakdown voltage is U_{b50} and breakdown takes place in wave tail region. Readings were taken when the breakdown occurred approximate at the same instant of the wave tail of the impulse. Table 6.2 shows the measured reading of propagation time from CRO and corresponding calculated propagation velocity for three electrode configurations with lightning impulse of 1.2/50 μs with both polarities.

Table 6.2 . Propagation data of breakdown channel in air in extremely non uniform field with li \pm 1.2/50 μs

| Gap distance (cm) | Needle - plane | | | | Rod - Plane | | | | Needle - Needle | | | |
|-------------------|------------------------------------|-------|---|-------|------------------------------------|-------|---|-------|------------------------------------|-------|---|-------|
| | Propagation time (μs) | | Propagation velocity (cm/ μs) | | Propagation time (μs) | | Propagation velocity (cm/ μs) | | Propagation time (μs) | | Propagation velocity (cm/ μs) | |
| | +li | -li | +li | -li | +li | -li | +li | -li | +li | -li | +li | -li |
| 3 | 0.365 | 0.350 | 8.22 | 8.57 | 0.415 | 0.335 | 7.23 | 8.96 | 0.370 | 0.375 | 8.11 | 8.00 |
| 4 | 0.350 | 0.355 | 11.43 | 11.27 | 0.400 | 0.350 | 10.00 | 11.43 | 0.365 | 0.380 | 10.96 | 10.53 |
| 5 | 0.360 | 0.355 | 13.89 | 14.08 | 0.400 | 0.350 | 12.50 | 14.29 | 0.375 | 0.375 | 13.33 | 13.33 |
| 6 | 0.375 | 0.380 | 16.00 | 15.79 | 0.400 | 0.360 | 15.00 | 16.67 | 0.365 | 0.360 | 16.44 | 16.67 |
| 7 | 0.362 | 0.380 | 19.34 | 18.42 | 0.350 | 0.370 | 20.00 | 18.92 | 0.365 | 0.365 | 19.18 | 19.18 |
| 8 | 0.350 | 0.390 | 22.86 | 20.51 | 0.350 | 0.385 | 22.86 | 20.78 | 0.370 | 0.380 | 21.62 | 21.05 |
| 9 | 0.390 | 0.390 | 23.08 | 23.08 | 0.340 | 0.390 | 26.47 | 23.08 | 0.375 | 0.375 | 24.00 | 24.00 |
| 10 | 0.375 | 0.390 | 26.67 | 25.64 | 0.350 | 0.400 | 28.57 | 25.00 | 0.375 | 0.370 | 26.67 | 27.03 |
| 11 | 0.385 | 0.390 | 28.51 | 28.21 | 0.350 | 0.400 | 31.43 | 27.50 | 0.375 | 0.375 | 29.33 | 29.33 |
| 12 | 0.370 | 0.390 | 32.43 | 30.77 | 0.380 | 0.400 | 31.58 | 30.00 | 0.380 | 0.375 | 31.58 | 32.00 |
| 13 | 0.370 | 0.390 | 35.14 | 33.33 | 0.375 | 0.400 | 34.67 | 32.50 | 0.380 | 0.380 | 34.21 | 34.2 |
| 14 | 0.375 | 0.390 | 37.33 | 35.89 | 0.375 | 0.400 | 37.33 | 35.00 | 0.385 | 0.380 | 36.36 | 36.84 |
| 15 | 0.380 | 0.400 | 39.47 | 37.50 | 0.375 | 0.400 | 40.00 | 37.50 | 0.385 | 0.380 | 38.96 | 39.47 |

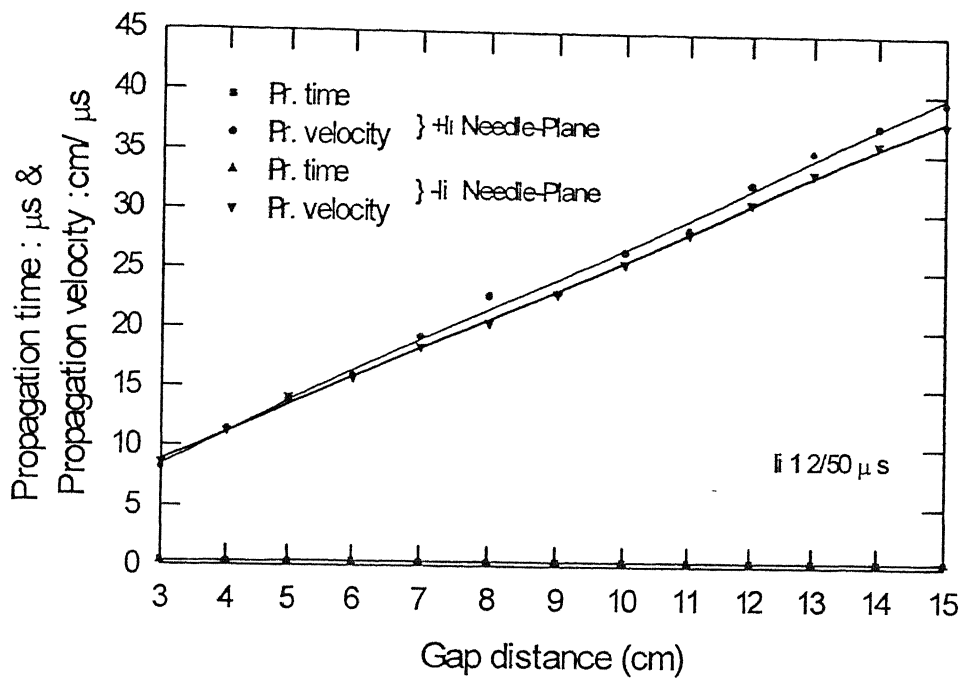


Fig 6.4 Propagation characteristics of air breakdown channel for Needle-Plane electrodes with $li \pm 1.2/50 \mu s$

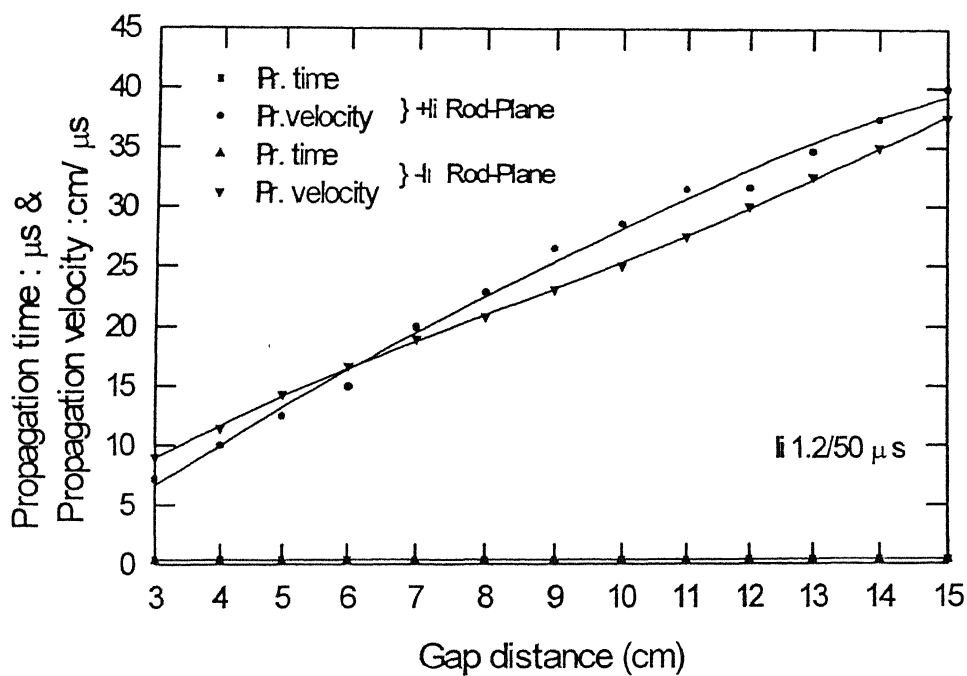


Fig 6.5 Propagation characteristics of air breakdown channel for Rod-Plane electrodes with $li \pm 1.2/50 \mu s$

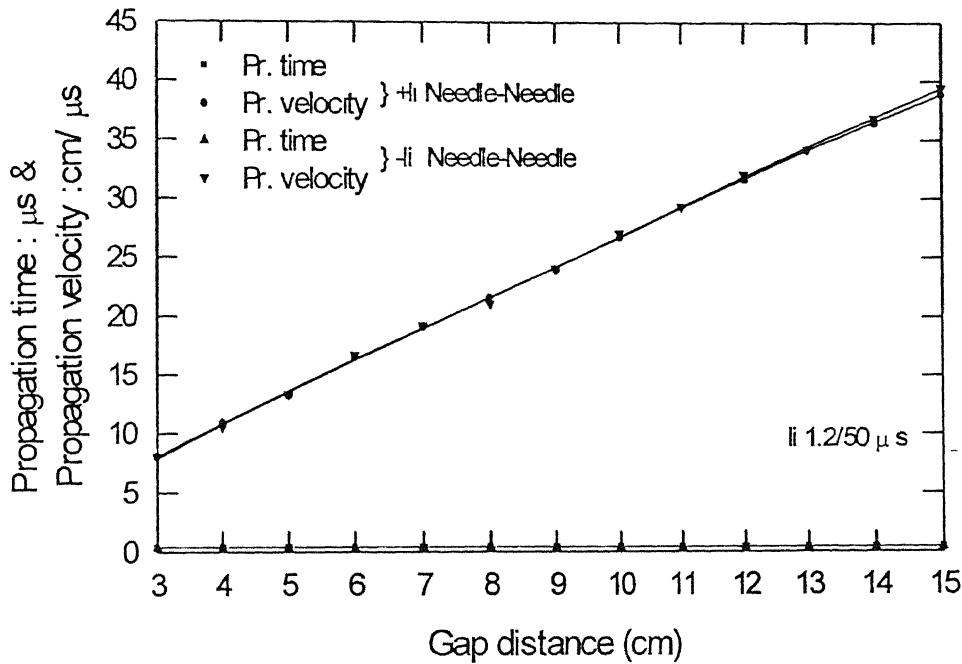


Fig 6.6 Propagation characteristics of air breakdown channel for Needle-Needle electrodes with $1.2/50 \mu s$

From figures 6.4-6 it can be observed that the nature of propagation characteristics is same as of switching impulse. Propagation time is almost constant and having values around half of the values obtain with switching impulse. Hence propagation velocity increases linearly of higher values from 7 to 40 cm/μs. The effect of polarity is also not present in these characteristics. Deviation from the linear curve is marginal for propagation velocity.

Chapter 7

Conclusions and Scope for Future Works

Important conclusions of this experimental investigation work are as follows

1. The breakdown voltage(U_{b50}) versus gap distance characteristics strongly depend upon the shape of electrodes, the applied impulse voltage wave shape and its polarity
2. The breakdown voltage(U_{b50}) increases as gap distance is increased for all the three electrode configurations and for all the waveshapes of either polarities. However the breakdown strength of air decreases as the distance between the electrodes is increased i.e. when the field becomes more extremely non uniform
3. The breakdown voltage(U_{b50}) characteristics with positive polarity shows the same nature of curve for switching and lightning impulse voltage waveshapes, but with negative polarity N-P and R-P electrodes have much higher breakdown voltages compared to N-N electrodes.
4. Polarity effect is conspicuous for N-P and R-P electrodes, but it is marginal for symmetrical mirror image electrodes like N-N. It also verifies the polarity effect is significant in case of non uniform field.
5. Breakdown characteristics measured with si1 & si2 wave shapes are of same nature.
6. The breakdown strength of air is lowest with positive polarity switching impulse voltages. So these overvoltages are more dangerous to the power system.
7. The slope of the line tangents to the U_{b50} -d curves depend upon the extent of stable PD process which appears before the breakdown
8. The electrode configurations N-P & R-P with positive polarity and N-N with negative polarity represents the most unfavorable condition as they have the lowest breakdown strength.
9. Average breakdown field intensity characteristics with switching impulse for N-P and R-P electrodes show an average potential gradient of about 5 kV/cm for positive and

between 10-15 kV/cm for negative polarity This verifies that breakdown under these conditions are accomplished with stable streamer discharge.

- 10 Average breakdown field intensity characteristics with lightning impulse for N-P and R-P electrodes show an average potential gradient of about 8 kV/cm for positive and about 15 kV/cm for negative polarity This verifies that development of stable streamer discharge is difficult for li compare to si on same conditions
11. Stable streamer discharge precede above a certain gap distance with switching impulse for R-P electrodes.
12. Breakdown strength of air is higher for lightning impulse compared to switching impulse for all the three electrode configurations with either polarity It verifies the dependence of the time to crest on the breakdown voltage and the development of stable PD is difficult with short duration pulses.
13. Leader propagation velocity depends upon the electrode configuration, gap distance and also on the shape of the applied voltage
14. On increasing the mean rate of rise i.e time to crest of the applied voltage the average leader propagation velocity increases
15. The nature of breakdown with positive and negative leader channel is similar.

Scope for future research

- Due to constrain of the impulse voltage generator rating and the clearance available in the laboratory, measurement could be performed for gap distances beginning at 2 cm to upto 15 cm only. Under such condition, only stable streamer discharges are able to precede the breakdown. It would be desirable to investigate the breakdown voltage characteristics for longer gap distances with such voltages
- In this study only those observation are taken for which instance of breakdown is approximately equal. If it is possible to breakdown the dielectric at a required instance in wave tail region then accurate variation of propagation time with voltage and gap distance can be analysed.

- Propagation velocity is calculated by taking shortest gap distance between the electrodes but normally the discharge does not take place in straight direction instead in some zig-zag direction
- Breakdown characteristics of SF_6 can be studied with same electrode configurations as this is most electronegative and insulating gas in power system

References

- 1 R. Arora and W. Mosch; "High Voltage Insulation Engineering"; Wiley Eastern Limited; 1995.
- 2 E. Kuffel and W. S. Zaengle; "High Voltage Engineering – Fundamentals"; Pergamon Press, Oxford; 1984
- 3 J. M. Meek, J. D. Craggs "Electrical Breakdown of Gases"; Clarendon Press, Oxford, 1953.
- 4 D. V. Razevig; "High Voltage Engineering"; translated by M. P. Chourasia; Khanna Publishers, Delhi; 1996
- 5 C. L. Wadhwa, "High Voltage Engineering", Wiley Eastern Limited; 1994.
- 6 M. A. Goffar Khan; " Investigation of Insulating Properties of Vacuum under High Voltage" Ph.D. Thesis, Deptt. of Electrical Engg.; I. I. T. Kanpur; 1995.
- 7 S. Singh, "Breakdown Properties of Atmospheric Air with Switching Overvoltages" M.Tech. Thesis, Deptt. of Electrical Engg.; I. I. T Kanpur; 1998.
- 8 D. B. Watson, S. K. Kho, "Impulse flashover Trajectory in Air in Non-uniform fields" IEEE Transactions on Electric Insulation, Vol 28, No.2, April 1993.
- 9 <http://www.geocities.com/CapeCanaveral/Lab/8063/lichtenb.htm>
- 10 <http://home.earthlink.net/~jimlux/hv/marx.htm>
